GEOMETRIC INTEGRATION AND ITS APPLICATIONS

C.J. Budd[1] and M.D. Piggott[2]

Abstract

This review aims to give an introduction to the relatively new area of numerical analysis called geometric integration. This is an overall title applied to a series of numerical methods that aim to preserve the qualitative (and geometrical) features of a differential equation when it is discretised. As the importance of different qualitative features is a rather subjective judgement, a discussion of the qualitative theory of differential equations in general is given first. The article then develops both the underlying theory of geometrical integration methods and then illustrates their effectiveness on a wide ranging set of examples, looking at both ordinary and partial differential equations. Methods are developed for symplectic ODEs and PDEs, differential equations with symmetry, differential equations with conservation laws and problems which develop singularities and sharp interfaces. It is shown that there are clear links between geometrically based methods and adaptive methods (where adaptivity is applied both in space and in time). A case study is given at the end of this article on the application of geometrical integration methods to problems arising in meteorology. From this we can see the advantages (and the disadvantages) of the geometric approach.

[1]Dept. of Mathematical Sciences, University of Bath, Claverton Down, Bath, BA2 7AY, UK. cjb@maths.bath.ac.uk

[2]Dept. of Mathematical Sciences, University of Bath, Claverton Down, Bath, BA2 7AY, UK. mapmdp@maths.bath.ac.uk

Contents

1 Introduction **3**

2 Qualitative properties **5**
- 2.1 A Partial Listing . . . 6
- 2.2 Why preserve structure? . . . 8

3 Hamiltonian Ordinary Differential Equations and Symplectic Integration **9**
- 3.1 The theory of Hamiltonian methods . . . 9
- 3.2 Symplectic numerical methods . . . 12
  - 3.2.1 Outline . . . 12
  - 3.2.2 Symplectic Runge-Kutta methods . . . 15
  - 3.2.3 Splitting and composition methods . . . 17
- 3.3 Examples of applications of symplectic integrators . . . 20
- 3.4 Error analysis - a brief overview . . . 26
  - 3.4.1 The backward error analysis of symplectic methods . . . 26
  - 3.4.2 An analysis of Splitting methods . . . 29

4 Conservation laws **32**
- 4.1 Outline . . . 32
- 4.2 Serendipitous and enforced conservation laws . . . 33
- 4.3 Discrete gradient methods . . . 35

5 Symmetry group methods **35**
- 5.1 Lie group methods . . . 36
  - 5.1.1 Example 1: Evolution on the sphere . . . 40
  - 5.1.2 Example 2: Rigid body motion . . . 42
- 5.2 Symmetries and reversing symmetries . . . 44
- 5.3 Scaling symmetries, temporal adaptivity and singularity capturing . . . 45
  - 5.3.1 Outline . . . 45
  - 5.3.2 Self-similar solutions . . . 47
  - 5.3.3 Numerical methods for scale invariant problems . . . 48
  - 5.3.4 Examples . . . 50

6 A comparison of methods **52**

7 Partial differential equations **58**
- 7.1 Symplectic methods for Hamiltonian PDEs . . . 58
  - 7.1.1 Basic theory . . . 58

8 Lagrangian and action based methods for PDEs **62**

9 Methods for partial differential equations that preserve all symmetries **66**

10 Noether's theorem for discrete schemes **71**

11 Spatial adaptivity, equidistribution and scaling invariance **74**
- 11.1 Scaling invariance of partial differential equations . . . 74
- 11.2 Spatial adaptivity . . . 75
- 11.3 Singularities in the nonlinear Schrödinger equation (NLS) . . . 77

11.4 The nonlinear diffusion equation 79

12 The Euler equations and some problems from meteorology 82

12.1 The Euler equation 82

12.1.1 The Arakawa Jacobian 83

12.1.2 Sine bracket type truncation 84

12.2 The semi-geostrophic equations, frontogenesis and prediction ensembles . . 86

12.2.1 Hamiltonian formulations 88

12.2.2 Links with moving mesh theory 89

12.2.3 Calculating Lyapunov exponents 90

13 Conclusion 91

1 Introduction

The modern study of natural phenomena described by both ordinary and partial differential equations usually requires a significant application of computational effort. To understand the design and operation of such computer algorithms, numerical analysis is essential. A huge amount of effort over the past fifty years (and earlier) has thus been applied to the research of numerical methods for differential equations. This research has led to many ingenious algorithms and associated codes for the computation of solutions to such differential equations. Most of these algorithms are based upon the natural technique of discretising the equation in such a way as to keep the local truncation errors associated with the discretisation as small as possible, to ensure that these methods are stable so that the local errors do not grow, and in adaptive methods, to use meshes which constrain such errors to lie within specified tolerance levels. The resulting discrete systems are then solved with carefully designed linear and nonlinear solvers often dealing with very large numbers of unknowns. When coupled with effective (a-priori and a-posteriori) error control strategies these methods can often lead to very accurate solutions of fairly general classes of differential equations, provided that the times for integration are not long and the solution remains reasonably smooth with bounded derivatives.

However, methods based on the analysis of local truncation errors do not necessarily respect, or even take into account, the qualitative and global features of the problem or equation. It can be argued that in some situations these global structures tell us more about the underlying problem than the local information given by the expression of the problem in terms of differentials. The recent growth of geometric integration has, in contrast, led to the development of numerical methods which systematically incorporate qualitative information of the underlying problem into their structure. Such methods are sometimes existing algorithms (such as the Gauss-Legendre Runge-Kutta methods or the Störmer-Verlet leapfrog method) that turn out to have excellent qualitative properties, developments of existing methods (such as adaptive procedures or Moser-Veselov integrators) for which qualitative information can be included in a natural way, or are entirely new methods, such as Lie group integrators which use special techniques to incorporate qualitative structure. As a side benefit to the incorporation of qualitative features, the resulting numerical schemes are often more efficient than other schemes and are also easier to analyse. This is because we may exploit the qualitative theory of the underlying differential equations (such as its Hamiltonian structure or group invariance) by using the powerful backward error analysis methods developed by Hairer, Reich and their co-workers [71, 72, 121].

As it is often unclear a-priori what the correct qualitative features of a problem are (and it is highly unlikely that one numerical method can preserve all of them — although Gauss-Legendre methods have a jolly good try at doing this), the development of geometric integration algorithms to solve scientific problems necessarily involves a dialogue between numerical analysts, applied mathematicians, engineers and scientists.

Some of the above comments may be exemplified by the following diagram. Given a differential equation which we seek to approximate using a numerical method, the left hand side of the diagram represents the use of classical methods for approximating the equation, whereas the right hand side displays the geometric integration philosophy.

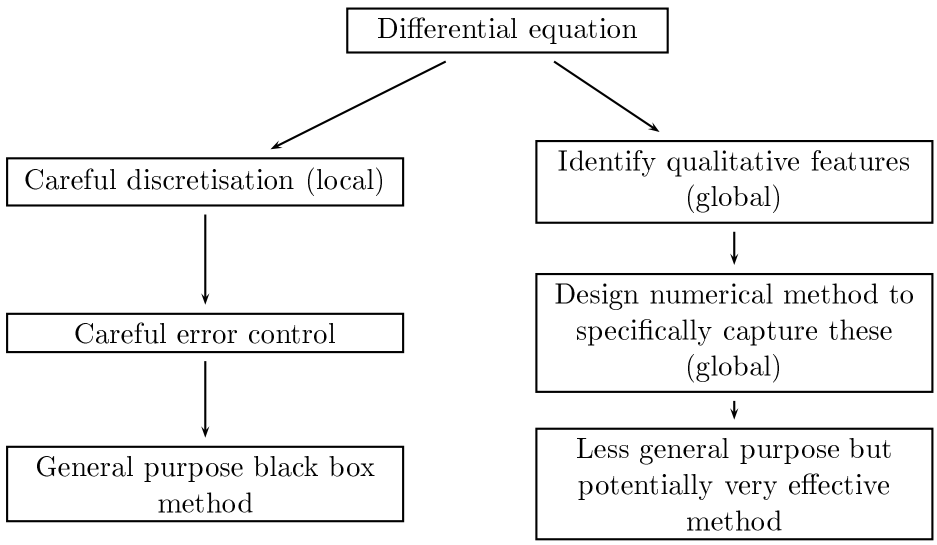

As a simple illustration, consider the harmonic oscillator problem

$$du/dt = v, \quad dv/dt = -u.$$

Qualitatively, this system has the property that its solutions are all periodic and bounded and that $u^2 + v^2$ is a conserved quantity of the evolution. A forward Euler discretisation of this system with time step h gives

$$U_{n+1} = U_n + hV_n, \quad V_{n+1} = V_n - hU_n.$$

It is easy to see that

$$U_{n+1}^2 + V_{n+1}^2 = \left(1 + h^2\right)\left(U_n^2 + V_n^2\right).$$

Thus, whilst over any finite time interval, the correct solution is obtained in the limit of $h \to 0$, the numerical method has lost all three qualitative features listed above. A geometrically based method instead aims to capture these.

The aim of this review is to introduce and explain, some ideas, methods, and techniques used in the field of geometric integration, basing our discussion around several carefully chosen examples. We will include some proofs of important results, but mostly will refer the reader to the literature for fuller explanations. We further aim to discuss how some of the mentioned ideas could be used in the very challenging problems arising in the fields of meteorology and numerical weather prediction. This discussion is necessarily incomplete and further details of geometric integration can be found in the recent reviews and discussions listed in the following references [25, 107, 69, 27, 128].

This review is organised as follows. In Section 2 we present an, obviously not exhaustive, description of some of the qualitative properties of both ordinary and partial differential equations that we have in mind.

In Sections 3, 4, 5 and 6 we look at methods for ordinary differential equations. In Section 3 we consider symplectic methods for Hamiltonian problems (including splitting and Runge-Kutta methods), looking at applications of these methods to a variety of problems in mechanics, and analysing their error through the use of backward error analysis. In Section 4 we consider methods that retain conservation laws of various forms. In Section 5 we look at a variety of methods that conserve symmetries of ordinary differential equations. These will include Lie group methods based upon Magnus series and/or approximations of the matrix exponential, methods for preserving reversing symmetries and time-adaptive methods for ordinary differential equations with scaling invariance symmetries. In particular developing methods for problems which allow the construction of numerical discretisations with uniform in time error estimates for certain problems. In Section 6 we make a comparison of various geometrically based methods for ordinary differential equations by comparing their performance for the (Hamiltonian) Kepler problem.

In Section 7, 8, 9, 10, 11 and 12 we look at geometric integration methods in the context of partial differential equations. In Section 7 we study Poisson bracket preserving methods as applied to Hamiltonian problems (such as the nonlinear wave equation and the nonlinear Schrödinger equation.) In Section 8 we look at methods which are derived from a Lagrangian formulation of a partial differential equation. In Section 9 we review the work of Dorodnitsyn [45] which extends symmetry based methods for ordinary differential equations to the construction of moving mesh methods for partial differential equations which preserve all of the symmetries of these equations. These are extended in Section 10 to methods which use a discrete form of Noether's theorem to ensure the conservation of quantities related to the invariance of the Lagrangian to continuous transformation groups. In Section 11 we continue to look at adaptive methods for partial differential equations, by developing in detail methods for scale invariant partial differential equations, which include the cases of the nonlinear diffusion equation and the nonlinear Schrödinger equation. We study numerical methods (based on moving mesh partial differential equations) which have proved to be especially effective in integrating these in the presence of interfaces and singularities. In Section 12 we focus our attention on some model problems arising in meteorology for which geometric based ideas may be beneficial. In particular looking at the calculation of weather fronts and making ensemble forecasts. We briefly discuss what possible impacts geometric integration could have on their computational analysis.

Finally, in Section 13 we present some concluding remarks, looking in particular at the advantages and disadvantages of geometric integration and the likely future developments in this new field.

2 Qualitative properties

In this section we shall briefly look at some of the qualitative and global features of a system described by a differential equation which we have in mind when we talk about geometric integration. The discussions of such qualitative features will, out of necessity (and the vast complexity of possible behaviours of solutions of differential equations), be very brief and introductory. We shall wherever possible include references to material where much further information may be found.

2.1 A Partial Listing

There are many possible qualitative features which may be present in systems modelled by ordinary or partial differential equations. We shall not attempt to give a complete listing, however below we give a partial listing which covers a wide variety of possibilities and mention how the different qualitative properties may be linked to one another.

1. *Geometrical structure* Deep properties of the phase space in which the system is defined give enormous insight into the overall properties of its solutions. Perhaps the most important of these arise in Hamiltonian problems.

2. *Conservation laws* Underlying many systems are conservation laws. These may include the conservation of total quantities (usually integrals over the domain in which the system evolves) such as mass, energy and momentum, or instead quantities which are conserved along particle trajectories and flows such as fluid density or potential vorticity. The loss of energy in a system describing planetary motion will inevitably lead to the planet so modelled spiralling into the sun, which is clearly incorrect qualitatively. Similarly it is widely accepted [42] that in large scale modelling of the oceans and atmosphere it is essential to conserve potential vorticity to retain the overall qualitative dynamics of the solution. The above are conservation laws associated directly with the manifold on which the solution evolves or the tangent bundle of this manifold, however, for Hamiltonian problems we may also have the conservation of symplectic structures in phase space which evolve on the co-tangent bundle and volume preservation in divergence-free systems which are conservation laws associated with the phase space in which the solution is posed. As is common with many such properties, there are deep relationships between them. For example the Hamiltonian of the solution is conserved in autonomous Hamiltonian systems and a wide class of Casimir functions are conserved along trajectories [103].

3. *Symmetries* Many systems are invariant under the actions of symmetries such as Lie group, scaling and involution symmetries. Such symmetries may or may not be retained in the underlying solution but there may exist solutions (self-similar solutions) which do not change when the symmetry group acts. The possible symmetries may include the following

   - *Galilean symmetries* such as translations, reflexions and rotations. One of the key problems in computer vision is to recognise an object which may be a translation or rotation of a known pattern. One way to do this is to associate invariants to the object (such as curvature) which do not change under the action of a Galilean symmetry. This is naturally achieved in the moving frames methods studied by [119] within the context of the geometric integration approach. The study of the motion of rigid bodies in three-dimensional space (such as a satellite or a robot arm) or the buckling of a cylindrical shell are dominated by the fact that such systems are invariant under Galilean symmetries [98].

- *Reversal symmetries* The solar system is an example of a system which is invariant under a time reversal, and more generally many physical systems are invariant under symmetries ρ satisfying the identity $\rho^2 = Id$. We can also ask whether a numerical method with time step h is *symmetric*, so that the inverse of taking such a time step is the same as replacing h by $-h$. (The forward Euler method does not have this property, in contrast to the trapezoidal rule which does.)
- *Scaling symmetries* Many physical problems have the property that they are invariant under rescalings in either time or space. This partly reflects the fact that the laws of physics should not depend upon the units in which they are measured or indeed should not have an *intrinsic* length scale. [10]. An example of such a scaling law is Newton's law of gravitation which is invariant under a rescaling in time and space. This invariance leads directly to Kepler's third law linking the period of a planet on an elliptical periodic orbit to the length of the major axis of the ellipse — determining this law does not involve solving the differential equation. A numerical method invariant under the same scaling law will exhibit a similar relation between (discrete) period and scale.
- *Lie group symmetries* These are deeper symmetries than those described above, often involving the invariance of the system to a (nonlinear) Lie group of transformations. An important example (which arises naturally in mechanics) is the invariance of a system to the action of the rotation group $SO(3)$. An excellent discussion of such symmetries is given in [118]. The review article [84] describes the numerical approach to computing solutions of ordinary differential equations with such symmetries.

4. *Asymptotic behaviours* The original development of numerical methods for differential equations centred on the study of minimising errors in the calculation of solutions over a fixed time T. However, when studying the *dynamics* of a system numerically and to gain insight into its long term behaviour we are often interested in the alternative question of taking a fixed method and applying it for an undefined number of time steps. Note that in a problem with widely varying time-scales (such as molecular dynamics where we try to model the behaviour of chemicals over seconds whilst molecular interactions occur over micro-seconds) the study of long term behaviour (measured in terms of the smallest time-scale) is unavoidable. Widely differing time-scales are natural in partial differential equations. For such studies we need to concentrate on the ability of a numerical method to preserve structurally stable features of the solution such as invariant sets, invariant curves and orbit statistics. A very thorough review of these issues and the way that numerical methods are used to study dynamical systems is given in the monograph [136] and fundamental contributions to the study of the preservation of invariant curves have been made by Beyn [13] (see also the work of Stoffer and Nip in this context [135]). An excellent example of such an investigation is the long term study of the solar system made by Sussman and Wisdom [139] in which numerical methods (special purpose splitting methods) are used to investigate whether the solar system has chaotic behaviour. As the errors of many 'conventional' methods accumulate exponentially with time, accurate qualitative investigations over long time using these methods is not possible, even if the methods are of high order and have very small local errors. Thus it is essential to use methods for which there is some control over the long term growth of errors, even if the local error made by such methods may appear to be very large in comparison to others. A hint of how this is possible is the fact that the differential

system under study may evolve in time so that over a long time its dynamics in some sense simplifies. For example it may ultimately evolve so that its dynamics is restricted to a low dimensional attractor (although its dynamics on this attractor may well be chaotic). Complex structures starting from arbitrary initial data may simplify into regular patterns [67]. Alternatively, the equation may have solutions which form singularities in finite time such as interfaces (singularities in curvature) weather fronts (derivative singularities) or combustion in which the solution itself becomes singular at a single point. All of these features can be incorporated into the design of a numerical scheme and should be reproduced by a good numerical method.

5. *Orderings in the solutions* The differential equation may possess some form of maximum principle which leads to a preservation of the solution orderings. For example, given two sets of initial data $u_0(x)$ and $v_0(x)$ for a partial differential equation, the solutions may respect the ordering that if $u_0(x) < v_0(x)$ for all x, then $u(x,t) < v(x,t)$ for all x and t. The linear heat equation $u_t = u_{xx}$ has this property as do many other parabolic equations. Maximum principles can play a significant role in understanding the *spatial* symmetries of the solution [55]. A related concept is that of solution convexity. Indeed, the preservation of the convexity of a pressure function across a front is an important feature in some areas of numerical weather prediction [39].

It is important to realise that these global properties may be closely linked to one another. For example, if the differential equation is derived from a variational principle linked to a Lagrangian function then, via Noether's theorem [118], each continuous symmetry of the Lagrangian leads directly to a conservation law for the underlying equation. This has a beautiful application to numerical analysis. If a numerical method is also based upon a Lagrangian and this Lagrangian has symmetries then the numerical method automatically has a discrete conservation law associated with this symmetry [47]. We will explore this relation in the section on partial differential equations.

Symmetry when coupled with solution orderings frequently leads to an understanding of the asymptotic behaviour of the equation. In particular, self-similar solutions (which are invariant under the action of a scaling group) can be used to bound the actual solution from above and below. The solution behaviour is then constrained to follow that of the self-similar solution [125]. Singularities in the equation often have more *local* symmetry than the general solution of the equation because the effects of boundary and initial conditions are less important [10]. Conversely solutions can have *hidden* symmetries [63] not evident in the actual equation.

Some natural questions to ask of a numerical method which attempts to emulate some or all of these properties are as follows.
What is the benefit (if any) of designing numerical methods which take into account qualitative properties of the underlying solution? For systems which possess more than one important qualitative property, how much of this structure can we hope to preserve? Which qualitative properties turn out to be more important, or beneficial, from a computational viewpoint?

2.2 Why preserve structure?

There are several reasons why it is worthwhile to preserve qualitative structure. Firstly, many of the above properties can be found in systems which occur naturally in applications. For example, large scale molecular or stellar dynamics can be described by Hamiltonian systems with many conservation laws. Mechanical systems evolve under rotational constraints, as do many of the problems of fluid mechanics. Partial differential equations possessing scaling symmetries and self-similarity arise in fluid and gas dynamics, combustion, nonlinear diffusion and mathematical biology. Partial differential equations with a Hamiltonian structure are important in the study of solitons (such as the KdV and nonlinear Schrödinger equation) and the semi-geostrophic equations in meteorology also have a Hamiltonian structure. The list could be virtually endless.

In designing our numerical method to preserve some structure we hope to see some improvements in our computations. For a start we will be studying a discrete dynamical system which has the same properties as the continuous one, and thus can be thought of as being in some sense close to the underlying problem in that stability properties, orbits and long-time behaviour may be common to both systems. Geometric structures often (using backward error analysis and exploiting the geometric structure of the discretisations) make it easier to estimate errors, and in fact local and global errors may well be smaller for no extra computational expense. Geometric integration methods designed to capture specific qualitative properties may also preserve additional properties of the solution *for free*. For example symplectic methods for Hamiltonian problems have excellent energy conservation properties and can conserve angular momentum or other invariants (which may not even be known in advance).

In conclusion, geometric integration methods (including Lie group methods, symplectic integrators, splitting methods, certain adaptive methods, etc.) can often 'go where other methods cannot'. They have had success in the accurate computation of singularities, long-term integration of the solar system, analysis of highly oscillatory systems (quantum physics for example). The list of application areas keeps on growing, see for example the many applications described by Leimkuhler in [90].

3 Hamiltonian Ordinary Differential Equations and Symplectic Integration

Probably the first significant area where geometric ideas were used was in the (symplectic) integration of Hamiltonian ordinary differential equations. This is natural as Hamiltonian systems (often incorporating constraints) have very important applications in mechanics, celestial and molecular dynamics and optics, and their analysis, since Hamilton's original papers, has always centred on the geometrical structure of the equations. We will start our investigation of geometric integration methods by focusing on such problems (later on we will investigate Hamiltonian partial differential equations). A detailed description of methods for Hamiltonian problems is given in [129], see also [136]. The numerical methods for solving such problems are usually called *symplectic* and include certain Runge-Kutta methods, splitting methods and methods based upon discretising the Lagrangian. We structure this discussion by first describing Hamiltonian systems, we then consider methods for such systems, and finally look at an analysis of the error of these methods using the backward error technique.

3.1 The theory of Hamiltonian methods

For classic introductions to this material see Arnold [6] and Goldstein [62]. Consider initially a mechanical system with generalised coordinates $\mathbf{q} \in \mathbb{R}^d$ and Lagrangian $L =$

$T - V$, where $T \equiv T(\mathbf{q}, \dot{\mathbf{q}})$ represents the kinetic energy of the system and $V \equiv V(\mathbf{q})$ its potential energy. The dynamics of such a system can be studied in terms of the calculus of variations by considering the action function constructed by integrating L along a curve $\mathbf{q}(t)$ and then computing variations of the action while holding the end points of the curve $\mathbf{q}(t)$ fixed (although it is sometimes advantageous not to impose this condition). See details of this derivation in [99] together with a detailed discussion of the numerical methods derived by discretising the action functional. We shall return to this topic in Section 8. It can be shown easily that this procedure leads to the following Euler-Lagrange equations describing the motion

$$\frac{d}{dt}\left(\frac{\partial L}{\partial \dot{\mathbf{q}}}\right) - \frac{\partial L}{\partial \mathbf{q}} = 0. \tag{1}$$

Hamilton recognised that these equations could be put into a form which allowed a more geometrical analysis. In particular he introduced the coordinates

$$\mathbf{p} = \frac{\partial L}{\partial \dot{\mathbf{q}}} \in \mathbb{R}^d,$$

which are the conjugate generalized momenta for the system. He further defined the Hamiltonian via a Legendre transformation as

$$H(\mathbf{p}, \mathbf{q}) = \mathbf{p}^T \dot{\mathbf{q}} - L(\mathbf{q}, \dot{\mathbf{q}})$$

and showed that (1) is equivalent to the following system of $2d$ first-order equations, called Hamilton's equations

$$\begin{aligned} \dot{\mathbf{p}} &= -\frac{\partial H}{\partial \mathbf{q}}, \\ \dot{\mathbf{q}} &= \frac{\partial H}{\partial \mathbf{p}}. \end{aligned} \tag{2}$$

This is called the *canonical form* for a Hamiltonian system. Note that for our considered mechanical system $H \equiv T + V$ and thus the Hamiltonian represents the total energy present.

More generally, if a system of ordinary differential is defined in terms of $\mathbf{u} \in \mathbb{R}^{2d}$ where $\mathbf{u} = (\mathbf{p}, \mathbf{q})^T$ with $\mathbf{p}, \mathbf{q} \in \mathbb{R}^d$ such that

$$\dot{\mathbf{u}} = \mathbf{f}(\mathbf{u}) \tag{3}$$

then this system is canonically Hamiltonian if

$$\mathbf{f}(\mathbf{u}) = J^{-1} \nabla H \tag{4}$$

where $H = H(\mathbf{p}, \mathbf{q})$ is the Hamiltonian function, ∇ is the operator

$$\left(\frac{\partial}{\partial p_1}, \frac{\partial}{\partial p_2}, \ldots, \frac{\partial}{\partial p_d}, \frac{\partial}{\partial q_1}, \ldots, \frac{\partial}{\partial q_d}\right),$$

and J is the skew-symmetric matrix

$$J = \begin{pmatrix} 0 & I_d \\ -I_d & 0 \end{pmatrix}. \tag{5}$$

Here I_d is the identity matrix of dimension d.

In this case $\mathbf{f}$ is called a Hamiltonian vector field. It is easy to see that if $\mathbf{f}_1$ and $\mathbf{f}_2$ are Hamiltonian vector fields then so is the vector field $\mathbf{f}_1 + \mathbf{f}_2$. We exploit this simple property in our analysis of splitting methods which follows shortly.

In addition to the conservation of the Hamiltonian a key feature of a Hamiltonian system is the *symplecticity* of its flow. The solution of the system (3) induces a transformation ψ on the phase space $\mathbb{R}^{2d}$ with associated Jacobian ψ'. Such a map is said to be *symplectic* if

$$\psi'^T J \psi' = J. \tag{6}$$

with J defined as above.

Symplectic maps have the very useful property that they combine to give other symplectic maps, as stated in the following.

LEMMA 3.1 *If ψ and φ are symplectic maps then so is the map $\psi \circ \varphi$*

Proof We can see this as follows. If ψ and φ are both symplectic maps then

$$(\psi'\varphi')^T J(\psi'\varphi') = \varphi'^T \psi'^T J \psi' \varphi' = \varphi'^T J \varphi' = J.$$

Symplecticity has the following, important, geometrical interpretation. If M is any 2-dimensional manifold in $\mathbb{R}^{2d}$, we can define $\Omega(M)$ to be the integral of the sum over the oriented areas, of its projections onto the (p_i, q_i) plane (so that if $d = 1$ this is the area of M). If ψ is a symplectic map, then $\Omega(M)$ is conserved throughout the evolution. In particular in one-dimension ($d = 1$) areas are conserved. A key result of Poincaré (1899) relating symplectic flows to Hamiltonian flows is the following.

THEOREM 3.1 *The flow $\psi(t)$ induced by a Hamiltonian function H via the differential equation (4) is symplectic.*

Proof If ψ' is the Jacobian matrix of the flow induced by the ordinary differential equation (4), then it follows from the definition of the Hamiltonian system that

$$\frac{d\psi'}{dt} = J^{-1} H'' \psi', \quad \text{with} \quad H'' = \begin{pmatrix} H_{pp} & H_{pq} \\ H_{pq} & H_{qq} \end{pmatrix}.$$

Hence

$$\frac{d}{dt}\left(\psi'^T J \psi'\right) = \psi'^T H'' J^{-T} J \psi' + \psi'^T H'' \psi' = 0.$$

However, when $t = 0$ we have $\psi' = I$ and hence $\left(\psi'^T J \psi'\right) = J$. The result then follows.

It can further be shown [69] that symplecticity holds iff a flow is Hamiltonian.

The symplecticity property is much stronger than simple preservation of $2d$-dimensional volume, since Hamiltonian systems preserve phase-space volume (Liouville's theorem) but it is possible to find volume preserving systems which are not Hamiltonian. From a perspective of dynamics, symplecticity plays a central role. In particular it means that behaviour of Hamiltonian systems is recurrent with solutions from any point in $\mathbb{R}^{2d}$ returning arbitrarily closely to their starting point. Furthermore (unlike dissipative systems) the dynamics of a Hamiltonian system cannot evolve onto a low dimensional attractor. Typical Hamiltonian dynamics is described by the celebrated KAM theorem [6] which describes how integrable and near integrable Hamiltonian systems (whose solutions are generically periodic or are confined to a torus) perturb (under periodic Hamiltonian perturbations) to tori (of highly irrational period) surrounded by regions of chaotic behaviour. As stated by [128] 'many properties that general systems only possess under exceptional circumstances appear generically in Hamiltonian systems'. Further details may be found in [6, 98, 118].

3.2 Symplectic numerical methods

3.2.1 Outline

Suppose now that a numerical one-step method of constant step size h is applied to approximate the solutions $\mathbf{u}(t)$ of (3) at time $t = nh$ by the vector $\mathbf{U}_n \in \mathbb{R}^{2d}$. We will assume for the moment that h is constant. This numerical scheme will induce a discrete flow mapping Ψ_h on $\mathbb{R}^{2d}$ which will be an approximation to the continuous flow map $\psi(h)$. We define the map Ψ_h to be symplectic if it also satisfies the identity (6). A natural geometric property that we would require of Ψ_h is that it should be symplectic if ψ is. We will now consider the construction of numerical methods with this property. We will call any numerical scheme which induces a symplectic map a *symplectic numerical method*. As we will see, such methods retain many of the other features (in particular the ergodic properties) of their continuous counterparts.

If the time step h is not constant, such as in an adaptive method, then particular care has to be taken with this definition and much of the advantage of using a symplectic scheme is lost [129] unless the equation defining h at each time step also preserves the geometric structure in some way. We will consider this issue further in Section 6.

The history of symplectic methods is interesting. Early work in the mathematics community which specifically aimed to construct symplectic methods for ordinary differential equations is given in de Vogelaere [144], Ruth [124] and Feng [54]. These early constructions were rather involved and much simpler derivations have followed, in particular see the work of Sanz-Serna and Calvo [129]. However, symplectic integrators themselves have been used for much longer than this. A lot of well established and very effective numerical methods have been successful precisely because they are symplectic even though this fact was not recognised when they were first constructed. Three examples of this serendipitous behaviour are Gauss-Legendre methods, related collocation methods and the Störmer-Verlet (leapfrog) methods of molecular dynamics. In the literature quoted above symplectic methods are generally constructed using one of four different methods

1. Generating functions
2. Runge-Kutta methods
3. Splitting methods
4. Variational methods

Of these four methods, method 1 tends to lead to methods which are cumbersome and difficult to use, however see [33] for details and examples. We consider method 4 in section 8 as it has a powerful application to partial differential equations. In this section we focus on methods 3 and 4.

Why bother? Whilst such methods preserve symplecticity and hence many of the qualitative features of the Hamiltonian problem they do not (in general) conserve the Hamiltonian itself (see Ge and Marsden [60]) unless an adaptive step h is used [86]. (However they can remain exponentially (in h) close to H for exponentially long times.) However, they usually have more favourable error growth properties. Invariant sets and orbit statistics converge even if the orbit is not followed with pointwise accuracy MacKay [96], McLachlan and Atela [106], Candy and Rozmus [31]. It is important also to observe that Hamiltonian systems arise naturally in partial differential equations (for example the nonlinear Schrödinger equation) for which the associated differential equations (say obtained through a semi-discretisation) are usually stiff. A conventional stiff solver such as a BDF method may introduce artificial dissipation into higher order modes, producing quite false qualitative behaviour. To resolve the energy transfer into the higher modes and to retain the correct dynamics of these modes a symplectic solver is essential.

It is worth saying that in computations small round-off errors introduce non-symplectic perturbations to Hamiltonian problems which can be an important factor in long term integrations. Some effort has been made to use integer arithmetic and lattice maps to remove the effects of round-off errors in such calculations, see the work of Earn and Tremaine [51].

Example To motivate the rest of this section we consider a simple, but important, example of a symplectic method. This is the second-order implicit, (symmetric) mid-point Runge-Kutta method, which for the problem (3) takes the form

$$\mathbf{U}_{n+1} = \mathbf{U}_n + h\mathbf{f}\left((\mathbf{U}_n + \mathbf{U}_{n+1})/2\right) = \mathbf{U}_n + hJ^{-1}\nabla H\left((\mathbf{U}_n + \mathbf{U}_{n+1})/2\right). \tag{7}$$

A proof that this method is indeed symplectic is instructive.

Proof For a sufficiently small time step h the implicit mid-point rule defines a diffeomorphism $\mathbf{U}_{n+1} = \Psi_h(\mathbf{U}_n)$. Differentiating (7) then gives

$$\Psi_h' = \frac{\partial \mathbf{U}_{n+1}}{\partial \mathbf{U}_n} = I + \frac{h}{2}J^{-1}H''\left((\mathbf{U}_n + \mathbf{U}_{n+1})/2\right)\left(I + \frac{\partial \mathbf{U}_{n+1}}{\partial \mathbf{U}_n}\right).$$

Hence, the Jacobian matrix of the transformation $\mathbf{U}_n \to \mathbf{U}_{n+1}$ is given by

$$\Psi_h'(\mathbf{U}_n) = \left[I - \frac{h}{2}J^{-1}H''\left((\mathbf{U}_n + \mathbf{U}_{n+1})/2\right)\right]^{-1}\left[I + \frac{h}{2}J^{-1}H''\left((\mathbf{U}_n + \mathbf{U}_{n+1})/2\right)\right]. \tag{8}$$

Note: This is a Cayley transformation. We shall return to this in the section on Lie group methods.
We have already mentioned that (6) is the condition we need to verify for a map to be symplectic, after substituting (8) into (6) we need to check that

$$\left[I + \frac{h}{2}J^{-1}H''\left((\mathbf{U}_n + \mathbf{U}_{n+1})/2\right)\right] J \left[I + \frac{h}{2}J^{-1}H''\left((\mathbf{U}_n + \mathbf{U}_{n+1})/2\right)\right]^T =$$
$$\left[I - \frac{h}{2}J^{-1}H''\left((\mathbf{U}_n + \mathbf{U}_{n+1})/2\right)\right] J \left[I - \frac{h}{2}J^{-1}H''\left((\mathbf{U}_n + \mathbf{U}_{n+1})/2\right)\right]^T.$$

The result now follows immediately from the symmetry of the Hessian matrix and the fact that $J^T = -J$.

Note: The above proof is independent of the specific form of the operator J, requiring only that J be skew-symmetric. Precisely similar arguments to the above can also be used to show that mid-point rule preserves the Poisson structure for systems with constant Poisson structure. This is very useful in studies of partial differential equations (see later). If J depends on U then can be shown to be *Almost Poisson*, that is preserves the Poisson structure up to second order, see [9]. The same idea is developed in *pseudo-symplectic methods* [8].

As we shall see presently, a powerful way of understanding and analysing such schemes is through the use of modified equation analysis. In particular, if $\mathbf{u}(t)$ is the solution of the equation and $\mathbf{U}_n$ the discrete solution, then modified equation analysis aims to find a differential equation *close* to the original so that the solution $\hat{\mathbf{u}}(t)$ of this lies much closer to $\mathbf{U}_n$ than the true solution $\mathbf{u}$ does. Generally we construct $\hat{\mathbf{u}}$ such that $\mathbf{U}_n - \hat{\mathbf{u}}(t_n) = \mathcal{O}(h^{N+1})$ with $N > r$, where r is the order of the numerical method. Suppose that the modified equation is

$$\frac{d\hat{\mathbf{u}}}{dt} = \hat{\mathbf{f}}(\hat{\mathbf{u}}).$$

Hairer [69] (see also Murua [116]) gives a construction of $\hat{\mathbf{f}}$ in terms of a B-series so that truncating a series of the form

$$\mathbf{f}_0(\hat{\mathbf{u}}) + h\mathbf{f}_1(\hat{\mathbf{u}}) + h^2\mathbf{f}_2(\hat{\mathbf{u}}) + \ldots \tag{9}$$

at order h^N gives an appropriate $\hat{\mathbf{f}}$ of order N as defined above. We give more details of this construction presently. Ideally the modified flow should have the same qualitative features as both the underlying equation and the discretisation. In this case the properties of the numerical *map* can be understood in terms of a smooth *flow* and thus analysed using methods from the theory of dynamical systems. This is discussed in [136] and has also been the motivation behind a series of meetings on *The dynamics of numerics and the numerics of dynamics* see [20].

Presently we will use this procedure to analyse the performance of certain symplectic methods. For the moment we observe, that a numerical method is symplectic if and only if each of the modified equations obtained by truncating (9) generates a Hamiltonian system. In particular the modified equation will have a modified Hamiltonian $H^0 + hH^1 + \ldots$. Ignoring for the moment the (exponentially small) difference between the modified flow and the discrete solution this leads to the important observation that

a symplectic discretisation of a Hamiltonian problem is a Hamiltonian perturbation of the original.

The importance of this observation cannot be over-emphasised. It implies that we can use the theory of perturbed Hamiltonian systems (in particular KAM theory) to analyse the resulting discretisation and it places a VERY strong constraint on the possible dynamics of this discrete system. It has been observed by Sanz-Serna that this procedure is not applicable to variable step methods as in this case the modified equation analysis breaks down. Whilst this is true in general, it can be overcome by a careful selection of h that preserves the Hamiltonian structure, and such choices may give improved methods [90, 68, 121]. However, there are limits to this form of analysis. The modified equations typically lead to asymptotic series that may break down for large step sizes, causing a break up of invariant curves. Furthermore there may be exponential effects beyond all orders (such as arise in chaotic flows) which will simply not be detected by this approach.

3.2.2 Symplectic Runge-Kutta methods

It is fortunate that an important (accurate and A-stable) class of Runge-Kutta methods, namely the Gauss-Legendre methods (also known as Kuntzmann and Butcher methods), also turn out to be symplectic methods. The implicit mid-point rule considered earlier is a member of this class. Whilst this gives a very useful class of methods applicable to a wide class of general Hamiltonian problems, the resulting methods are highly implicit and for specific problems splitting methods, which may be explicit, may be preferable. To explain these Runge-Kutta methods, in this sub-section we review the results in [129]. Consider a standard s-stage Runge-Kutta method with Butcher tableau

$$\begin{array}{c|c} c & A \\ \hline & b^T \end{array}$$

where $c, b \in \mathbb{R}^s$ and $A \equiv (a_{i,j}) \in \mathbb{R}^{s \times s}$. The following result (Lasagni [89], Sanz-Serna [127] and Suris [138], see also [129]) gives a complete characterisation of all symplectic Runge-Kutta methods

THEOREM *A necessary and sufficient condition for a Runge-Kutta method to be symplectic is that for all* $1 \leqslant i, j \leqslant s$

$$b_i a_{ij} + b_j a_{ji} - b_i b_j = 0. \tag{10}$$

Note that the necessity of condition (10) requires that the method have no redundant stages, i.e. the method be irreducible, see [129]. We can immediately see that if the matrix A was lower triangular then (10) would imply that $b_i = 0$, $\forall i$, this obviously contradicts the consistency condition $\sum b_i = 1$, and therefore we can conclude that symplectic Runge-Kutta methods must be implicit. This is not an ideal state of affairs, however we shall see presently that in a number of very important situations methods which are both symplectic and explicit may be found.

The proof of this result is a consequence of the fact that any method satisfying (10) automatically preserves any *quadratic* invariant of the solution of the equation to which it is applied (a point we return to in Section 4). In other words, any invariant of the form

$$u^T A u$$

for an appropriate matrix A. The symplecticity condition is a quadratic invariant of the variational equation

$$\psi' = J^{-1} H''(\mathbf{u}) \psi$$

associated with the Hamiltonian equation. Thus applying the Runge-Kutta method to this derived equation gives the desired result, see [16].

All Gauss-Legendre methods have this property (and the implicit mid-point rule is simply the lowest order method of this form). For example the second (implicit mid-point) and fourth order Gauss-Legendre methods have the form

$$\begin{array}{c|c} \frac{1}{2} & \frac{1}{2} \\ \hline & 1 \end{array} \qquad \begin{array}{c|cc} \frac{3-\sqrt{3}}{6} & \frac{1}{4} & \frac{3-2\sqrt{3}}{12} \\ \frac{3+\sqrt{3}}{6} & \frac{3+2\sqrt{3}}{12} & \frac{1}{4} \\ \hline & \frac{1}{2} & \frac{1}{2} \end{array}$$

and condition (10) can be seen to be satisfied for both methods. The fact that all Gauss-Legendre are symplectic implies that we can derive symplectic methods of arbitrarily high order.

The natural partitioning present in the Hamiltonian problem (2) suggests that we may think about using different numerical methods for different components of the problem. We shall now consider *partitioned Runge-Kutta* methods, where for our problem at hand we integrate the p components of (2) with the Runge-Kutta method given by the first Butcher tableau below, and the q components of (2) with the second tableau below.

$$\begin{array}{c|c} c & A \\ \hline & b^T \end{array} \qquad \begin{array}{c|c} \tilde{c} & \tilde{A} \\ \hline & \tilde{b}^T \end{array}$$

As we have done for symplectic Runge-Kutta methods we may now classify symplectic partitioned Runge-Kutta methods with the following result.

THEOREM *A necessary and sufficient condition for a partitioned Runge-Kutta method to be symplectic is that for all* $1 \leqslant i, j \leqslant s$

$$b_i = \tilde{b}_i, \quad b_i \tilde{a}_{ij} + \tilde{b}_j a_{ji} - b_i \tilde{b}_j = 0. \tag{11}$$

The same comment as above about the need for irreducibility of the methods applies here, for more details see [1]. For the special case of problems where the Hamiltonian takes the separable form $H(p, q) = T(p) + V(q)$, only the second part of (11) is required for symplecticity.

An example of such a method is given by Ruth's third-order method [124] — one of the first symplectic methods appearing in the literature, it has the tableau

$$\begin{array}{c|ccc} & 7/24 & 0 & 0 \\ c & 7/24 & 3/4 & 0 \\ & 7/24 & 3/4 & -1/24 \\ \hline & 7/24 & 3/4 & -1/24 \end{array} \qquad \begin{array}{c|ccc} & 0 & 0 & 0 \\ \tilde{c} & 2/3 & 0 & 0 \\ & 2/3 & -2/3 & 0 \\ \hline & 2/3 & -2/3 & 1 \end{array}$$

For problems with a separable Hamiltonian (e.g. in celestial mechanics) the functional T often takes the special form $T(p) = p^T M^{-1} p/2$, with M a constant symmetric invertible matrix (see the examples later). In this case Hamilton's equations (2) have the equivalent second order form

$$\ddot{q} = -M^{-1}V_q.$$

The fact that this special form for T arises often can now be seen to be a consequence of Newton's second law. The form that Hamilton's equations now take suggests the use of *Runge-Kutta-Nyström* methods, see [73]. The tableau here is of the form

$$\begin{array}{c|c} c & A \\ \hline & b^T \\ \hline & B^T \end{array}$$

which corresponds to the method given by

$$\begin{aligned} Q_i &= q_n + c_i h M^{-1} p_n - h^2 \sum_{j=1}^{s} a_{ij} M^{-1} V_q(Q_j), \\ p_{n+1} &= p_n - h \sum_{i=1}^{s} B_i V_q(Q_i), \\ q_{n+1} &= q_n + h M^{-1} p_n - h^2 \sum_{i=1}^{s} b_i M^{-1} V_q(Q_i). \end{aligned}$$

We now state a result giving conditions for a Runge-Kutta-Nyström method to be symplectic, see [117].

THEOREM *The s-stage Runge-Kutta-Nyström given by the above tableau is symplectic if for all $1 \leqslant i, j \leqslant s$*

$$b_i = B_i(1 - c_i), \quad B_i(b_j - a_{ij}) = B_j(b_i - a_{ji}) \tag{12}$$

3.2.3 Splitting and composition methods

These methods exploit natural decompositions of the problem, and particular of the Hamiltonian and have been used with very great success in studies of the solar system and of molecular dynamics [90, 131]. Much recent work in this field is due to Yoshida and McLachlan. The main idea behind splitting methods is to decompose the discrete flow Ψ_h as a composition of simpler flows

$$\Psi_h = \Psi_{1,h} \circ \Psi_{2,h} \circ \Psi_{3,h} \ldots,$$

where each of the sub-flows is chosen such that each represents a simpler integration (perhaps even explicit) of the original. A geometrical perspective on this approach is to find useful geometrical properties of each of the individual operations which are preserved under combination. Symplecticity is just such a property, but we often seek to preserve reversibility and other structures.

Suppose that a differential equation takes the form

$$\frac{d\mathbf{u}}{dt} = \mathbf{f} = \mathbf{f}_1 + \mathbf{f}_2.$$

Here the functions $\mathbf{f}_1$ and $\mathbf{f}_2$ may well represent different physical processes in which case there is a natural decomposition of the problem (say into terms related to kinetic and potential energy).

The most direct form of splitting methods decompose this equation into the two problems

$$\frac{d\mathbf{u}_1}{dt} = \mathbf{f}_1 \quad \text{and} \quad \frac{d\mathbf{u}_2}{dt} = \mathbf{f}_2$$

chosen such that these two problems can be integrated *exactly in closed form* to give explicitly computable flows $\Psi_1(t)$ and $\Psi_2(t)$. We denote by $\Psi_{i,h}$ the result of applying the corresponding continuous flows $\psi_i(t)$ over a time h. A simple (first-order) splitting is then given by the *Lie-Trotterr formula*

$$\Psi_h = \Psi_{1,h} \circ \Psi_{2,h}. \tag{13}$$

Suppose that the original problem has Hamiltonian $H = H_1 + H_2$, then as observed earlier this is the composition of two problems with respective Hamiltonians H_1 and H_2. The differential equation corresponding to each Hamiltonian leads to an evolutionary map $\psi_i(t)$ of the form described above. By definition, as ψ_i is the exact solution of a Hamiltonian system, it must follow that each operator $\Psi_{i,h}$ is a symplectic map. Hence, by Lemma 3.1, the combined map must also be symplectic. Thus operator splitting in this context automatically generates a symplectic map.

An interesting example of such a procedure in the context of a partial differential equation, are the so called *equilibrium models* for calculating advective and reactive chemical flows of the form

$$u_t + a u_x = -g(u, v), \quad v_t = g(u, v).$$

To apply a splitting method to this system, an advective step without reaction is determined exactly by using the method of characteristics applied to the total concentration $c = u + v$. This step is then followed by a reactive step without advection. These models are widely used in the chemical industry and a numerical analysis of splitting methods for advection problems is given in [91]. Indeed, procedures of this form are widely used in any process where there are clearly two interacting components and each component is treated separately, see for example [130].

The Lie-Trotter splitting (13) introduces local errors proportional to h^2 at each step and a more accurate decomposition is the *Strang splitting* given by

$$\Psi_h = \Psi_{1,h/2} \circ \Psi_{2,h} \circ \Psi_{1,h/2}. \tag{14}$$

This splitting method has a local error proportional to h^3.

A proof of these error estimates obtained by using the Baker-Campbell-Hausdorff formula will be given presently.

Example 1. Suppose that a Hamiltonian system has a Hamiltonian which can be expressed as a combination of a kinetic energy and a potential energy term as follows

$$H(\mathbf{u}) = H_1(\mathbf{u}) + H_2(\mathbf{u}) \equiv T(\mathbf{p}) + V(\mathbf{q}).$$

so that

$$\frac{d\mathbf{p}}{dt} = -H_{2,q}(\mathbf{q}), \quad \frac{d\mathbf{q}}{dt} = H_{1,p}(\mathbf{p}).$$

This splitting of H is usually referred to as a separable or P-Q splitting. We immediately have that

$$\Psi_{1,h} = I - hH_{2,q} \quad \text{and} \quad \Psi_{2,h} = I + hH_{1,p}$$

where I represents the identity mapping.

Applying the Lie-Trotter formula directly to this splitting gives the *symplectic Euler method* (SE)

$$\mathbf{p}_{n+1} = \mathbf{p}_n - hH_{2,q}(\mathbf{q}_n), \quad \text{and} \quad \mathbf{q}_{n+1} = \mathbf{q}_n + hH_{1,p}(\mathbf{p}_{n+1}). \tag{15}$$

A more sophisticated splitting method for this problem based upon the Strang splitting is

$$\mathbf{p}_{n+1/2} = \mathbf{p}_n - \frac{h}{2}H_{2,q}(\mathbf{q}_n), \quad \mathbf{q}_{n+1} = \mathbf{q}_n + hH_{1,p}(\mathbf{p}_{n+1/2}), \quad \mathbf{p}_{n+1} = \mathbf{p}_{n+1/2} - \frac{h}{2}H_{2,q}(\mathbf{q}_{n+1}).$$

For systems with such separable Hamiltonians we may combine subsequent Strang splittings (as described above) to give (after relabelling) the celebrated *Störmer-Verlet method* (SV)

$$\begin{aligned} \mathbf{q}^{n+1/2} &= \mathbf{q}^{n-1/2} + hT_p(\mathbf{p}^n), \\ \mathbf{p}^{n+1} &= \mathbf{p}^n - hV_q(\mathbf{q}^{n+1/2}). \end{aligned}$$

The same method is obtained by apply the two-stage Lobatto IIIA-B Runge-Kutta pair to this separable case (see [69]).

A form of this method appeared in the molecular dynamics literature [143] many years before anyone realised that its remarkable success in that field was due to the fact that it was in fact a very efficient symplectic method.

Example 2 Yoshida splittings.

The Strang splitting has the desirable property that it is symmetric so that $\Psi_h^{-1} = \Psi_{-h}$. By combining symmetric splittings, Yoshida [146] derived a series of remarkable high order methods. Given a symmetric second order *base method* $\Psi_h^{(2)}$, for example in [146] Yoshida considers the case where the base method is given by the Strang splitting (14). Yoshida then constructs the method

$$\Psi_h^{(4)} = \Psi_{x_1 h}^{(2)} \circ \Psi_{x_0 h}^{(2)} \circ \Psi_{x_1 h}^{(2)}.$$

He proved that $\Psi_h^{(4)}$ is indeed a fourth-order symmetric method if the weights are chosen as

$$x_0 = -\frac{2^{1/3}}{2 - 2^{1/3}}, \quad x_1 = \frac{1}{2 - 2^{1/3}}.$$

If the problem being considered is Hamiltonian and the second-order method is symplectic then our newly constructed fourth-order method will also be symplectic. This procedure can be extended and generalized as follows. Given a symmetric integrator $\Psi_h^{(2n)}$ of order $2n$, for example when $n = 1$ we are simply restating the above construction and when $n = 2$ we may take the method constructed above. The method given by the composition

$$\Psi_h^{(2n+2)} = \Psi_{x_1 h}^{(2n)} \circ \Psi_{x_0 h}^{(2n)} \circ \Psi_{x_1 h}^{(2n)}$$

will be a symmetric method of order $2n+2$ if the weights are chosen as

$$x_0 = -\frac{2^{1/(2n+1)}}{2-2^{1/(2n+1)}}, \quad x_1 = \frac{1}{2-2^{1/(2n+1)}}.$$

Note: When considering partial differential equations McLachlan [103] uses alternative splittings of the Hamiltonian into linear and nonlinear components. We return to this decomposition presently.

3.3 Examples of applications of symplectic integrators

Before looking at the error analysis of these various symplectic methods we consider their application to four examples, the harmonic oscillator, the pendulum, Molecular and stellar dynamics

Example 1 **The Harmonic oscillator.**

This well studied problem has a separable Hamiltonian of the form

$$H(p,q) = \frac{p^2}{2} + \frac{q^2}{2},$$

and has solutions which are circles in the (p,q) phase space. The associated differential equations are

$$\frac{dq}{dt} = p, \quad \frac{dp}{dt} = -q.$$

Consider now the closed curve

$$\Gamma \equiv p^2 + q^2 = C^2,$$

the action of the solution operator of the differential equation is to map this curve into itself (conserving the area πC^2 of the enclosed region). The standard *forward Euler method* applied to this system gives the scheme

$$p_{n+1} = p_n - hq_n, \quad q_{n+1} = q_n + hp_n,$$

so that Ψ_h is the operator given by

$$\Psi_h \mathbf{v} = \begin{pmatrix} 1 & -h \\ h & 1 \end{pmatrix} \mathbf{v}, \quad \text{with} \quad \det(\Psi_h) = 1 + h^2.$$

It is easy to see that in this case, Γ evolves through the action of the discrete map Ψ_h to the new circle given by

$$p_{n+1}^2 + q_{n+1}^2 = C^2(1+h^2)$$

and the area enclosed within the discrete evolution of Γ has increased by a factor of $1+h^2$. Periodic orbits are not preserved by the forward Euler method — indeed all such discrete orbits spiral to infinity. Similarly, a discretisation using the backward Euler method leads to trajectories that spiral towards the origin.

Consider now the *symplectic Euler method* applied to this example. This gives rise to the discrete map

$$p_{n+1} = p_n - hq_n, \quad q_{n+1} = q_n + h(p_n - hq_n) = (1-h^2)q_n + hp_n.$$

The discrete evolutionary operator is then simply the matrix

$$\Psi_h \begin{pmatrix} p \\ q \end{pmatrix} = \begin{pmatrix} 1 & -h \\ h & 1-h^2 \end{pmatrix} \begin{pmatrix} p \\ q \end{pmatrix}$$

which can easily be checked to be symplectic. For example $\det(\Psi_h) = 1$. The circle Γ is now mapped to the ellipse

$$(1-h^2+h^4)p_{n+1}^2 - 2h^3 p_{n+1}q_{n+1} + (1+h^2)q_{n+1}^2 = C^2$$

which has the same enclosed area. The symplectic Euler map is not symmetric in time so that

$$\psi_h^{-1} \neq \psi_{-h}.$$

Observe that the symmetry of the circle has been destroyed through the application of this mapping.

It is also easy to see that if

$$A = \begin{pmatrix} 1 & -\frac{h}{2} \\ -\frac{h}{2} & 1 \end{pmatrix}$$

then

$$\Psi_h^T A \Psi_h = A.$$

Consequently, invariant curves of the map Ψ_h are given by the solutions of

$$\hat{H}(p_n, q_n) \equiv p_n^2 + q_n^2 - hp_n q_n = C^2,$$

which are ellipses with major and minor axes of lengths $C(1 + h/2)$ and $C(1 - h/2)$ respectively. Observe that the modified Hamiltonian function $\hat{H}$ is an $\mathcal{O}(h)$ perturbation of the original Hamiltonian. Thus the symplectic Euler method preserves the qualitative features of bounded solutions and periodic orbits lost by both the forward and backward Euler methods.

In figure 1 we compare the original periodic orbit with the perturbed periodic orbit in the case of $h = 0.25$, with starting values $p = 0, q = 1$.

Next consider the *Störmer-Verlet* method. This gives the discrete map

$$p_{n+1/2} = p_n - hq_n/2, \quad q_{n+1} = q_n + h(p_n - hq_n/2),$$

$$p_{n+1} = p_{n+1/2} - \frac{h}{2}\left(q_n + h\left(p_n - \frac{h}{2}q_n\right)\right).$$

The discrete evolutionary operator ψ_h is now the symplectic matrix

$$\Psi_h \mathbf{v} = \begin{pmatrix} 1-h^2/2 & -h+h^3/4 \\ h & 1-h^2/2 \end{pmatrix} \mathbf{v}.$$

The curve Γ is to order h^2 mapped to a circle of the same radius. The Störmer-Verlet method preserves the symmetry of the circle to this order, and indeed is also symmetric in time so that $\psi^{-1} = \psi_{-h}$.

Finally we consider the implicit mid-point rule. For this we have

$$C \begin{pmatrix} p_{n+1} \\ q_{n+1} \end{pmatrix} = C^T \begin{pmatrix} p_n \\ q_n \end{pmatrix},$$

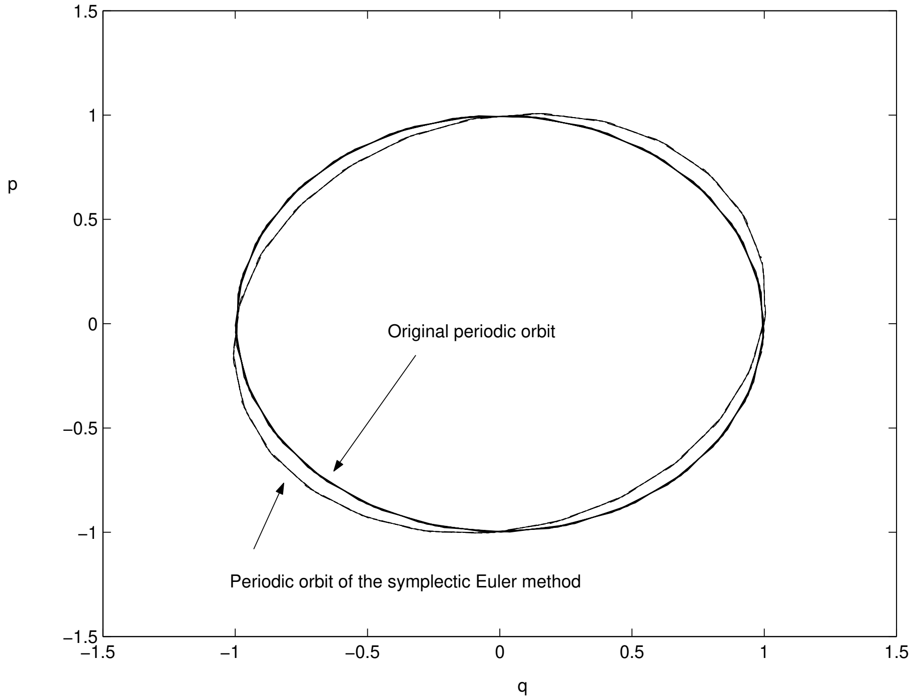

Figure 1: *Periodic orbit of the symplectic Euler method compared with the original periodic orbit.*

where

$$C = \begin{pmatrix} 1 & \frac{h}{2} \\ -\frac{h}{2} & 1 \end{pmatrix}.$$

Observe that $CC^T = \left(1 + h^2/4\right) I$. The evolution operator is then simply

$$\Psi_h = C^{-1} C^T.$$

Observe further that if $\mathbf{U_n} = (p_n, q_n)^T$ then

$$\left(1 + h^2/4\right) \mathbf{U}_{n+1}^T \mathbf{U}_{n+1} = \mathbf{U}_{n+1}^T C^T C \mathbf{U}_{n+1} = \mathbf{U}_n^T C C^T \mathbf{U}_n = \left(1 + h^2/4\right) \mathbf{U}_n^T \mathbf{U}_n.$$

Hence the quadratic invariant $\mathbf{U}_n^T \mathbf{U}_n$ is exactly preserved by this method. This feature is shared by all symplectic Runge-Kutta methods.

Figure 2 demonstrates the effect of applying some of these methods to the set Γ.

Example 2 **The pendulum**

The simple pendulum is a Hamiltonian system, the solution of which by symplectic methods is discussed in [147] and [73]. For small values of p and q it reduces to the Harmonic oscillator and it has periodic orbits which are close to circles. For larger values the periodic orbits evolve towards heteroclinic connexions. For this problem we have the Hamiltonian

$$H(p, q) = \frac{1}{2} p^2 + \cos(q),$$

and associated differential equations

$$\frac{dq}{dt} = p, \quad \frac{dp}{dt} = -\sin(q).$$

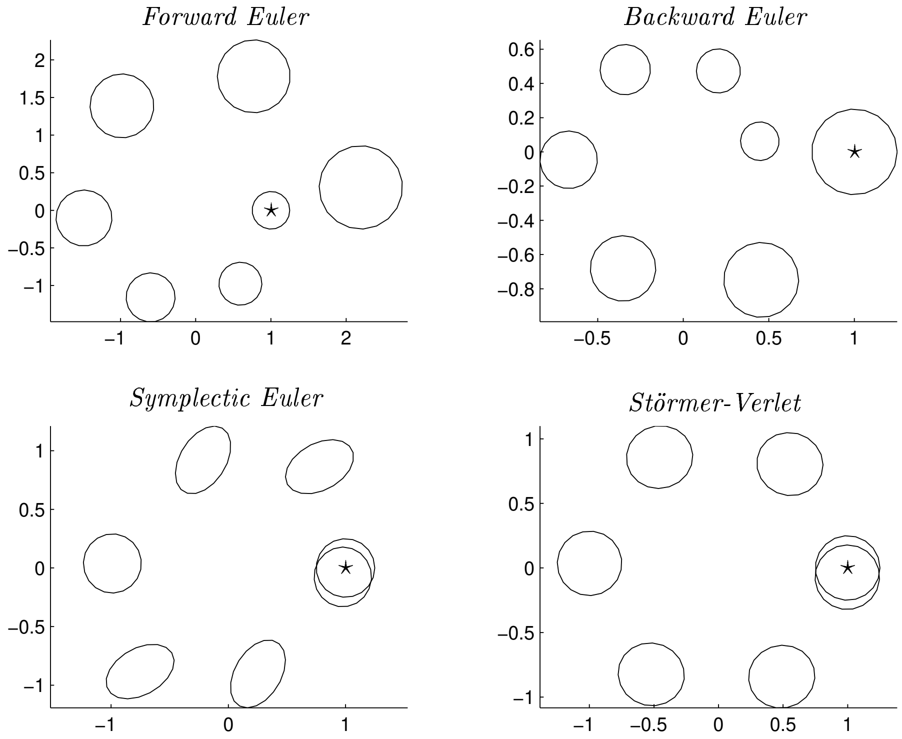

Figure 2: *Dynamics of four numerical methods applied to the harmonic oscillator problem. Forward and Backward Euler both have time step $2\pi/24$ and symplectic Euler and Störmer-Verlet have time step $2\pi/12$. The $\star$ is placed in the centre of the circle of initial conditions.*

As above we apply the symplectic Euler method to the system to give the discrete system

$$p_{n+1} = p_n - h \sin q_n, \quad q_{n+1} = q_n + hp_{n+1}.$$

In figure 3 we consider applying this method for a variety of values of h. For small values much of the original structure of the phase space is preserved. Observe the persistence of the periodic orbits, now distorted into ellipses as in the last example. For larger values of h this structure starts to break down with periodic orbits breaking up into invariant tori. For still larger values of h chaotic behaviour is observed. All of these figures are very similar to those of the 'standard map' in Hamiltonian dynamics [94] with dynamics determined by the results of the KAM theorem.

In this case the modified equation analysis presented in the next section predicts that to leading order the symplectic Euler method has the same dynamics as a Hamiltonian system with the modified Hamiltonian

$$\tilde{H} = \frac{p^2}{2} - \cos q - \frac{h}{2} p \sin(q) + \frac{h^2}{12}(\sin^2(p) + p^2 \cos(q)) - \frac{h^3}{12} p \cos(q) \sin(q) + \mathcal{O}(h^4),$$

and it is level sets of this that are also plotted in figure 3. Observe that for small p and q this reduces to the modified Hamiltonian of the harmonic oscillator.

Example 3 **The many body problem**

The classical equations for a system of $N > 1$ particles (or heavenly bodies) interacting via a potential force V can be written in Hamiltonian form (2), with the Hamiltonian

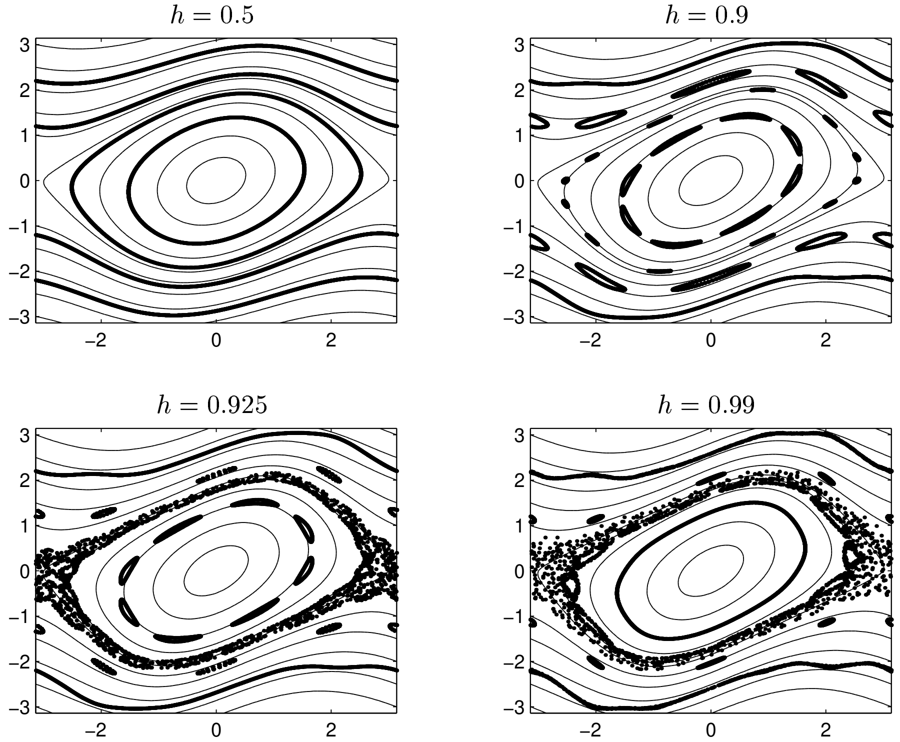

Figure 3: *Dynamics of the symplectic Euler method applied to the pendulum problem.*

function given by

$$H(\mathbf{p},\mathbf{q}) = \frac{1}{2}\sum_{i=1}^{N} m_i^{-1}\mathbf{p}_i^T\mathbf{p}_i + \sum_{i<j} V_{i,j}\left(\|\mathbf{q}_i - \mathbf{q}_j\|\right). \tag{16}$$

Here the m_i represent masses of objects with positions and momenta $q_i, p_i \in \mathbb{R}^3$. $V(r)$ represents some potential function, for example r^{-1} for gravitational problems and the Lennard-Jones potential $r^{-12} - r^{-6}$ for problems in molecular dynamics [3]. Here $\|\cdot\|$ is the Euclidean distance. We would like to integrate these equations for long times where many near collisions (and hence large forces and velocities) may occur, whilst conserving the energy H and the total angular momentum of the system $L = \sum_{i=1}^{N} p_i \times q_i$. In practice L is relatively easy to conserve as it is a quadratic invariant.

As before we shall consider here three numerical schemes. The simplest possible is the forward (explicit) Euler method (FE)

$$\begin{aligned}\mathbf{p}^{n+1} &= \mathbf{p}^n - hH_q(\mathbf{p}^n,\mathbf{q}^n),\\ \mathbf{q}^{n+1} &= \mathbf{q}^n + hH_p(\mathbf{p}^n,\mathbf{q}^n).\end{aligned}$$

The Hamiltonian is again separable, so we may use the symplectic Euler method (SE)

$$\begin{aligned}\mathbf{p}^{n+1} &= \mathbf{p}^{n+1} - hH_q(\mathbf{p}^n,\mathbf{q}^n),\\ \mathbf{q}^{n+1} &= \mathbf{q}^n + hH_p(\mathbf{p}^{n+1},\mathbf{q}^n).\end{aligned}$$

and the Störmer-Verlet method.

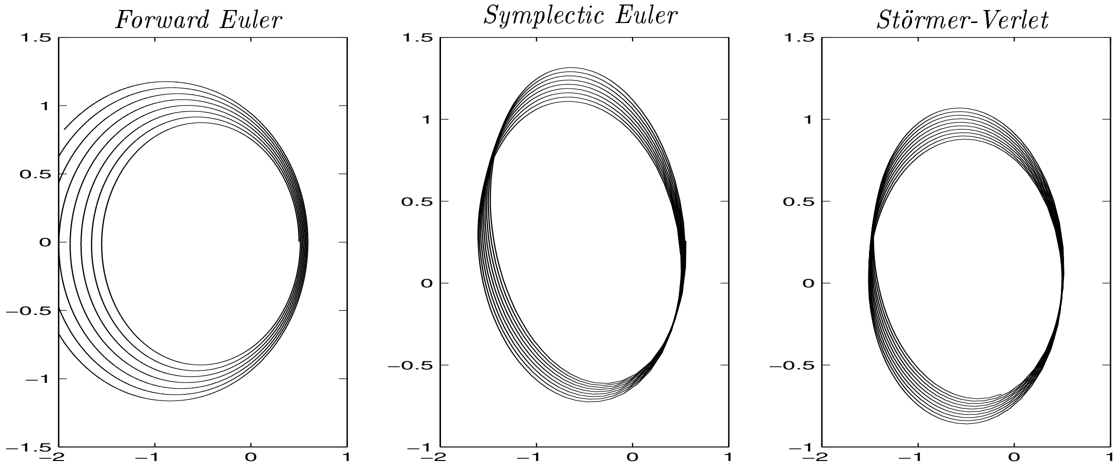

Figure 4: *Kepler trajectories with eccentricity of 0.5 computed with the forward Euler (h=0.002), symplectic Euler (h=0.1) and Störmer-Verlet (h=0.1) methods.*

Example 4 **Stellar dynamics and the Kepler problem**

The Kepler (or two-body) problem, describing the motion under gravity of a planet around large stellar mass is a special case of example 3 which may be written as a Hamiltonian system with

$$H(p_1, p_2, q_1, q_2) = \frac{1}{2}(p_1^2 + p_2^2) - \frac{a}{\sqrt{q_1^2 + q_2^2}}, \tag{17}$$

so that $V(r) = r^{-1}$ in (16). The exact dynamics of this system exactly preserve H which represents total energy, as well as the angular momentum given by

$$L = q_1 p_2 - q_2 p_1.$$

In addition, the problem has rotational, time-reversal and scaling symmetries, which we shall consider presently. In figure 4 we show some trajectories computed with the three methods introduced above. For the initial data used here the exact solution is an ellipse of eccentricity $e = 0.5$ with the origin at one focus. Notice that the forward Euler trajectory spirals outwards (in a similar manner to behaviour observed for the Harmonic oscillator) and so does not accurately reproduce the periodic solution to this problem. The symplectic Euler does better in this respect, the numerical solution lies much closer to an ellipse, however it exhibits clockwise precession (the ellipse rotates) about the origin.

In figure 5 we consider both the growth in the trajectory error (computed using the Euclidean norm) and the conservation (or lack of it) of Hamiltonian (or energy) for our methods. The forward Euler method acts to increase the energy of the system leading to a monotonic growth in the Hamiltonian. In contrast the Hamiltonian whilst not constant for the symplectic methods exhibits a bounded error. The symplectic methods have *linear* trajectory error growth as opposed to the *quadratic* growth observed in the non-symplectic methods. The various peaks in these graphs correspond to close approaches between the planet and the star.

These results are summarized in the following table, given in [69]. Note that both the symplectic Euler and Störmer-Verlet methods preserve the quadratic invariant of the angular momentum exactly.

Method	Global error	Error in H	Error in L
FE	$\mathcal{O}(t^2 h)$	$\mathcal{O}(th)$	$\mathcal{O}(th)$
SE	$\mathcal{O}(th)$	$\mathcal{O}(h)$	0
SV	$\mathcal{O}(th^2)$	$\mathcal{O}(h^2)$	0

See [69, 129] for similar experiments and discussions, as well as proofs and explanations of the apparent superiority of symplectic over non-symplectic methods.

More sophisticated methods for the N-body problem have been developed in the astrophysics literature. These methods have largely been based upon splitting the problem into a collection of independent two-body problems plus a potential term accounting for mutual planetary interactions, as well as careful integration of certain parts of close approach orbits. They have been used to compute the evolution of the solar system for many millions of years. In particular Sussman and Wisdom [139] computed the evolution of the nine planets for 100 million years using a time step of 7.2 days. They found that the solar system as a whole is chaotic with a Lyapunov exponent of 4 million years, and in particular they verified earlier work by showing that the motion of Pluto is chaotic with a Lyapunov exponent of 10 to 20 million years. Another calculation is presented by Wisdom and Holman in [145], they calculated the evolution of the outer five planets for 1.1 billion years with a time step of 1 year and produced similar results. A possible disagreement between the chaos exhibited in numerical simulations and classical stability theories for the solar system is discussed and resolved by Murray and Holman in [115].

Note that for problems with close approaches, and hence large forces and velocities, some form of adaptivity often needs to be employed and we discuss this later in the section on temporal adaptivity and singularities.

3.4 Error analysis - a brief overview

We now give a brief overview of the methods used to analyse the behaviour of symplectic and splitting methods. These ideas are covered in much greater detail elsewhere and for the most part we refer the reader to this literature.

3.4.1 The backward error analysis of symplectic methods

As described earlier, backward error analysis (or modified equation analysis) is the procedure for analysing a numerical method by finding a modified differential equation which has a flow which approximates the discrete flow better than the original equation. The modified equations can be constructed by using a simple iterative procedure outlined in Hairer [72]. Many deep theorems related to backward error analysis are given in [121]. This is a very rich field of analysis which we only touch on here, for a review and a discussion of its applicability to various problems see Griffiths and Sanz-Serna [66].

We now give a more detailed derivation of the standard backward error formula. Suppose that $\mathbf{u}' = \mathbf{f}(\mathbf{u})$ is the original equation with flow $\psi(t)$ and that $\hat{\mathbf{u}}' = \hat{\mathbf{f}}(\hat{\mathbf{u}})$ is the modified equation. We will suppose that for small h we can develop an asymptotic series for $\hat{\mathbf{f}}$ of the form

$$\hat{\mathbf{f}}(\mathbf{u}) = \mathbf{f}(\mathbf{u}) + h\mathbf{f}_1(\mathbf{u}) + h^2\mathbf{f}_2(\mathbf{u}) + \dots .$$

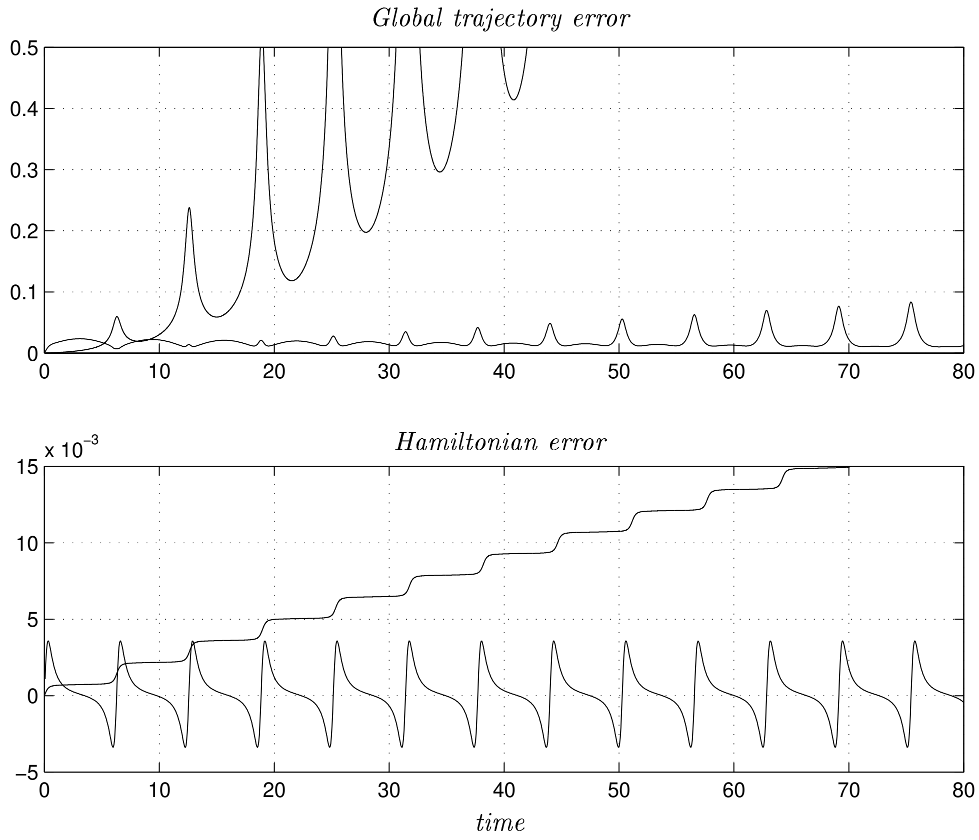

Figure 5: *Global trajectory error measured with Euclidean norm in four-dimensional phase space, and error in Hamiltonian for the Kepler problem with eccentricity* $e = 0.5$*. Methods shown are the forward Euler* ($h = 0.0001$) *lying in general above symplectic Euler* ($h = 0.005$)*.*

Assume that at some initial time $\mathbf{u} = \hat{\mathbf{u}}$. Using a simple Taylor series we can expand the solution of the modified ordinary differential equation so that

$$\hat{\mathbf{u}}(t+h) = \mathbf{u} + h(\mathbf{f} + h\mathbf{f}_2 + h^2\mathbf{f}_3 + \ldots) + \frac{h^2}{2}(\mathbf{f}' + h\mathbf{f}' + \ldots)(\mathbf{f} + \ldots) + \ldots.$$

We want to compare this solution with the action of the discrete operator Ψ_h. In general, for a consistent scheme, there will be functions $\mathbf{d}_k(h)$ so that

$$\Psi_h \mathbf{u} = \mathbf{u} + h\mathbf{f}(\mathbf{u}) + h^2\mathbf{d}_2(\mathbf{u}) + h^3\mathbf{d}_3(\mathbf{u}) + \ldots.$$

We can now equate the above two expressions. Taking terms at orders h^2 and h^3 gives

$$\mathbf{f}_2 = \mathbf{d}_2 - \frac{1}{2}\mathbf{f}'\mathbf{f} \quad \text{and} \quad \mathbf{f_3} = \mathbf{d}_3 - \frac{1}{6}\left(\mathbf{f}''(\mathbf{f},\mathbf{f})(\mathbf{u}) + \mathbf{f}'\mathbf{f}'\mathbf{f}(\mathbf{u})\right) - \frac{1}{2}\left(\mathbf{f}'\mathbf{f}_2(\mathbf{u}) + \mathbf{f}_2'\mathbf{f}(\mathbf{u})\right).$$

This procedure can be continued to all orders and a Maple program to do this is described in [72]. In general it gives an asymptotic rather than a convergent series, which diverges if all terms are summed, but which can be optimally truncated to give errors which are (potentially exponentially) small in h.

An example given in [69] and [66] is the blow-up or nonlinear heat equation. We consider this here as an example of backward error analysis and return to it later for a fuller discussion of the application of scale invariant adaptive methods. The blow-up equation is given by

$$u' = u^2, \quad u(0) = 1. \tag{18}$$

Significantly, this equation has singular solution $u(t) = 1/(1-t)$ which becomes infinite as $t \to 1$.

When approximated by the Forward Euler method this problem has a discrete solution which is bounded for all time and does not in any way reproduce the singular behaviour. This will be true of any explicit method when applied to this problem. (In our later discussion on scale invariant methods we will show how this property can be recovered). In this case we have $\mathbf{d}_2 = \mathbf{d}_3 = \ldots = 0$. Applying backward error analysis, the modified equation for (18) under this discretisation then takes the form

$$\hat{f}(u) = u^2 - hu^3 + (3/2)h^2u^4 - (8/3)h^3u^5 + \ldots.$$

The modified system does not admit singular solutions and is qualitatively much closer to the solution of the Forward Euler method than the original.

A key feature underlying the analytical approach of backward error analysis is the question of whether qualitative features of the underlying equation are reflected in the modified equation.

Hairer [69] uses an inductive argument to show that if the underlying equation is Hamiltonian and the method is symplectic then the modified system constructed as above is also Hamiltonian. In particular there are smooth functions H_j such that

$$\mathbf{f}_j(\mathbf{u}) = J^{-1}\nabla H_j(\mathbf{u}).$$

For the Harmonic oscillator problem considered earlier, we have already seen that to leading order we have

$$H(\mathbf{u}) = \frac{1}{2}\left(p^2 + q^2\right) \quad \text{and} \quad H_1(\mathbf{u}) = -\frac{1}{2}pq.$$

It has also been shown that if the underlying system is reversible in time and a symmetric method (eg. Störmer-Verlet) is used to solve it, then the resulting modified system is also reversible [74]. In addition Reich [121] proves that if f lies in a Lie algebra $\mathfrak{g}$ and the numerical method defines a discrete flow remaining within the associated Lie group G (see the section on Lie group methods later), then the $\hat{f}$ associated with the modified system also lies in $\mathfrak{g}$.

Reich [121] and many others have presented conditions for the error between the modified equation, the discrete solution and the underlying differential equation. This error depends upon the truncation point of the series used to generate the modified equations. This is, in general, an *asymptotic* series which diverges if continued as an expansion with an infinite number of terms, but which has superconvergent properties if truncated optimally. (See similar results for the study of asymptotic series in general which also demonstrate exponential convergence when optimally truncated [34]). In particular, it can be shown [12] that an optimally truncated modified equation has an exponentially small error such that if ψ_h is the discrete flow and $\varphi_{N,h}$ the flow of the modified equation when truncated at the point N then there is a γ which depends on the method, a constant h^* and an optimal $N(h)$ so that

$$\|\Psi_h - \varphi_{N,h}\| < h\gamma e^{-h^*/h}.$$

If the underlying system is Hamiltonian, this result extends to the theorem that the discrete Hamiltonian closely approximates the (constant) Hamiltonian of the modified problem over exponentially long time intervals. Indeed, in this case

$$\hat{H}(y_n) = \hat{H}(y_0) + \mathcal{O}(e^{-h^*/2h}),$$

so that although the actual Hamiltonian is not conserved a modified form of it is, to a very good approximation, conserved over very long time intervals. This explains the results described in the calculations presented for the Kepler problem.

The pendulum equation discussed in the examples above has Hamiltonian

$$H = \frac{p^2}{2} - \cos(q).$$

When using the implicit mid-point rule the modified Hamiltonian is [69] given by

$$\hat{H} = \frac{p^2}{2} - \cos(q) + \frac{h^2}{48}\left(\cos(2q) - 2p^2\cos(q)\right).$$

For *sufficiently small* values of h the modified Hamiltonian $\hat{H}$ is extremely well conserved. As we have seen from the earlier experiments, this agreement breaks down (with a consequent loss of integrability) when h takes larger values.

3.4.2 An analysis of Splitting methods

The basic tool for analysis of splitting methods is the celebrated Baker-Campbell-Hausdorff (BCH) formula [142] which allows an analysis of splitting methods to be made in terms of the (lack of) commutativity of the operators associated with the splitting.

To motivate this procedure, consider the system

$$\frac{d\mathbf{u}}{dt} = \mathbf{f}(\mathbf{u}) = \mathbf{f}_1 + \mathbf{f}_2$$

such that the two systems $d\mathbf{u_i}/dt = \mathbf{f}_i$ have respective flows ψ_t^i (which may be calculated exactly or approximately using a discrete (high order) method). Associated with each such flow is the *Lie derivative* D_i defined by its action on the function F so that

$$\frac{d}{dt}F(\mathbf{u}_i(t)) = (D_i F)(\mathbf{u}_i(t)) = F'(\mathbf{u}_i)f_i(\mathbf{u}_i)$$

where $\mathbf{u}_i(t)$ is the solution of the associated differential equation. Then if $d\mathbf{u_i}/dt = \mathbf{f_i}(\mathbf{u_i})$ we have $d\mathbf{u}_i/dt = D_i\mathbf{u}_i(t)$, $d^2\mathbf{u}_i/dt^2 = D_i^2\mathbf{u}_i(t)$, etc. As a consequence we may express the flow φ_t^i as an exponential of the form

$$\varphi_t^i\mathbf{u}_0 = \exp(tD_i)\mathbf{u}_0 = \sum_n \frac{t^n D_i^n}{n!}\mathbf{u}_0,$$

and compose two flows in the manner

$$\left(\varphi_t^1 \circ \varphi_s^2\right) u_0 = \exp(tD_1)\exp(sD_2)\mathbf{u}_0.$$

Thus we see how a flow can be thought of in terms of the exponential of an operator. Now suppose that X and Y are general operators with associated exponentials

$$\exp(hX) = I + hX + \frac{h^2}{2}X^2 + \ldots, \quad \exp(hY) = I + hY + \frac{h^2}{2}Y^2 + \ldots,$$

then the combined exponential (applying one operator and then the next) is given by

$$\exp(hX)\exp(hY),$$

whereas the simultaneous action of the two is given by

$$\exp(hX + hY).$$

If X and Y commute then these two operations are the same, however in general they are different, and the BCH formula gives a precise description of this difference.

THEOREM *For the operators hX and hY defined above we have*

$$\exp(hX)\exp(hY) = \exp(hZ)$$

where

$$hZ = hX + hY + \frac{h^2}{2}[X,Y] + \frac{h^3}{12}([X,X,Y] + [Y,Y,X]) + \ldots \tag{19}$$

where $[X,Y]$ is the commutator of the operators X and Y given by

$$[X,Y] = XY - YX, \quad [X,X,Y] = [X,[X,Y]], \quad etc$$

.

Proof See Varadarajan [142].

We compare this with the operation of evolving under the action of $hX + hY$ given by $\exp(hX + hY)$. If hX and hY are discrete operators applied over a time period h then the principle error introduced by operator splitting is given by the order h^2 contribution $h^2[X,Y]/2$.

Sanz-Serna [128] considers analysing splitting methods using the BCH formula as follows

1. Constructing modified systems corresponding to the discrete operators in the splitting (this is trivial for separable problems).

2. Writing these flows in terms of exponentials X and Y as above.

3. Using BCH to construct the modified equation for the splitting method.

A detailed analysis of this procedure is described in [116].

Example Consider the use of the symplectic Euler method when applied to the Harmonic oscillator problem

$$\frac{du}{dt} = v, \quad \frac{dv}{dt} = -u$$

so that

$$\frac{d\mathbf{u}}{dt} = \begin{pmatrix} 0 & 1 \\ -1 & 0 \end{pmatrix} \mathbf{u} \equiv A\mathbf{u}.$$

The continuous flow map ψ_h is then the rotation matrix

$$\psi_h \mathbf{u} = \exp(hA) = \begin{pmatrix} \cos(h) & \sin(h) \\ -\sin(h) & \cos(h) \end{pmatrix} \mathbf{u}.$$

The symplectic Euler method decomposes the matrix A into the two matrices A_1 and A_2 where

$$A_1 = \begin{pmatrix} 0 & 1 \\ 0 & 0 \end{pmatrix} \quad \text{and} \quad A_1 = \begin{pmatrix} 0 & 0 \\ -1 & 0 \end{pmatrix}.$$

Thus

$$\exp(hA_1) = \begin{pmatrix} 1 & h \\ 0 & 1 \end{pmatrix} \quad \text{and} \quad \exp(hA_2) = \begin{pmatrix} 1 & 0 \\ -h & 1 \end{pmatrix}$$

giving

$$\begin{aligned} \exp(hA_1)\exp(hA_2) &= \begin{pmatrix} 1-h^2 & h \\ -h & 1 \end{pmatrix} \\ &= \begin{pmatrix} \cos(h) & \sin(h) \\ -\sin(h) & \cos(h) \end{pmatrix} + \begin{pmatrix} -h^2/2 & 0 \\ 0 & h^2/2 \end{pmatrix} + \mathcal{O}(h^3). \end{aligned}$$

Observe that

$$\frac{h^2}{2}[A_1, A_2] = \begin{pmatrix} -h^2/2 & 0 \\ 0 & h^2/2 \end{pmatrix}$$

so that the above analysis is fully consistent with this result.

In contrast we may apply the same analysis to the *Strang splitting*. This gives

$$\begin{aligned} \exp(hX/2)\exp(hY)\exp(hX/2) &= \exp(hX/2)\exp(hY + hX/2 + h^2[Y,X]/4 + \ldots) \\ &= \exp(hY + hX + h^2[Y,X]/4 + h^2[X,Y]/4 + h^2[X,X]/8 + \ldots). \end{aligned}$$

The identities $[Y,X] + [X,Y] = 0$ and $[X,X] = 0$ imply that the dominant error to the Strang splitting is zero — accounting for the improved accuracy of this method. Indeed the next term in this construction is given by

$$\frac{h^3}{12}\left([Y,Y,X] - \frac{1}{2}[X,X,Y]\right),$$

demonstrating the improved accuracy of this method.

Returning to our example, it is easy to see that

$$\exp(hA_1/2)\exp(hA_2)\exp(hA_1/2) = \begin{pmatrix} 1-h^2/2 & h-h^3/4 \\ -h & 1-h^2/2 \end{pmatrix} = \exp(hA_1+hA_2)+\mathcal{O}(h^3).$$

This same procedure can be applied to general splitting decompositions of the form [104]

$$\varphi^2_{b_m h}\circ\varphi^1_{a_m h}\circ\varphi^2_{b_{m-1}h}\circ\dots\varphi^1_{a_1 h}.$$

Careful choices of the coefficients $a_1,\dots,b_m$ lead to higher order methods. A particular example of which is the Yoshida method described earlier which combines time-symmetric methods (such as the Störmer-Verlet method) with both *positive* and *negative* time steps to derive higher order methods. More recently Blanes and Moan [15] have constructed a series of higher order methods which are considerably more efficient than the Yoshida splittings and which remove the above error to leading and higher orders.

4 Conservation laws

4.1 Outline

The backward error analysis of Hamiltonian systems described in the last section has shown that a modified form of the Hamiltonian of a problem is conserved to within an exponentially small error by a symplectic method. As conservation laws are universal in physical applications, we can ask the question of how we should design a numerical method to capture them. Whilst the Hamiltonian (and many other quantities) are conserved in a Hamiltonian system, many other problems (which are not themselves Hamiltonian) have invariants. In this section we consider how well these can be conserved. Conservation laws have had a major impact in the development of schemes in (for example) fluid dynamics with the Arakawa scheme [4] for conserving energy and enstrophy (in partial differential equations) In another important study de Frutos and Sanz-Serna [56] give an example of a conserving second-order method applied to the KdV equation outperforming a non-conserving third-order method, despite the fact that the higher order method has smaller local truncation errors. In [93] Li and Vu-Quoc (in reference to numerical discretisations of the nonlinear Klein-Gordon equations) state that *in some areas, the ability to preserve some invariant properties of the original differential equation is a criterion to judge the success of a numerical simulation.*

We can think of a conservation law associated with the solutions of a differential equation as follows. Suppose that the underlying differential equation is $d\mathbf{u}/dt = \mathbf{f}(\mathbf{u})$, then a conservation law is given by the constraint $I(\mathbf{u}(t)) = const$ so that the solution evolves on the constraint manifold $\mathcal{M}$ where

$$\mathcal{M} = \{\mathbf{x}\in\mathbb{R}^d : I(\mathbf{x}) = I(\mathbf{u}_0)\}.$$

We distinguish these examples, where the manifold $\mathcal{M}$ arises as part of the solution (and is a natural constraint), from differential algebraic equations in which the differential equation system is underdetermined and the manifold $\mathcal{M}$ acts as an enforced constraint. First the bad news. Even in symplectic methods we cannot (with non-adaptive time steps) exactly conserve the underlying Hamiltonian, or indeed, in general anything other than *quadratic* invariants, Ge and Marsden [60]. Thus we need to look further than the symplectic methods outlined in the last section. Various approaches have been developed including moving frames (see Olver [119] as well as the references therein), discrete gradients, projection and methods based on Noether's theorem.

4.2 Serendipitous and enforced conservation laws

Now the good news. Many useful invariants can be preserved, either by general methods or by purpose designed methods.

A *linear* invariant takes the form

$$I = A\mathbf{u}$$

and a *quadratic* invariant the form

$$I = \mathbf{u}^T C\mathbf{u},$$

where C is a symmetric or skew-symmetric square matrix. Angular momentum in the Kepler problem and in molecular dynamics is an example of a quadratic invariant. We will see the usefulness of the preservation of quadratic invariants when we consider the performance of a variety of methods, including the implicit mid-point rule, to the problem of rigid body motion.

The following theorem gives a broad classification of methods which conserve a wide class of such invariants.

THEOREM *(i) All Runge-Kutta and multi-step methods preserve linear invariants (ii) Runge-Kutta methods satisfying the condition (10) preserve quadratic invariants (iii) In a splitting method, if Ψ_h^i are methods that conserve quadratic invariants, then so does the composition of these methods.*

Proof We now present a proof of (ii) following Sanz-Serna and Calvo [129]. From the general structure of a Runge-Kutta method it is possible to write

$$\begin{aligned} \mathbf{u}_{n+1}^T C\mathbf{u}_{n+1} &= \mathbf{u}_n^T C\mathbf{u}_n + 2h\sum_{i=1}^{s} b_i \mathbf{k}_i^T C\mathbf{Y}_i \\ &\quad + h^2 \sum_{i,j=1}^{s} (b_i b_j - b_i a_{ij} - b_j a_{ji})\mathbf{k}_i^T C\mathbf{k}_j, \end{aligned} \tag{20}$$

where $\mathbf{k}_i = \mathbf{f}(\mathbf{Y}_i)$ and $\mathbf{Y}_i = \mathbf{u}_n + h\sum_j a_{ij}\mathbf{k}_j$. However, from

$$0 = \frac{d}{dt}\left(\mathbf{u}^T C\mathbf{u}\right) = \mathbf{u}^T C\mathbf{f}(\mathbf{u}),$$

and the symmetry or skew-symmetry of C, we see that the first sum in (20) vanishes. The result now follows since the second sum in (20) vanishes provided that the symplecticity condition (10) holds.

The other two parts of this theorem have similarly simple proofs.

We can extend this theorem to say that for a partitioned systems with quadratic invariant $I(\mathbf{p},\mathbf{q}) = \mathbf{p}^T S\mathbf{q}$, S a constant square matrix, I is conserved if the system is integrated by a symplectic partitioned Runge-Kutta method, i.e. a method satisfying (11), see [129] for additional details.

This very nice property of Runge-Kutta methods cannot be easily extended to other classes of ordinary differential equation solvers. Indeed, quadratic invariants are in general NOT preserved by linear multi-step methods. For example the trapezoidal rule

$$u_{n+1} = u_n + \frac{h}{2}\left(f\left(u_n\right) + f\left(u_{n+1}\right)\right)$$

(which is equivalent to the implicit mid-point rule for linear problems but differs for nonlinear problems) possesses many nice properties (such as symmetry) but does not preserve quadratic invariants (and hence is not symplectic). Although this may seem to limit the potential usefulness of this latter method it is shown in [129] that the trapezoidal rule can be considered to be a symplectic map when applied to a system equivalent to the original but after a reversible change of coordinates, methods which satisfy this are called conjugate symplectic in [129]. Thus many of the nice features of symplectic maps are inherited by this method.

A more general equation may have deeper invariants. An important class of such are isospectral flows of the form

$$\frac{d}{dt}u = [A, u] \equiv Au - uA$$

where u and A are now matrices. Such flows have the entire spectrum of u as an invariant, provided that the matrix A is skew symmetric, and arise naturally in the computation of the Lyapunov exponents of a system. They also arise in the study of Lie group solvers which will be considered in the next section.

The theorem cannot be extended to more complicated invariants. For example polynomial invariants of degree three or greater are in general not conserved, it is shown in [69] for example that no Runge-Kutta method can conserve all such invariants.

Faced with this problem, an obvious way to conserve a particular invariant is to simply enforce it during the evolution by continually projecting the solution onto the constraint manifold. An example of this procedure might be an integration of the many body problem with conservation of energy and angular momentum enforced. In another example we can consider a matrix equation in which we require that the determinant of the matrix at each stage of the evolution should be unity. This can be enforced by dividing the discrete solution obtained at each stage by its determinant scaled appropriately. Hairer [70] discusses such a procedure in which a standard numerical method is used to advance the solution by one step and the resulting calculated value is then projected (say using the Euclidean norm) on to the constraint manifold. This procedure can be systematised by using Lagrange multipliers.

Whilst this procedure may seem natural it has two significant disadvantages. Firstly, the projection procedure inevitably reduces the information present in the calculation. Secondly, it is far from clear that enforcing a natural constraint in any way is reproducing the correct geometrical features of the problem. It is quite possible that the dynamics on the manifold itself is completely wrong. Hairer makes this clear in [69] in which he applies this procedure to the Kepler problem using both the forward Euler and the symplectic Euler methods. He finds that good qualitative agreement is obtained only when *all* of the invariants of the problem are maintained, and indeed if only one (for example energy) is maintained then the overall performance of the method can in fact be degraded.

4.3 Discrete gradient methods

We now briefly discuss a more general approach for constructing methods which preserve conservation laws. These methods are termed *discrete gradient* methods and are based on the observation that an ODE problem $\dot{u} = f(u)$ with the invariant or first integral $I(u)$ may be written in the equivalent skew-gradient form

$$\frac{du}{dt} = S(u)\nabla I(u), \quad S^T = -S. \tag{21}$$

Given a vector field f and first integral I there will in general be no uniqueness in the choice of S. One particular choice is given by $S = (f(\nabla I)^T - (\nabla I)f^T)|\nabla I|^{-2}$. However, some problems may naturally be posed in such a way that an S is given immediately, for example in Hamiltonian or Poisson systems. In general the method is then constructed by discretising (21) and forming the discrete skew gradient system, or discrete gradient method

$$\frac{u^{n+1} - u^n}{\Delta t} = \tilde{S}(u^{n+1}, u^n, \Delta t)\tilde{\nabla} I(u^n, u^{n+1}), \tag{22}$$

where $\tilde{S}$ is a consistent ($\tilde{S}(u, u, 0) = S(u)$) skew-symmetric matrix and $\tilde{\nabla} I$ is defined to be a discrete gradient of I, that is

$$I(u') - I(u) = \tilde{\nabla} I(u', u).(u' - u), \quad \text{and} \quad \tilde{\nabla} I(u, u) = \nabla I(u).$$

The discretisation given by (22) can now be proven to conserve I

$$\begin{aligned} I(u^{n+1}) - I(u^n) &= \tilde{\nabla} I(u^{n+1}, u^n).(u^{n+1} - u^n) \\ &= \Delta t\, \tilde{\nabla} I(u^{n+1}, u^n)^T \tilde{S}(u^{n+1}, u^n, \Delta t)\tilde{\nabla} I(u^{n+1}, u^n) \\ &= 0. \end{aligned}$$

There are many possible ways to choose the discrete gradient and the skew-symmetric matrix $\tilde{S}$ see [108], one possible choice of each is given by $\tilde{S}(u, u', \tau) = S((u + u')/2)$ and

$$\tilde{\nabla} I(u, u')_i = \frac{I(u^{(i)}) - I(u^{(i-1)})}{u'_i - u_i}$$

where $u^{(i)} = (u'_1, \ldots, u'_i, u_{i+1}, \ldots, u_m)$, called the coordinate increment discrete gradient in [108] and attributed to Itoh and Abe [85].

The above construction can be extended to derive methods which preserve more than one first integral, and also to cases where I is a Lyapunov exponent see [107]. Once a symmetric integral conserving method has been constructed using this technique (the method may be made symmetric by choosing $\tilde{S}$ and $\tilde{\nabla} I$ such that $\tilde{S}(x, x', \tau) = \tilde{S}(x', x, -\tau)$ and $\tilde{\nabla} I(x, x') = \tilde{\nabla} I(x', x)$), the ideas of Yoshida as discussed earlier may be used to construct higher-order methods.

5 Symmetry group methods

Whilst geometric methods were originally developed to solve Hamiltonian problems a very significant development of geometrical ideas has been in the computation of the solutions of problems with symmetries. Here we can distinguish between problems which have an underlying symmetry (such as a rotational symmetry) which the solutions may or may not share, or problems in which the solutions evolve on manifolds which are invariant under the action of a symmetry group. This situation becomes rather more complex for partial differential equations and we return to these later. In this section we consider progressively the development of methods for problems with Lie group, reversing and scaling symmetries. Here we start with a very general set of ideas and then specialise to a case where adaptivity and symmetry work together.

5.1 Lie group methods

This section summarises many of the ideas which are discussed in the very general survey article by Iserles et. al. [84].

In the previous section we looked at problems in which the solutions were constrained to lie on a manifold $\mathcal{M}$. The task of discretising a system consistently with this manifold invariant is greatly assisted when $\mathcal{M}$ is *homogeneous*, namely when it is subjected to a transitive group action of a Lie group G with identity e and we can think of points on the manifold as being coupled by the group action. In other words there is a function $\lambda : G \times \mathcal{M} \to \mathcal{M}$ such that for every $g_1, g_2 \in G$ and $u \in \mathcal{M}$

$$\lambda(g_1, \lambda(g_2, u)) = \lambda(g_1 g_2, u), \quad \text{with} \quad \lambda(e, u) = u$$

and for all $u_1, u_2 \in \mathcal{M}$ there is a g such that $\lambda(g, u_1) = u_2$.

Invariance of $\mathcal{M}$ under the action of such a Lie group G is a very strong special case of the invariants discussed in the last section. Homogeneous manifolds include Lie groups themselves, spheres, tori, Stiefel and Grassmann manifolds. An important example of such a problem is the evolution of an orthogonal matrix. Substantial work has been done by Iserles, Munthe-Kaas, Nørsett, Zanna and their co-workers [82, 83, 84, 112, 113, 114, 149] on the construction of efficient numerical schemes which ensure that solutions of appropriate differential equations evolve on such manifolds.
The most direct examples of homogeneous manifolds occur when $\mathcal{M}$ is equal to the Lie group G. Although this appears to be a special case, Munthe-Kaas and Zanna [114] have shown that, provided a numerical method can be constructed so that solutions of the differential equation evolve on a Lie-group, then these methods can be extended in a straightforward manner to every homogeneous space acted on by that group. Thus we can consider this simpler case only, and the remainder of this sub-section will be on this topic.

Accordingly, suppose that G is a Lie group, we will consider the following differential equation.

$$\mathbf{u}' = A(t, \mathbf{u})\mathbf{u}, \quad t \geqslant 0, \qquad \mathbf{u}(t_0) = \mathbf{u}_0 \in G, \tag{23}$$

where $A : \mathbb{R}^+ \times G \to \mathfrak{g}$, and $\mathfrak{g}$ is the *Lie algebra* of G. Typically G will be a matrix Lie group and $\mathbf{u}$ a matrix. The motivation for considering this differential equation is the following lemma.

LEMMA *If $\mathfrak{g}$ is the Lie algebra of the group G then the solutions $\mathbf{u}$ of the differential equation (23) are constrained to evolve on the Lie group G.*

Some examples of such matrix Lie groups and their corresponding Lie algebras are as follows

Lie group	Lie algebra
$SL_n = \{u : \det(u) = 1\}$	$\mathfrak{sl}_n = \{A : \mathrm{trace}(A) = 0\}$
$O_n = \{u : u^T u = I\}$	$\mathfrak{so}_n = \{A : A^T + A = 0\}$
$SO_n = \{u : u^T u = I, \det(u) = 1\}$	$\mathfrak{so}_n = \{A : A^T + A = 0\}$
$Sp_n = \{u : u^T J u = J\}$	$\mathfrak{sp}_n = \{A : JA + A^T J = 0\}$
$GL_n = \{u : \det(u) \neq 0\}$	$\mathfrak{gl}_n =$ all matrices

Observe, for example, that whilst the Lie group of orthogonal matrices forms a nonlinear manifold, the Lie algebra of skew symmetric matrices comprises a linear vector space. This is true for all of the other examples. Numerical solvers for the differential equation (23) tend to work on elements of the Lie algebra of G rather than the elements of G itself precisely because nonlinear constraints on G become linear constraints on $\mathfrak{g}$. Thus it is important to have methods which allow you to move from the Lie algebra to the Lie group. The most important such method is the *exponential map* which acts as a map between the Lie algebra and the corresponding Lie group. For $A \in \mathfrak{g}$ it is defined by

$$\exp(A) = \sum_{n=0}^{\infty} \frac{A^n}{n!}.$$

Calculating, or approximating, the exponential map plays an important role in most Lie group solvers as it allows us to transfer calculations from the (nonlinear) Lie group on to the (linear) Lie algebra. However, it is not an easy map to evaluate. MATLAB employs several alternative methods (empm, ..., expm3) for computing the exponential function, but finding the matrix exponential will always be an expensive process. Numerical methods have been used to find easy to compute approximations to it it, for a review of many such methods see [111], and for a geometric perspective see [32]. For certain cases it can be computed using a finite sum. For example if $A \in \mathfrak{so}_3$ then Rodrigues formula [98] gives

$$\exp(A) = I + \frac{\sin(\alpha)}{\alpha} A + \frac{1}{2}\left(\frac{\sin(\alpha/2)}{\alpha/2} A^2\right) \quad \text{where} \quad A = \begin{pmatrix} 0 & -\omega_3 & \omega_2 \\ \omega_3 & 0 & -\omega_1 \\ -\omega_2 & \omega_1 & 0 \end{pmatrix},$$

and

$$\alpha = \sqrt{\omega_1^2 + \omega_2^2 + \omega_3^2}.$$

It is worth observing that for certain Lie groups we may identify other maps between the Lie algebra and the Lie group which are much easier to compute than the exponential map. A notable example of such is the *Cayley map* defined by

$$\mathrm{cay}(A) = (I - A/2)^{-1}(I + A/2)$$

which requires one matrix inversion rather than an infinite sum.

LEMMA *If $A \in \mathfrak{so}_n$ then cay$(A) \in O_n$.*

Proof. Let $O = (I - A/2)^{-1}(I + A/2)$ then

$$O^T = (I + A^T/2)(I - A^T/2)^{-1} = (I - A/2)(I + A/2)^{-1} = (I + A/2)^{-1}(I - A/2) = O^{-1}.$$

This result may be extended to show that the Cayley map also works for the symplectic group, i.e. it maps $\mathfrak{sp}_n$ into Sp_n.

Most Lie-group solvers follow a set pattern: Let us assume that the underlying group is finite-dimensional. By Ado's theorem, it then follows that the Lie algebra $\mathfrak{g}$ is isomorphic to a matrix algebra (a subset of $\mathfrak{gl}_m(R)$, the Lie algebra of $m \times m$ real matrices). For simplicity's sake (and with moderate loss of generality) we can thus stipulate that $\mathfrak{g}$ is a matrix Lie algebra. The equation (23) is *pushed* to the underlying Lie algebra $\mathfrak{g}$, solved there and the solution is *pulled back* to G with the exponential map. (In the restricted class of problems described above this step can be replaced by an application of the Cayley map.) This operation may take place repeatedly in the course of a single time step and is displayed in the following diagram,

Lie group: $\quad \mathbf{u}' = A(t, \mathbf{u})\mathbf{u}$

$$\begin{tikzcd}
\mathbf{U}_n \arrow[d, "\text{push-forward}"'] & & \mathbf{U}_{n+1} \\
\sigma_n \arrow[rr, "\text{numerical method}"] & & \sigma_{n+1} \arrow[u, "\text{pull-back}"']
\end{tikzcd}$$

Lie algebra: $\quad \sigma' = \mathrm{dexp}_\sigma^{-1} A(t, e^\sigma \mathbf{U}_n)$

Here $A : \mathbb{R}^+ \times G \to \mathfrak{g}$ and $\sigma(t)$ evolves on the Lie algebra $\mathfrak{g}$. The numerical method is devised to solve a differential equation for σ rather than for u. The pull-back for matrix Lie algebras is the standard matrix exponential (or Cayley map),

$$\mathbf{U}_{n+1} = e^{\sigma_{n+1}} \mathbf{U}_n.$$

In contrast, the push-forward projects the equation onto the Lie algebra. For the exponential map it is given by the *dexpinv equation*

$$\sigma' = \sum_{l=0}^{\infty} \frac{B_l}{l!} ad_\sigma^l A(t, e^\sigma \mathbf{U}_n), \quad t \geqslant t_0, \qquad \sigma(t_n) = 0,$$

where $\{B_l\}_{l=0}^{\infty}$ are *Bernoulli numbers,* defined by

$$\frac{x}{e^x - 1} = \sum_{k=0}^{\infty} B_k \frac{x^k}{k!}$$

while the *adjoint operator ad_x* in a Lie algebra is an iterated commutator,

$$ad_x^l y = \overbrace{[x, [x, \ldots, [x, y] \cdots]]}^{l \text{ times}}, \qquad l \geqslant 0.$$

For a proof of this result see Hairer [69]. A similar expression to the dexpinv equation (the dcayinv equation) can be derived for the Cayley transform, see Iserles [82].

We can now use a numerical scheme to integrate the dexpinv equation. Here the constraint on this solver is that all computed solution should lie in the Lie algebra. However, as the Lie algebra is a linear vector space this is easy: as long as the numerical method employs just linear-space operations and commutators, it is bound to produce $\sigma_{n+1} \in \mathfrak{g}$. An important example of such methods are the *Runge–Kutta/Munthe-Kaas* (RKMK) schemes, which in the present formalism apply a (typically, explicit) Runge–Kutta method to the dexpinv equation, appropriately truncated [112]. For example, a classical third-order Runge–Kutta method, applied to the Lie-group equation (23), reads

$$\begin{aligned}
\mathbf{k}_1 &= A(t_n, \mathbf{U}_n)\mathbf{U}_n, \\
\mathbf{k}_2 &= A(t_n + \frac{1}{2}h, \mathbf{U}_n + \frac{1}{2}h\mathbf{k}_1)(\mathbf{U}_n + \frac{1}{2}h\mathbf{k}_1), \\
\mathbf{k}_3 &= A(t_{n+1}, \mathbf{U}_n - h\mathbf{k}_1 + 2h\mathbf{k}_2)(\mathbf{U}_n - h\mathbf{k}_1 + 2h\mathbf{k}_2), \\
\mathbf{v} &= h\left(\frac{1}{6}\mathbf{k}_1 + \frac{2}{3}\mathbf{k}_2 + \frac{1}{6}\mathbf{k}_3\right), \\
\mathbf{U}_{n+1} &= \mathbf{U}_n + \mathbf{v}.
\end{aligned}$$

In general this cannot be expected to keep $\{\mathbf{U}_n\}_{n=0}^{\infty}$ in G. However, as soon as we change the configuration space from G to $\mathfrak{g}$, solve there and pull back, the ensuing RKMK scheme,

$$\begin{aligned}
\mathbf{k}_1 &= A(t_n, \mathbf{U}_n), \\
\mathbf{k}_2 &= A(t_n + \frac{1}{2}h, e^{\frac{1}{2}h\mathbf{k}_1}\mathbf{U}_n), \\
\mathbf{k}_3 &= A(t_{n+1}, e^{-h\mathbf{k}_1 + 2h\mathbf{k}_2}\mathbf{U}_n), \\
\mathbf{v} &= h\left(\frac{1}{6}\mathbf{k}_1 + \frac{2}{3}\mathbf{k}_2 + \frac{1}{6}\mathbf{k}_3\right), \\
\mathbf{U}_{n+1} &= \exp\left(\mathbf{v} + \frac{h}{6}[\mathbf{v}, \mathbf{k}_1]\right)\mathbf{U}_n,
\end{aligned}$$

respects the Lie-group structure.

A different example of a class Lie-group solvers can be obtained from a direct manipulation of the dexpinv equation, in particular when the Lie-group equation is linear,

$$\mathbf{u}' = A(t)\mathbf{u}.$$

Perhaps the most powerful approach is to exploit the *Magnus expansion.* This is an explicit solution of the dexpinv equation for the linear problem above and which has the following form

$$\begin{aligned}
\sigma(t) = &\int_0^t A(\xi)\, d\xi - \frac{1}{2}\int_0^t\int_0^{\xi_1} [A(\xi_2), A(\xi_1)]\, d\xi_2\, d\xi_1 \\
&+ \frac{1}{4}\int_0^t\int_0^{\xi_1}\int_0^{\xi_2} [[A(\xi_3), A(\xi_2)], A(\xi_1)]\, d\xi_3\, d\xi_2\, d\xi_1 \\
&+ \frac{1}{12}\int_0^t\int_0^{\xi_1}\int_0^{\xi_1} [A(\xi_3), [A(\xi_2), A(\xi_1)]]\, d\xi_3\, d\xi_2\, d\xi_1 + \cdots,
\end{aligned} \qquad (24)$$

see Magnus [97]. The analysis and numerical implementation of Magnus expansions is a far-from-trivial task and it is investigated in depth, using techniques from graph theory and quadrature, in [83]. Significantly, the Magnus expansion can be truncated at any point to give an approximation to σ which is comprised of linear operations and commutators, and thus must lie in the Lie algebra $\mathfrak{g}$. This is a key to the effective use of these methods. When applied to the problem $\mathbf{u}' = A(t)\mathbf{u}$ a typical method based upon the Magnus series [83], [149] replaces $A(t)$ locally by an interpolation polynomial $\hat{A}$ and then solves the equation $\mathbf{u}' = \hat{A}\mathbf{u}$ locally on the interval $[t_n, t_n + h]$ by using a truncated form of (24) and an appropriate quadrature method. Careful exploitation of the way in which the commutators are calculated can significantly reduce the computation labour in this calculation. Zanna [149] has also extended this method to certain classes of nonlinear equations.

Example If an interpolation polynomial of degree one is used with a two point Gaussian quadrature and the Magnus expansion is truncated at the fourth term then the following order four method is obtained [69] (where we make the assumption that the exponential is evaluated exactly)

$$U_{n+1} = \exp\left(\frac{h}{2}(A_1 + A_2) + \frac{\sqrt{3}h^2}{12}[A_2, A_1]\right) U_n, \tag{25}$$

where $A_{1,2} = A(t_n + x_{1,2}h)$ with x_i the Gauss points $1/2 \pm \sqrt{3}/6$.

An alternative to using the Magnus expansion is the *Fer expansion.* In this we write the solution of the Lie-group equation $\mathbf{u}' = A(t)\mathbf{u}$ in the form

$$\mathbf{u}(t) = \exp\left[\int_0^t A(\xi)d\xi\right]\mathbf{z}(t), \qquad t \geqslant 0,$$

where $\mathbf{z}$ obeys the linear equation

$$\mathbf{z}' = \left[\sum_{l=1}^{\infty} \frac{(-1)^l}{(l+1)!} ad^l_{\int_0^t A(\xi)d\xi} A(t)\right]\mathbf{z}, \quad t \geqslant 0, \qquad \mathbf{z}(t_0) = \mathbf{u}(t_0).$$

This procedure can be iterated, ultimately producing the solution $\mathbf{u}$ as an infinite product of exponentials.

An important feature of RK/Munthe-Kaas, Magnus and Fer methods is that their implementation involves repeated computation of commutators. This activity, which represents the lion's share of computational expense, can be simplified a very great deal by exploiting linear dependencies among commutators. The analysis of this phenomenon is amenable to techniques from the theory of Lie algebras and constitutes the theme of [113]. See also the work of Blanes et. al. [14] in the derivation of *optimal* Lie group methods which evaluate a minimum number of commutators.

5.1.1 Example 1: Evolution on the sphere

We now consider an example of a differential equation evolving on the sphere S_2. We use an example given in [53], where it is used to demonstrate how to construct solutions to problems on manifolds with the matlab toolbox DiffMan. The problem is given by

$$\frac{d\mathbf{u}}{dt} = A(t)\mathbf{u}(t), \quad A(t) = \begin{pmatrix} 0 & t & -\cos(t)/2 \\ -t & 0 & t/2 \\ \cos(t)/2 & -t/2 & 0 \end{pmatrix}, \quad \mathbf{u}(0) = \begin{pmatrix} 0 \\ 0 \\ 1 \end{pmatrix}. \tag{26}$$

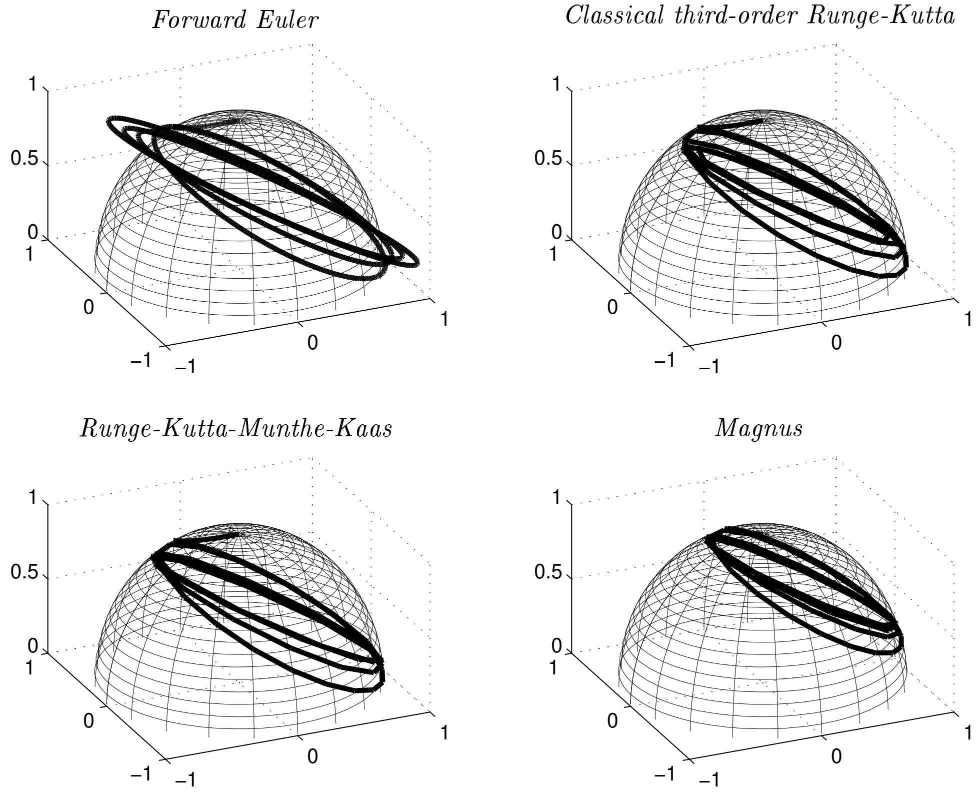

Figure 6: *The dynamics of four methods applied to problem (26). Forward Euler is shown for 1400 steps of length 0.005. Classical RK, RKMK and Magnus methods are all shown for 70 steps of length 0.1.*

The matrix A is obviously a map from $\mathbb{R}$ into $\mathfrak{so}(3)$ and thus the quadratic quantity $I(\mathbf{u}) = \mathbf{u}^T\mathbf{u}$ is an invariant of system (26), i.e.

$$u_1^2(t) + u_2^2(t) + u_3^2(t) = u_1^2(0) + u_2^2(0) + u_3^2(0), \quad t \geqslant 0,$$

and the solution evolves on the two-sphere S^2. In the case that u was a 3×3 matrix we would be in the situation of u evolving on the Lie group O_2.

Figure 6 demonstrates the behaviour of four numerical methods applied to problem (26). As we have seen in previous examples the forward Euler method exhibits a growth in I and the solution curve consequently leaves the surface of the sphere. The RK method exhibits a monotonic decrease in I from 1 to less than 0.8, thus the numerical solution again leaves the surface of the sphere, however this time heading towards the origin. As expected from the previous section the RKMK and Magnus methods both exactly conserve I and hence evolve on the desired solution manifold.

5.1.2 Example 2: Rigid body motion

For our second example we consider the more subtle, nonlinear, physically based problem of a rigid body with centre of mass fixed at the origin. The body moves according to the Euler equations

$$\begin{aligned}
\dot{u}_1 &= (I_2 - I_3)u_2u_3/I_2I_3 \\
\dot{u}_2 &= (I_3 - I_1)u_3u_1/I_3I_1 \\
\dot{u}_3 &= (I_1 - I_2)u_1u_2/I_1I_2
\end{aligned}$$

where (I_1, I_2, I_3) are the moments of inertia about coordinate axes and (u_1, u_2, u_3) the body angular momenta. We may write this in our Lie group form

$$\dot{\mathbf{u}} = A(t, \mathbf{u})\mathbf{u},$$

where

$$A(t, \mathbf{u}) = \begin{pmatrix} 0 & I_3^{-1}u_3 & -I_2^{-1}u_2 \\ -I_3^{-1}u_3 & 0 & I_1^{-1}u_1 \\ I_2^{-1}u_2 & -I_1^{-1}u_1 & 0 \end{pmatrix}$$

is a map from $\mathbb{R}^3$ into $\mathfrak{so}(3)$ as in the previous example.

This problem has the additional structure of being able to be written in the non-canonical Hamiltonian form

$$\dot{\mathbf{u}} = \{\mathbf{u}, H\}, \tag{27}$$

where the conserved Hamiltonian function and the bracket operation on functions of $\mathbf{u}$ are given by

$$H(\mathbf{u}) = \frac{1}{2}\left(\frac{u_1^2}{I_1} + \frac{u_2^2}{I_2} + \frac{u_3^2}{I_3}\right), \quad \{F, G\}(\mathbf{u}) = -\mathbf{u} \cdot (\nabla F \times \nabla G). \tag{28}$$

(See [98, 118] for further details of the bracket operation, including the properties it must satisfy.) Following these operations through we can see that our rigid body system may be written

$$\dot{\mathbf{u}} = \mathbf{u} \times \nabla H(\mathbf{u}) \equiv J(\mathbf{u})\nabla H(\mathbf{u}). \tag{29}$$

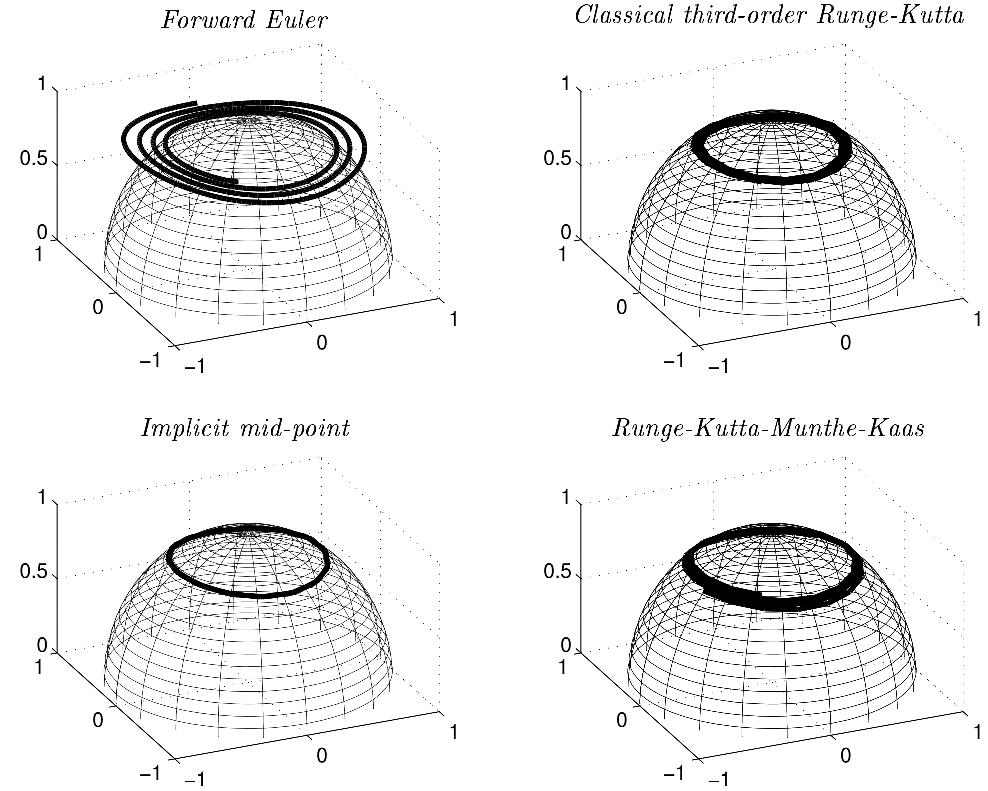

Figure 7: *The dynamics of four methods applied to the rigid body problem. Forward Euler is shown for 500 steps of length 0.02. Classical RK, RKMK and implicit mid-point methods are all shown for 50 steps of length 0.2.*

Here $J(\mathbf{u})$ is the skew-symmetric matrix

$$J(\mathbf{u}) = \begin{pmatrix} 0 & -u_3 & u_2 \\ u_3 & 0 & -u_1 \\ -u_2 & u_1 & 0 \end{pmatrix}. \tag{30}$$

Since functions of $\mathbf{u}$ also evolve in the same manner as (27), we can obtain the additional conserved quantity of the system

$$S(\mathbf{u}) = u_1^2 + u_2^2 + u_3^2,$$

by observing that

$$\frac{d}{dt} S(\mathbf{u}) = \{S, H\}(\mathbf{u}) = -\mathbf{u} \cdot (\mathbf{u} \times \nabla H),$$

which is obviously zero. Notice that we can say further that $\{S, F\} = 0$ for all functions F, and so conservation of S follows from the form of the bracket operation and not the Hamiltonian, a quantity of this type is known as a *Casimir invariant* and such invariants arise very naturally in many Hamiltonian problems. We will consider these in more detail in the section on partial differential equations.

The conservation of S tells us that the motion of our system evolves on the sphere, and conservation of H that motion also evolves on an ellipsoid. An ideal numerical scheme will reproduce both of these invariants.

Figure 7 shows the behaviour of some numerical methods applied to this problem with $I_1 = 7/8$, $I_2 = 5/8$ and $I_3 = 1/4$, and initial condition chosen such that $\mathbf{u}^T\mathbf{u} = 1$. As we have come to expect now the forward Euler method exhibits a growth in both S and H and can be seen to leave the surface of the sphere. The RK method exhibits a decrease in both S and H and also leaves the sphere. The RKMK method (applied to the problem written in the form $\dot{\mathbf{u}} = A(t, \mathbf{u})\mathbf{u}$ rather than the Hamiltonian form (29)) preserves S and so the numerical solution lies on the sphere, although H is not conserved and hence the solution is not a closed curve. In the case of the implicit mid-point rule both S and H are conserved (since they are both quadratic invariants we know this from an earlier discussion), and the solution can be seen to be a closed curve lying on the surface of the sphere — exactly the ideal scenario we mentioned earlier.

The special form that J takes, and hence also the bracket operation, means that this problem is of *Lie-Poisson* type. That is we may write our skew-symmetric matrix (30) as

$$J_{ij}(\mathbf{u}) = \sum_{k=1}^{3} c_{ij}^k u_k,$$

where c_{ij}^k are structure constants for a Lie algebra, in this case $\mathfrak{so}(3)$. See [98, 118] for further details. For a splitting based numerical method designed to preserve this structure see [102], [11], and for methods designed to preserve the Casimirs and Hamiltonians of such system see [52]. A recent review and comparison of various methods for this system may be found in [28].

5.2 Symmetries and reversing symmetries

A manifold invariant under the action of a Lie group has a very special structure. However, a symmetry of a system need not satisfy all of the conditions of a Lie group of symmetries as outlined above. In particular, we may consider a general set of symmetries $\mathbf{h}$ from a phase space to itself such that if the underlying equation is

$$\frac{d\mathbf{u}}{dt} = \mathbf{f}(\mathbf{u})$$

and $\mathbf{v} = \mathbf{h}(\mathbf{u})$ is a map from the phase space to itself, then the new system will take the form

$$\frac{d\mathbf{v}}{dt} = \mathbf{g}(\mathbf{v}).$$

This system has $\mathbf{h}$ as a *symmetry* if $\mathbf{f} = \mathbf{g}$ and a *reversal symmetry* if $\mathbf{f} = -\mathbf{g}$ (so that the arrow of time is reversed in this case). A special case of symmetries, namely scaling symmetries, is considered in the next section. Symmetries relate the vector field at the two points $\mathbf{u}$ and $\mathbf{h}(\mathbf{u})$ and simplify and organise phase space.

The construction of methods which preserve symmetries and reversal symmetries is described in detail in [109] and [107] and we follow their treatment here. They are important because many systems have symmetries and these help to reduce the complexity of the flow. Hamiltonian problems typically have reversing symmetries and this structure can be rather more easily preserved under a (variable time step) discretisation than symplecticity. Leimkuhler [90] recommends the use of reversible adaptive methods when calculating the energy exchange in close approach orbits in the Kepler problem and in molecular dynamics and constructs some very effective methods with this property.

A special case occurs when $\mathbf{h}$ is a linear involution such that $\mathbf{h}^2 = Id$. In mechanics this arises with systems (p, q) with the action $\mathbf{h}(p, q) = (-p, q)$. The system is then reversible if

$$\mathbf{f}(\mathbf{h}(\mathbf{u})) = -\mathbf{h}(\mathbf{f}(\mathbf{u})).$$

The action of this map reverses the arrow of time. In this case if the flow map induced by the differential equation is ψ_t then

$$\mathbf{h}^{-1} \circ \psi_t \circ \mathbf{h} = \psi_t^{-1} = \psi_{-t}.$$

It is highly desirable that such systems should be integrated by numerical methods which preserve this reversible nature. In particular, if Ψ_h is the map on phase space induced by the numerical method then $\mathbf{h}$-reversibility is equivalent to time reversibility

$$\mathbf{h}^{-1} \circ \Psi_h \circ \mathbf{h} = \Psi_h^{-1}.$$

For a self-adjoint method we have further that

$$\Psi_h^{-1} = \Psi_{-h}.$$

In particular, a method such as the forward Euler method is not reversible, whereas the implicit mid-point rule does have this property.

These methods are studied in detail in [133], [134] where it is shown that they have many of the nice features of symplectic methods (for example a reversible version of the KAM theorem exists, see Lamb and Roberts [88], and this can be used to justify some results similar to those obtained for symplectic methods applied to Hamiltonian problems), but the desirable property that variable time steps may also be used. These methods are extended in [77], where a fully explicit time-reversible, variable time step Störmer-Verlet method is derived. See also the papers [79], [38], [17] where such methods are analysed in detail.

5.3 Scaling symmetries, temporal adaptivity and singularity capturing

5.3.1 Outline

We shall consider now a special class of ordinary differential equation problems which are invariant under scaling symmetries which are a subset of linear symmetries. For such problems the Lie group is diagonalisable and all operations commute. Thus it may seem that this is a very restricted class of problems. However, it encompasses a wide class of differential equations that arise very naturally in theoretical physics, especially in considering systems which have no intrinsic length or time scales. We call such problems, and the methods used to solve them *scale invariant*. A natural approach to studying such problems is the use of *adaptive methods*. These have had a bit of a bad press in the geometric integration literature following the discovery by Sanz-Serna and his co-workers [129] that symplectic methods with variable time steps often do not perform as well as similar methods with fixed time steps. This is because the variable time step methods could not, in general be analysed by using the backward error analysis methods described in Section 3.4.1. However, we demonstrate in this section that the additional structure given by scaling invariance when coupled with a geometrically designed adaptive method allows us to construct adaptive schemes with the remarkable property that they have uniform errors for all time (ie. no error growth with time) when used to approximate self-similar solutions of the ordinary differential equations.

Suppose that we consider the differential equation system

$$\frac{d\mathbf{u}}{dt} = \mathbf{f}(\mathbf{u}), \quad \mathbf{u} = (u_1, u_2, \ldots, u_N), \quad \mathbf{f} = (f_1, f_2, \ldots, f_N).$$

A *scaling symmetry* of such an equation is an invariance under the linear transformation

$$t \to \lambda^{\alpha_0} t, \quad u_i \to \lambda^{\alpha_i} u_i, \quad i = 1, \ldots, N,$$

where $\lambda > 0$ is an arbitrary scalar. The condition for this is that for all $\lambda > 0$

$$f_i(\ldots, \lambda^{\alpha_j} u_j, \ldots) = \lambda^{\alpha_i - \alpha_0} f_i(\ldots, u_j, \ldots).$$

This is a slight generalisation of previous sections as we are now allowing time to transform as well.

Note that such a definition may easily be extended to differential algebraic equations. This is especially useful when studying semi-discretisations of scale invariant partial differential equations.

The transformation above may be defined in terms of the vector $\boldsymbol{\alpha} = (\alpha_0, \alpha_1, \ldots, \alpha_N)$ and a system of differential equations may be invariant under the action of many such scaling groups. The vectors $\boldsymbol{\alpha}$ describing this set of invariances then form a (commutative) vector space.

Scaling symmetries arise very naturally in ordinary (and indeed partial) differential equations where they express an invariance of the equation to the units in which it is expressed. It is for this reason that many of the equations of mathematical physics have *polynomial* nonlinearities [10] as it is precisely these which are covariant under the action of such symmetries. For the purposes of numerical discretisations, scale invariant problems have a delicious structure. Consider the two operations of scaling and discretisation acting on a system of differential equations. If the discretisation is a multi-step, a Runge-Kutta or a Taylor series method then *the operations of scaling and discretisation commute.* The only other transformation with this properly is an affine transformation. Technically, such methods are *covariant* with respect to *linear* changes of variables, a result established in [107]. It is certainly not a property enjoyed by the action of a general Lie group. It is this observation which allows us the possibility of an easy derivation of scale invariant discretisations which admit discrete self-similar solutions.

To motivate this discussion we consider two examples of scale invariant equations. The first, which we looked at earlier in the discussion of backward error analysis is the blow-up equation

$$\frac{du}{dt} = u^2 \tag{31}$$

which is invariant under the scaling

$$t \to \lambda t, \quad u \to \lambda^{-1} u.$$

The second example is the (two-dimensional) Kepler problem

$$\dot{x} = u, \quad \dot{u} = -ax/\sqrt{x^2 + y^2}, \quad \dot{y} = v, \quad \dot{v} = -ay/\sqrt{x^2 + y^2}.$$

This system is left unchanged following the rescaling

$$t \to \lambda t, \quad (x, y) \to \lambda^{2/3}(x, y), \quad (u, v) \to \lambda^{-1/3}(u, v),$$

for any arbitrary positive constant λ. We saw in a previous section that this problem can also be written in canonical Hamiltonian form (2), with Hamiltonian

$$H(x,y,u,v) = \frac{u^2}{2} + \frac{v^2}{2} - \frac{a}{\sqrt{x^2+y^2}}.$$

It is then immediate that the Hamiltonian scales in the manner

$$H(\lambda^{2/3}x, \lambda^{2/3}y, \lambda^{-1/3}u, \lambda^{-1/3}v) = \lambda^{-2/3}H(x,y,u,v)$$

from which we may deduce the 'conservation law'

$$\frac{2}{3}xH_x + \frac{2}{3}yH_y - \frac{1}{3}uH_u - \frac{1}{3}vH_v = -\frac{2}{3}H.$$

The scaling invariance of the Kepler problem transforms one solution to another, and when applied to periodic orbits immediately gives us Kepler's third law relating the cube of the semi-major axis of a periodic orbit to the square of its period. We observe also that the Kepler problem is invariant under the action of the rotation group O_2, and hence scaling and more general Lie groups may act together here.

5.3.2 Self-similar solutions

Whilst not all solutions of scale invariant systems of ODEs are themselves scale invariant, those that are play a special role in the overall theory. They are often attractors and therefore describe the long term asymptotics of more general solutions. A self-similar solution has the (invariant) form given by

$$u_i(\lambda^{\alpha_0}t) = \lambda^{\alpha_i}u_i(t).$$

It is easy to show that all such solutions take the form

$$u_i = t^{\alpha_i/\alpha_0}v_i$$

where the *constants* v_i satisfy the *algebraic* equation

$$\alpha_i v_i = \alpha_0 f_i(\ldots, v_j, \ldots).$$

Self-similar solutions often describe singularities in the system. For the blow-up equation (31), the self-similar solutions are in fact all possible solutions, up to time translation, and these have the form

$$u(t) = \frac{1}{T-t}$$

where T is arbitrary. A singularity described by a self-similar solution can also occur in Kepler's problem in a finite time T provided that the angular momentum of the system is zero. This is called *gravitational collapse* and occurs when a particle falls into the sun. An example of a solution with this property is the following self-similar solution.

$$\begin{aligned} x &= \left(\frac{9}{2}\right)^{1/3}(T-t)^{2/3}, \\ u &= -\left(\frac{2}{3}\right)\left(\frac{9}{2}\right)^{1/3}(T-t)^{-1/3}, \\ y &= v = 0. \end{aligned} \tag{32}$$

5.3.3 Numerical methods for scale invariant problems

We immediately observe that conventional numerical methods, including symplectic ones, fail to reproduce the gravitational collapse, or indeed any singular in finite time phenomenon, if a fixed time step is used. An explicit method such as forward Euler will always give a bounded solution, and an implicit method may not have algebraic equations soluble as real numbers for all time steps. Some form of adaptivity therefore needs to be used for this problem, or indeed a large number of problems which have the common feature of developing singularities in a finite time. Thus we are strongly motivated to use an adaptive approach for this problem despite the difficulties of applying backward error analysis outlined in [129].

More generally, we can further say that adaptive methods fall naturally within the geometric integration framework as fixed mesh methods impose constraints on the solution process whereas adaptivity allows the solution and method to evolve together. What we mean here is that if we reparameterize time it is possible for us to derive numerical methods which are themselves invariant under the scaling transformation. We now follow this through for the general case and by looking at the examples of the blow-up and gravitational collapse problems, examine what benefits we achieve.

To describe the adaptive approach we introduce a map which describes a rescaling of the time variable in terms of a new computational or fictive variable τ, given by

$$\frac{dt}{d\tau} = g(u).$$

We impose the constraint that $g(\lambda^{\alpha_i} u_i) = \lambda^{\alpha_0} g(u)$. For the blow-up problem a suitable choice is $g(u) = 1/u$ and for the Kepler problem in one-dimension a suitable choice is $g(x, u) = x^{3/2}$.

The motivation for introducing this new times variable is that the system describing u_i and t in terms of τ is then invariant under the scaling transformation with τ *fixed*, so that if $(t(\tau), u_i(\tau))$ is a solution, then so is $(\lambda^{\alpha_0} t(\tau), \lambda^{\alpha_i} u_i(\tau))$. Therefore, a numerical discretisation of our new system with fixed computational time step $\Delta\tau$ is also invariant, in that if $(t_n, u_{i,n})$ are discrete approximations to $t(n\Delta\tau), u_i(n\Delta\tau))$, then whenever $(t_n, u_{i,n})$ is a solution of our set of discrete equations induced by the discretisation then $(\lambda^{\alpha_0} t_n, \lambda^{\alpha_i} u_{i,n})$ is also a solution.

The rescaling in time is often called a Sundman transformation [90] and has the following direct link with adaptivity. If we take equal steps $\Delta\tau$ in the fictive time variable, then this will correspond to real time steps $\Delta t_n = t_{n+1} - t_n$. To leading order we then have

$$\Delta t_n = g(u)\Delta\tau$$

and hence we have a simple means of adapting the real time step.

Rescaling the whole system then gives

$$\frac{du_i}{d\tau} = h_i(u), \quad \frac{dt}{d\tau} = g(u), \tag{33}$$

where $h_i \equiv g f_i$. Observe that this transformation has had the effect of changing a problem with a variable step size into one with a constant step size $\Delta\tau$. Thus we may now use the full power of the analytical techniques developed for fixed time steps on these problems. Stoffer and Nipp [135] used precisely this procedure for analysing the existence of invariant curves in variable time step discretisations of ODEs.

For the gravitational collapse problem with $a = 1$ an application of this procedure gives

$$\begin{aligned}\frac{dx}{d\tau} &= x^{3/2}u,\\ \frac{du}{d\tau} &= -\frac{1}{x^{1/2}},\\ \frac{dt}{d\tau} &= x^{3/2}.\end{aligned} \tag{34}$$

Observe that whereas this system is scale invariant it has lost its symplectic structure. A device to recover this structure (the Poincaré transform) is discussed presently. The choice of power $3/2$ in the function g is also arrived at in [17] by equalising the amount of fictive time required for both strong and weak collision events, this property has some similarity with Kepler's third law which our scaling invariant method automatically inherits (see later) and therefore the common choice of $3/2$ should be unsurprising.

The secret behind the use of the scale invariant adaptive methods is a careful discretisation of the extended system (33), in which all equations in this system are discretised to the same order of accuracy.

For example, consider a forward Euler discretisation of (34) with constant step size $\Delta\tau$.

$$\begin{aligned}x_{n+1} - x_n &= x_n^{3/2}u_n\Delta\tau\\ u_{n+1} - u_n &= -x_n^{-1/2}\Delta\tau\\ t_{n+1} - t_n &= x_n^{3/2}\Delta\tau.\end{aligned} \tag{35}$$

The following properties of linear multi-step discretisations of the scaled system (33) are listed below.

1. Linear multi-step or Runge-Kutta discretisations of our transformed system (for the above example (34)) have relative local truncation errors which are independent of scale.
2. Global properties of the continuous solution which are derived from scaling invariance may be inherited by the numerical scheme, one example being Kepler's third law.
3. Any continuous self-similar solutions of the problem are uniformly (in time) approximated by discrete self-similar solutions admitted by the numerical method. These discrete solutions also inherit the stability of the continuous ones.

The importance of points 1 and 3 can be seen from the following. Suppose we are computing a solution to a problem in which a singularity is forming, and that the formation is progressively described through the action of the scaling group. Our adaptive numerical method will continue to compute with no overall loss in relative accuracy.

To elaborate on the first part of point 3 we firstly define a *discrete self-similar solution* of the discretised system. This is a discrete solution which has the property that it is invariant under the same changes of scale as the original. In particular a discrete self-similar solution $(t_n, u_{i,n})$ must take the form

$$u_{i,n} = z^{\alpha_i n}V_i, \quad t_n = z^{\alpha_0 n}T,$$

for appropriate V_i, T and z satisfying a suitable algebraic equation. We now state the connexion between the discrete and self-similar solutions via the following theorem.

THEOREM *Let $u_i(t)$ be a self-similar solution of our ordinary differential equation, then for sufficiently small $\Delta\tau$ there is a discrete self-similar solution $(t_n, u_{i,n})$ of the discrete scheme approximating our rescaled system such that for* **all** n

$$u_i(t_n) = u_{i,n}(1 + \mathcal{O}(\Delta\tau^p))$$

where p is the order of the discretisation and the constant implied in the $\mathcal{O}(\Delta\tau^p)$ term does not depend on n.

Proof. See [26].

The most interesting physical self-similar solutions are those which act as attractors since they determine asymptotic behaviour of more general solutions. The stability result mentioned in point 3 ensures that we are not destroying this property in our numerical method.

Crucial to the success of this method is the calculation of the function $g(u)$. This can be done a-priori by finding solutions to the functional equation

$$g(\ldots, \lambda^{\alpha_i} u_i, \ldots) = \lambda^{\alpha_0} g(\ldots, u_i, \ldots),$$

by differentiating with respect to λ, setting $\lambda = 1$ and then solving the resulting linear hyperbolic equation. (This has many possible solutions, all of which are in principle appropriate functions g.) This procedure can be automated in Maple. Alternatively (and maybe preferably) g can be estimated a-posteriori. If the underlying system is scale invariant, then indeed error estimates obtained using the Milne device do lead to equations which are first order discretisations of the equation $dt/d\tau = g$ with scale invariant functions g, however, we should note that the higher order accuracy in the approximation of self-similar solutions is lost in the use of such methods. Research is ongoing in the application and analysis of a-posteriori scale invariant methods.

5.3.4 Examples

Now we see how this theorem applies to our two examples. Firstly consider the blow-up equation

$$\frac{du}{dt} = u^2.$$

Taking $g(u) = 1/u$ we end up with the following rescaled equation

$$\frac{du}{d\tau} = u, \quad \frac{dt}{d\tau} = u^{-1}.$$

Now consider an implicit mid-point rule discretisation of this system, this gives the discrete system

$$u_{n+1} - u_n = \frac{\Delta\tau}{2}\left(u_n + u_{n+1}\right), \quad t_{n+1} - t_n = \frac{2\Delta\tau}{u_n + u_{n+1}}.$$

Now seek a discrete self-similar solution in the form of

$$u_n = z^{-n} V, \quad t_n = z^n.$$

Substituting gives

$$\left(z^{-(n+1)} - z^{-n}\right) V = \frac{\Delta\tau}{2} V \left(z^{-(n+1)} - z^{-n}\right), \quad z^{n+1} - z^n = \frac{2\Delta\tau}{V\left(z^{-(n+1)} + z^{-n}\right)}$$

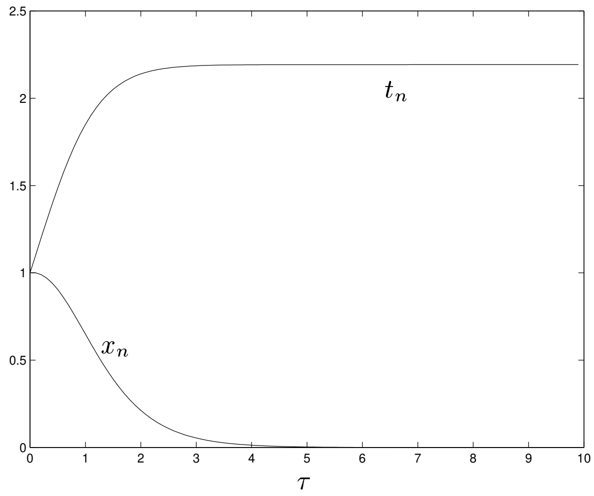

Figure 8: *Convergence properties of t_n and x_n as functions of τ.*

so that, dividing by factors of z^n we have

$$(1-z) = \frac{\Delta\tau}{2}(1+z), \quad \text{and} \quad z - 1 = \frac{2z\Delta\tau}{V(1+z)},$$

and hence

$$z = \frac{1-\Delta\tau/2}{1+\Delta\tau/2} \quad \text{and} \quad V = -(1-(\Delta\tau/2)^2).$$

Thus

$$t_n = \left(\frac{1-\Delta\tau/2}{1+\Delta\tau/2}\right)^n, \quad u_n = -(1-(\Delta\tau/2)^2)\left(\frac{1-\Delta\tau/2}{1+\Delta\tau/2}\right)^{-n},$$

so that

$$u_n = -(1-(\Delta\tau/2)^2)t_n^{-1}.$$

Now the true self-similar solution is $u = -1/t$ so that we see we have *uniformly* approximated this to an accuracy of $\Delta\tau^2$.

We now look at some results from an implementation of the forward Euler discretisation to solve the gravitational collapse problem with initial conditions $x = 1$ and $u = 0$, at (without loss of generality) $t = 1$. The true solution for these initial conditions is not self-similar, but it evolves towards a true self-similar solution as the collapse time T is approached.

In Figure 8 we plot t_n and x_n both as functions of τ. Observe that t_n tends towards the constant value of $T_{\Delta\tau}$ whilst x_n tends to zero. In Figure 9 we present a plot of x_n as a function of t_n in this case. Observe the singular nature of collapse of the solution.

Now compare these results with the theoretical predictions. Our transformed system (34) has the collapsing self-similar solution (from (32))

$$x = Re^{2\mu\tau/3}, \quad u = -ve^{-\mu\tau/3}, \quad t = T - e^{\mu\tau} \tag{36}$$

where

$$\mu = -\left(\frac{9}{2}\right)^{1/2}.$$

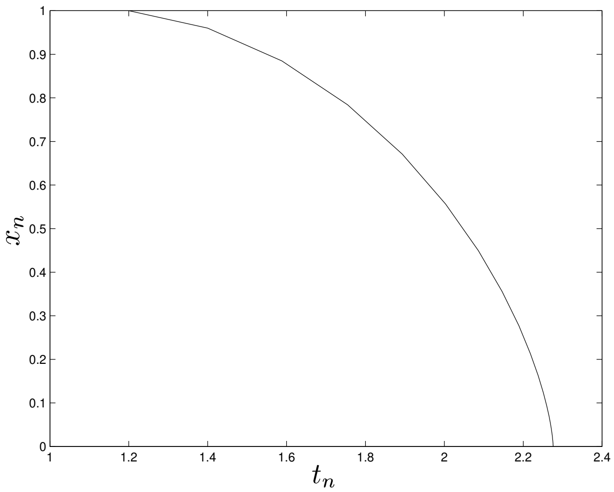

Figure 9: *The collapse of x_n as $t_n \to T_{\Delta\tau}$.*

Observe that as $\tau \to \infty$ we have $x \to 0$, $|u| \to \infty$ and $t \to T$, and that $t = T - 1$ at $\tau = 0$. Similarly our numerical scheme (35) admits a discrete collapsing self-similar solution of the form

$$x_n = \hat{X} z^{2n/3}, \quad u_n = -\hat{V} z^{-n/3}, \quad t_n = T_{\Delta\tau} - z^n.$$

Comparing with (36) we see that z is an analogue of $\exp(\mu\Delta\tau)$ if $n\Delta\tau = \tau$. Here $|z| < 1$ so that $x_n \to 0$, $|u_n| \to \infty$ and $t_n \to T_{\Delta\tau}$ as $n \to \infty$, (c.f. [35]). $T_{\Delta\tau}$ is a discrete collapse time which need not necessarily coincide with the true collapse time T, however as $\Delta\tau \to 0$ we have $T_{\Delta\tau} \to T$. Substituting into our forward Euler discretisation we find the values of the constants:

$\Delta\tau$	$\hat{X}$	$\hat{V}$	z
0.2	1.46704	1.04761	0.64461
0.1	1.55633	1.07440	0.80584
0.05	1.60298	1.08760	0.89852

notice that in agreement with the theory we have

$$\hat{X} = X(1 + \mathcal{O}(\Delta\tau)), \quad \hat{V} = V(1 + \mathcal{O}(\Delta\tau)), \quad z = e^{\mu\Delta\tau}(1 + \mathcal{O}(\Delta\tau^2))$$

where from (32) we have

$$X = 1.65096, \quad V = 1.100642,$$

and $\exp(\mu\Delta\tau)$ takes the values 0.65425, 0.80886, and 0.89937 for the three choices of $\Delta\tau$ above. See [26] for further results and examples.

6 A comparison of methods

To conclude this discussion on ordinary differential equations we now look at a comparison of different geometrically based methods (for example methods designed around the symplectic structure or around the scaling structure) applied to the same problem, and we also look at some non geometrical methods. In keeping with our earlier discussion we look at the Kepler two-body problem, which exhibits both a Hamiltonian structure as well as various symmetries, and study periodic solutions with high eccentricity where errors might be expected to be introduced during the close approaches.

We gave the Hamiltonian for Kepler's problem in equation (17), Hamilton's corresponding equations are

$$\dot{p}_i = -\frac{q_i}{(q_1^2 + q_2^2)^{3/2}}, \quad \dot{q}_i = p_i, \quad i = 1, 2. \tag{37}$$

We may think of q representing the position and p the velocity of a heavenly body moving (in a two-dimensional pane) around the sun positioned at the origin of our coordinate system. In our idealized state considered here both objects have the same mass. Throughout this section we take the initial conditions for this problem to be

$$q_1(0) = 1 - e,\ q_2(0) = 0,\ p_1(0) = 0,\ p_2(0) = \sqrt{\frac{1+e}{1-e}}$$

the exact solution is given by a conic section. We consider here the case of an ellipse (periodic solutions of period 2π), i.e. we consider eccentricities between zero and one, $0 \leqslant e < 1$. Along with the Hamiltonian which represents the total energy of the system, the angular momentum of the system given by $L(\mathbf{q}, \mathbf{p}) = q_1 p_2 - q_2 p_1$ is also a conserved quantity.

For this problem large forces are experienced close to the origin, i.e. when the planet passes close by the other (near-collision), whereas away from the origin the effect of the force is more sedate. From the standpoint of equidistributing the local truncation error of a numerical method between two adjacent time steps at any point on the orbit, it is often considered desirable to use a method which incorporates an adaptive time stepping strategy. In [129] symplectic methods with standard adaptive time stepping strategies are tested and disappointingly they are shown to behave in a non-symplectic way. Thus although an individual step of an individual orbit may be symplectic, the overall map on the whole of phase space may not be symplectic. Moreover, there is no obvious shadowing property, in that backward error analysis is hard to apply and the solution of the numerical method is not closely approximated by the solution of a nearby Hamiltonian system. As a consequence, the symplectic method with a (badly chosen) variable time step exhibits a quadratic rather than linear error growth for large times. For other discussions regarding this matter see [132, 134].

To overcome this problem we may consider other ways of varying the time step, and not concentrate exclusively on symplectic integrators. An obvious method for performing temporal adaptivity is through the Sundman transform we discussed in the previous section for preserving scaling symmetries. However, as we shall now see there is a problem with this approach for Hamiltonian problems (especially if our aim is to approximate invariant curves such as periodic orbits rather than singular behaviour). Kepler's problem is scaling invariant under the transformation

$$t \to \lambda t, \quad (q_1, q_2) \to \lambda^{2/3}(q_1, q_2), \quad (p_1, p_2) \to \lambda^{-1/3}(p_1, p_2),$$

for any arbitrary positive constant λ. Suppose that we perform the Sundman transform with the function

$$g = (q_1^2 + q_2^2)^{3/4}.$$

This gives the new, scale invariant, system

$$\frac{dp_i}{d\tau} = -q_i(q_1^2 + q_2^2)^{-3/4}, \quad \frac{dq_i}{d\tau} = p_i(q_1^2 + q_2^2)^{3/4}, \quad i = 1, 2. \tag{38}$$

However in general this procedure fails to preserve any Hamiltonian structure present in a problem. Since the function g has been chosen in a special way any numerical method applied to (38) will preserve the scaling invariance of the problem, as in the previous section. There would appear no particular reason to use a symplectic method on the transformed system. The question arises as to whether there is any way to construct a method which manages to preserve both the Hamiltonian and scaling invariance properties for problems such as Kepler's problem which possess them both.

Reich [121] and Hairer [68] combine the use of symplectic methods with adaptive time stepping through the use of the *Poincaré transformation*, see also [90]. Suppose that the original Hamiltonian H is time independent. Now, with $e = H(\mathbf{p}_0, \mathbf{q}_0)$ introduce a modified Hamiltonian $\hat{H}$ defined by

$$\hat{H}(\mathbf{p}, \mathbf{q}, t, e) = g(\mathbf{p}, \mathbf{q})\{H(\mathbf{p}, \mathbf{q}) - e\}, \tag{39}$$

the Hamiltonian system corresponding to $\hat{H}$ is given by

$$\begin{aligned}
\frac{d\mathbf{p}}{d\tau} &= -g\nabla_q H - \{H - e\}\nabla_q g, \\
\frac{d\mathbf{q}}{d\tau} &= g\nabla_p H + \{H - e\}\nabla_p g, \\
\frac{dt}{d\tau} &= g, \\
\frac{de}{d\tau} &= 0.
\end{aligned} \tag{40}$$

Here $(\mathbf{p}, t)^T$ and $(\mathbf{q}, e)^T$ are now conjugate variables in the extended phase space $\mathbb{R}^{2d} \times \mathbb{R}^2$. Along the *exact* solution of the problem $H(\mathbf{p}, \mathbf{q}) = e$, and thus the first two equations of (40) simply reduce in this case to a system transformed by using the Sundman transformation described earlier. We may thus think of the last terms in (40) as perturbations of the Sundman transformed system which make the system Hamiltonian. We can obviously now apply a symplectic method with fixed time step $\Delta\tau$ to the transformed system and the favourable properties of such methods should follow. Notice that the function g is performing exactly the same rôle that it did in the Sundman transform method of performing time reparameterization. The scale invariant choices for g derived above therefore also gives a Poincaré transformed system which is scale invariant without the need to scale τ.

For simplicity we discretise this system using the Symplectic Euler method to achieve a first-order symplectic method. The Poincaré transformation has the disadvantage that it destroys the separability property of the Hamiltonian and therefore the symplectic Euler method applied to this problem is implicit. We use Newton iteration to solve the nonlinear equations, however it is possible in this case to simply solve a quadratic equation, see Hairer [68].

For comparison we form a time-reversible, second order, angular momentum conserving method by applying the second-order Lobatto IIIa-b pair to the Sundman transformed system, the method is usually termed the adaptive Verlet method [79], see also [77, 90]. An explanation for the reciprocal choice of time step update is given in [38]. For the Kepler problem described earlier, with function g depending only on $\mathbf{q}$ this scheme can be

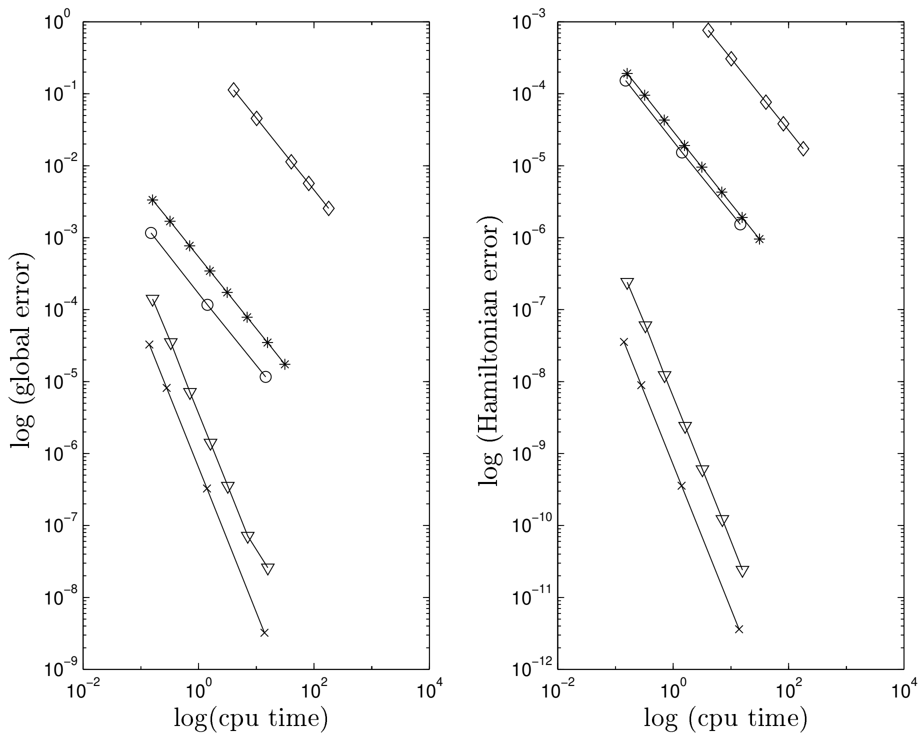

Figure 10: *Kepler problem with eccentricity of 0.5 for 10 orbits. Symplectic Euler ($\star$), Störmer-Verlet (∇), Sundman Symplectic Euler ($\diamond$), Poincare Symplectic Euler ($\circ$), adaptive Verlet Sundman ($\times$).*

written as (where $r = \sqrt{q_1^2 + q_2^2}$)

$$
\begin{aligned}
\mathbf{q}_{n+1/2} &= \mathbf{q}_n + \frac{\Delta\tau}{2\rho_n}\mathbf{p}_n \\
\rho_{n+1} &= \frac{2}{g(\mathbf{q}_{n+1/2})} - \rho_n \\
\mathbf{p}_{n+1} &= \mathbf{p}_n - \frac{\Delta\tau}{2}\left\{\frac{1}{\rho_n} + \frac{1}{\rho_{n+1}}\right\}\frac{\mathbf{q}_{n+1/2}}{r^3_{n+1/2}} \\
\mathbf{q}_{n+1} &= \mathbf{q}_{n+1/2} + \frac{\Delta\tau}{2\rho_{n+1}}\mathbf{p}_{n+1} \\
t_{n+1} &= t_n + \frac{\Delta\tau}{2}\left\{\frac{1}{\rho_n} + \frac{1}{\rho_{n+1}}\right\}
\end{aligned}
$$

In figure 10 we show the results of applying the SE and SV methods to the untransformed Kepler problem as well as SE and adaptive Verlet applied to the Sundman transformed system and SE applied to the Poincaré transformed system. For this experiment we only integrate for 10 orbits of eccentricity 0.5 — a fairly simple problem. Straight away we see the correct order for the methods with both the fixed and variable step size formulations. The adaptive methods which preserve either the symplectic or reversible properties can be seen to have better performance even for this problem where adaptivity is not vital for efficiency. However the symplectic Euler method applied to the Sundman transformed system demonstrates a definite reduction in performance, presumably due to the loss of both symplecticity and reversibility.

We perform a similar experiment in figure 11, this time for a higher eccentricity of 0.9,

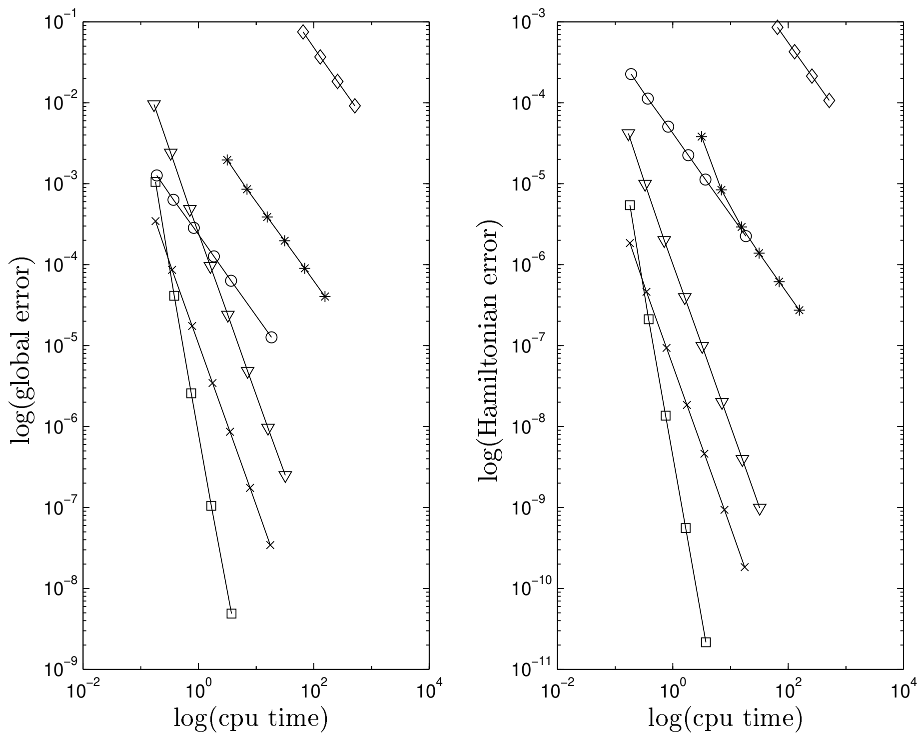

Figure 11: *Kepler problem with eccentricity of 0.9 for 10 orbits. Symplectic Euler ($\star$), Störmer-Verlet (∇), Sundman Symplectic Euler ($\diamond$), Poincare Symplectic Euler ($\circ$), adaptive Verlet Sundman ($\times$), Ruth's third order method ($\Box$).*

where adaptive methods should come into their own. We see the desired result of the adaptive methods designed to preserve symplecticity or reversibility performing well in comparison to their fixed step size counterparts. Again, the symplectic Euler method applied to the Sundman transformed system is seen to perform poorly. Ruth's third order method is also included for comparison purposes.

In figure 12 we again perform computations for the problem with eccentricity of 0.9, but now integrate over the much longer time scale of 1000 orbits. Again we see the improvements the use of adaptive time stepping affords, although this example clearly demonstrates that for high accuracy the use of high-order methods appears to be beneficial.

Finally in figure 13 we demonstrate the desirable linear error growth property of the methods which preserve symplecticity or reversibility applied to this problem. We also include the classical third-order Runge-Kutta method mentioned in a previous section, it can be seen to exhibit quadratic error growth demonstrating the fact that for long-term simulations a geometric integrator is to be preferred in many situations. Note that no effort has been made to choose fictive time steps in a consistent manner here, and therefore no conclusions regarding the relative accuracies of these methods should be inferred.

Similar experiments are carried out by Calvo et. al. in [30]. They come to the similar conclusion that for Hamiltonian problems a code based on high-order Gauss formulae with Poincaré transformations may outperform standard software.

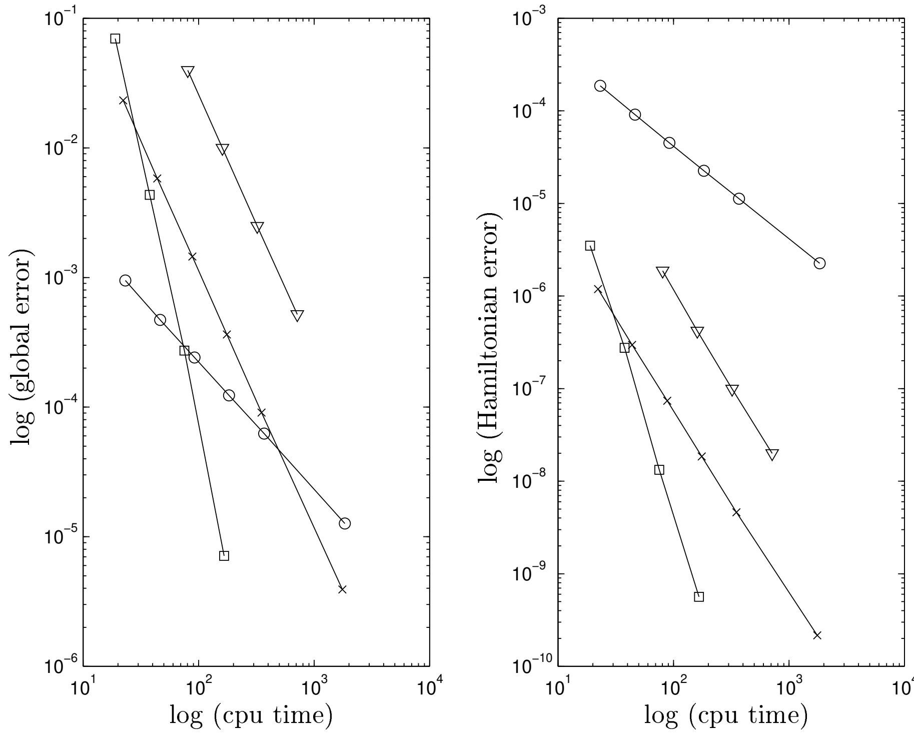

Figure 12: *Kepler problem with eccentricity of 0.9 for 1000 orbits. Störmer-Verlet (∇), Poincare Symplectic Euler ($\circ$), adaptive Verlet Sundman ($\times$), Ruth's third order method ($\Box$).*

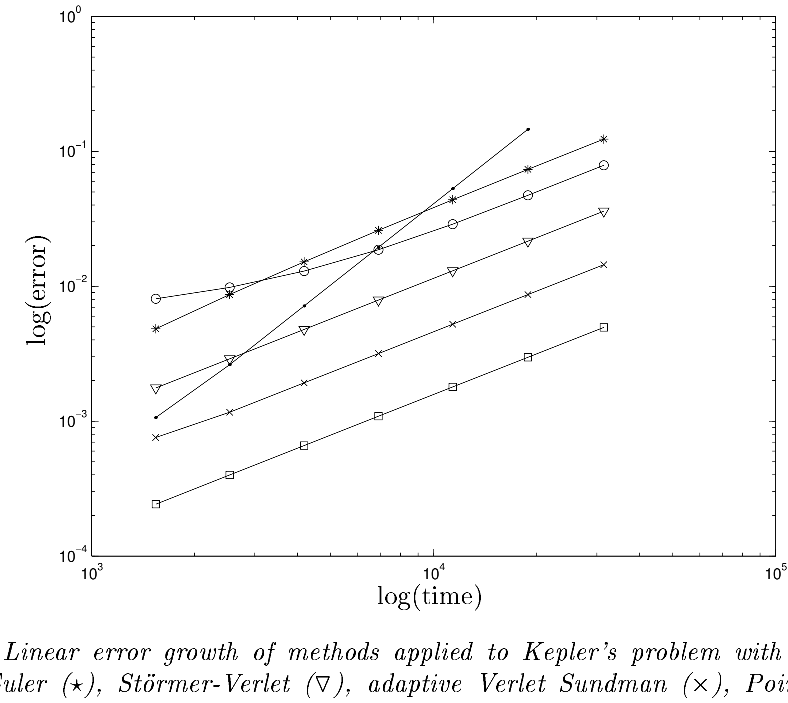

Figure 13: *Linear error growth of methods applied to Kepler's problem with eccentricity 0.5. Symplectic Euler ($\star$), Störmer-Verlet (∇), adaptive Verlet Sundman ($\times$), Poincare Symplectic Euler ($\circ$), Ruth's third order method ($\Box$). For comparison third-order classical Runge-Kutta ($\cdot$) is shown, clearly exhibiting quadratic error growth.*

7 Partial differential equations

There has been far less treatment of partial differential equations in the geometric integration literature than that of ordinary differential equations. Indeed the excellent accounts of geometric integration by Hairer [69], McLachlan & Quispel [107] and by Sanz-Serna [128] do not mention PDEs at all. For certain types of PDE (eg. strongly hyperbolic) this is understandable as they represent significantly more complex systems than ODEs and when discretised as systems of ODEs are far more complex to work with and are usually stiff — containing widely different timescales. On the other hand, it is precisely geometrically based methods which are well placed to deal with them as the spatial variation implicit in such problems adds a very strong geometric structure to the ODE systems which we can subsequently exploit. An important example of this is an extension of the symmetry group methods described in Section 5.3 to include the spatial variable so that we strongly couple spatial and temporal structures. Here adaptivity plays a central rôle in all of our calculations — indeed adaptivity finds a natural geometrical setting. We start our discussion however by looking at Hamiltonian PDEs and then at PDEs with a Lagrangian structure.

7.1 Symplectic methods for Hamiltonian PDEs

Many partial differential equations can be put into a Hamiltonian formulation and admitted symmetries of this formulation can lead, via Noether's theorem, to conservation laws. There are several approaches aimed at exploiting this structure in discretisations of the equations, all of which can loosely be labelled geometrical. One is based upon using the Hamiltonian formulation of the PDEs on multi-symplectic structures, generalising the classical Hamiltonian structure by assigning a distinct symplectic operator for each space direction and time [18], [19], [122]. Variational integrators [99] (see also the next section) generalise Veselov-type discretisations of PDEs in variational form. In this section we will look at methods for discretising the Hamiltonian PDEs using a Poisson bracket approach and/or various splitting methods. In sections 9 and 10 we look at the use of semi-discretisations (in space) of the equations and discrete analogues of Noether's theorem.

7.1.1 Basic theory

Here we summarise some of the ideas presented in the monograph by Olver [118].
Many differential equations of the form

$$\mathbf{u}_t = \mathbf{F}(x, \mathbf{u}, \mathbf{u}_x, \mathbf{u}_{xx}, ..)$$

can be represented in the Hamiltonian form

$$\mathbf{u}_t = \mathscr{D}\left(\frac{\delta \mathscr{H}}{\delta \mathbf{u}}\right), \quad \mathscr{H}[\mathbf{u}] = \int H(x, \mathbf{u}, \mathbf{u}_x, ..)\, dx.$$

Typically the domain of integration in the above is the real line or the circle (corresponding to periodic boundary conditions for the PDE). In this expression $\mathscr{H}$ is a functional map from the function space in which $\mathbf{u}$ is defined to the real line. The variational (or functional) derivative $\delta\mathscr{H}/\delta\mathbf{u}$ is the function defined via the Gateaux derivative

$$\left(\frac{d}{d\varepsilon}\mathscr{H}[\mathbf{u} + \varepsilon\mathbf{v}]\right)_{\varepsilon=0} = \int \frac{\delta \mathscr{H}}{\delta \mathbf{u}}\, v\, dx,$$

so that if u is a scalar function and $H \equiv H(u, u_x)$ then

$$\frac{\delta \mathscr{H}}{\delta u} = \frac{\partial H}{\partial u} - \frac{\partial}{\partial x}\left(\frac{\partial H}{\partial u_x}\right).$$

The operator $\mathscr{D}$ is *Hamiltonian* if given the functionals $\mathscr{P}[\mathbf{u}]$ and $\mathscr{L}[\mathbf{v}]$ it generates a Poisson bracket $\{.,.\}$ given by

$$\{\mathscr{P}, \mathscr{L}\} = \int \frac{\delta \mathscr{P}}{\delta \mathbf{u}} \cdot \mathscr{D} \frac{\delta \mathscr{L}}{\delta \mathbf{u}}\, dx.$$

Where the Poisson bracket must satisfy the skew symmetry condition

$$\{\mathscr{P}, \mathscr{L}\} = -\{\mathscr{L}, \mathscr{P}\}$$

and the Jacobi identity

$$\{\{\mathscr{P}, \mathscr{L}\}, \mathscr{R}\} + \{\{\mathscr{L}, \mathscr{R}\}, \mathscr{P}\} + \{\{\mathscr{R}, \mathscr{P}\}, \mathscr{L}\} = 0,$$

for all functionals $\mathscr{P}$, $\mathscr{L}$ and $\mathscr{R}$.

The Hamiltonian partial differential equation describing the time evolution of the system is then given by

$$\mathbf{u}_t = \{\mathbf{u}, \mathscr{H}\}.$$

Such Hamiltonian systems have invariants (Casimirs) which are functionals $\mathscr{C}$ which satisfy

$$\{\mathscr{C}, \mathscr{F}\} = 0 \quad \text{for all functionals} \quad \mathscr{F},$$

and so these invariants are not associated with properties of the Hamiltonian, they arise through any degenerate nature of the Poisson structure. In particular, Casimirs are conserved during the evolution. The Hamiltonian functional $\mathscr{H}$ is conserved when it is not explicitly dependent on time.

We now give three examples of such PDEs which we will refer to throughout this section.

Example 1 The nonlinear wave equation.

In this case $\mathbf{u} = (p, q)^T$, $\mathscr{D}$ is the *canonical* Poisson operator given by

$$\mathscr{D} = \begin{bmatrix} 0 & -1 \\ 1 & 0 \end{bmatrix} \quad \text{and} \quad H = \frac{p^2}{2} + \frac{q_x^2}{2} + V(q).$$

Thus, the partial differential equation is then

$$\begin{pmatrix} p_t \\ q_t \end{pmatrix} = \begin{pmatrix} -\delta\mathscr{H}/\delta q \\ \delta\mathscr{H}/\delta p \end{pmatrix} = \begin{pmatrix} q_{xx} - V'(q) \\ p \end{pmatrix}.$$

Example 2 The KdV equation.

This integrable equation is used to describe the motion of water waves in long channels. It has soliton solutions which can be determined by using the inverse scattering transformation. It is described in detail in Drazin and Johnson's monograph on solitons [49]. In this case

$$\mathscr{D} = \frac{\partial}{\partial x} \quad \text{and} \quad H = -\frac{u^3}{6} + \frac{u_x^2}{2}.$$

The associated PDE is then

$$u_t = \frac{\partial}{\partial x}\left(\frac{\delta \mathscr{H}}{\delta u}\right) = \frac{\partial}{\partial x}\left(-\frac{u^2}{2} - u_{xx}\right)$$

so that

$$u_t + u u_x + u_{xxx} = 0.$$

Example 3 The one-dimensional nonlinear Schrödinger equation.

This is an important example of an integrable PDE which models the modulational instability of water waves and is also used to describe the dynamics of lasers and of nonlinear optics. In a later section we will look at cases of determining the singular solutions for this equation posed in three dimensions which have a rather different behaviour from the soliton solutions which occur in one dimension.

In the one-dimensional case we take $u = (\psi, \bar{\psi})^T$ where ψ and $\bar{\psi}$ are treated as independent variables, we take $\mathscr{D}$ to be i times the canonical Poisson operator and

$$H(\psi, \bar{\psi}) = \psi_x \bar{\psi}_x - \frac{1}{2}\psi^2 \bar{\psi}^2.$$

The corresponding partial differential equation is then given by

$$i\psi_t = \frac{\delta \mathscr{H}}{\delta \bar{\psi}} = -\psi_{xx} - \psi|\psi|^2.$$

This system has many conserved quantities including $\mathscr{H}$, $\int |u|^2 \, dx$ and

$$\int |\psi_{xx}|^2 + 2|\psi|^6 - 6|\psi_x|^2|\psi|^2 - ((|\psi|^2)_x)^2 \, dx.$$

Hamiltonian wave equations of the form described in the examples above have been studied in great detail by many authors. An excellent survey of results and methods is given by McLachlan in [103]. The basic approach suggested by these authors is to discretise $\mathscr{H}$ and $\mathscr{D}$ separately to obtain a symplectic set of ordinary differential equations. In this paper McLachlan recommends that (pseudo) spectral methods should be used whenever possible to discretise the equations in space, in particular differential operators such as $\mathscr{D}$ (in the KdV example) as finite differences introduce excessive dispersion into the system. Indeed, it is considered essential that the higher modes typically present in Hamiltonian PDEs should be correctly resolved.

The resulting system of ordinary differential equations can then be integrated using a symplectic method, typically based upon one of the splitting methods described in Section 3. Two types of splitting can be considered, both based upon a natural decomposition of the Hamiltonian. If $\mathbf{u} = (p, q)^T$ and $\mathscr{H} = T(p) + V(q)$ then a $P - Q$ splitting can be used exactly as before, with explicit time integration at each stage.

An alternative, potentially more stable, and certainly recommended method is to use an $L - N$ splitting. In this it is assumed that $\mathscr{H}$ can be decomposed as

$$H(\mathbf{u}) = L(\mathbf{u}) + N(\mathbf{u})$$

where L corresponds to the linear dynamics of the partial differential equation associated with the higher order derivatives and N is typically a nonlinear operator associated with lower order derivatives. In this case the time flow of the vector field corresponding to L is typically integrated by using a Fourier transform.

It is significant that Casimirs, which are invariants of the flow, are in general conserved by symplectic splitting methods. This is a natural consequence of the results described in Section 4.

We now describe two examples of the use of these methods taken from [103].

Example 1 The nonlinear wave equation.

As described above this is given by

$$\frac{\partial q}{dt} = p, \quad \frac{\partial p}{dt} = q_{xx} - V'(q),$$

and we consider this with periodic boundary conditions on the interval $[0, 2\pi]$. A convenient way of discretising the Hamiltonian formulation of this equation is to use a spectral method. Accordingly, applying a full spectral decomposition in space gives

$$p(x,t) = \sum_m p_m(t)e^{imx}, \quad q(x,t) = \sum_m q_m(t)e^{imx}.$$

Substituting into the partial differential equation leads to the following system of ordinary differential equations

$$\dot{q}_m = p_m, \quad \dot{p}_m = m^2 q_m - \frac{1}{2\pi}\int_0^{2\pi} V'\left(\sum q_k e^{ikx}\right) e^{-imx}\, dx.$$

This system is canonically Hamiltonian, with conjugate variables q_m and p_{-m} and Hamiltonian

$$H = \frac{1}{2}p_0^2 + \sum_{m\neq 0}(p_m p_{-m} + m^2 q_m q_{-m} + \frac{1}{2\pi}\int_0^{2\pi} V\left(\sum q_m e^{imx}\right)\, dx.$$

Note that the function H above is simply $\mathscr{H}/2\pi$ where $\mathscr{H}$ is defined as in the example and the operator $\mathscr{D}$ is the same in both cases. McLachlan suggests that this system should be discretised by truncating p, q (and hence H) to a finite number of modes and evaluating the integral inside H by using a trapezoidal quadrature rule. This leads to the Hamiltonian system

$$\dot{q}_m = p_m, \quad \dot{p}_m = -m^2 q_m - (FV'(F^{-1}q))_m,$$

where F is the discrete Fourier transform used to map between Fourier space and the solution space. Difficulties arise in this discretisation due to aliasing of the nonlinear terms, which can be reduced by padding the solution with zeros.

Both the $P - Q$ and the $L - N$ splittings may be used on this system. For the $P - Q$ splitting we can use an explicit Störmer-Verlet method exactly as before. For the $L - N$ splitting the problem is decomposed as

$$L: \quad \dot{q}_m = p_m, \quad \dot{p}_m = -m^2 q_m$$

and

$$N: \quad \dot{q}_m = 0, \quad \dot{p}_m = -(FV'(F^{-1}q))_m.$$

In this splitting, the linear system L is the harmonic oscillator and can be integrated explicitly. Similarly the nonlinear system N has a trivial integral. It is shown in [103] that for weakly nonlinear problems the $L-N$ splitting has both a smaller truncation error and no linear stability limit, making them generally preferable to $P-Q$ splittings.

Example 2 The nonlinear Schrödinger equation

We consider again the one-dimensional NLS equation

$$i\psi_t + \psi_{xx} + \psi|\psi|^2 = 0, \quad \psi(0,t) = \psi(L,t).$$

This partial differential equation is integrable and can be solved by using the inverse scattering transform [49]. It admits plane wave solutions $\psi = \exp(2i|a|^2 t)a$ and in the symmetric case with $\psi(x,t) = \psi(L-x,t)$ it also admits homoclinic (localised wave-packet type) orbits connecting the periodic orbits which have fine spatial structure. It is possible to devise discretisations of the equation which are themselves integrable [2] and the latter authors recommend this approach when resolving the structure of the homoclinic solutions. If instead a standard Runge-Kutta-Merson method in time is used together with a central difference discretisation in space then there is a rapid flow of energy into the high frequencies due to poor resolution of the spatial structure, and temporal chaos in the time-series (a phenomenon not present in the underlying system). In both cases the spatial mesh introduces a large perturbation from integrability.

Instead a symplectic (integrable) method based on the $L-N$ splitting can be used in the form

$$L: \quad i\psi_t + \psi_{xx} = 0, \quad N: \quad i\psi_t + \psi|\psi|^2 = 0.$$

In [103] a spectral decomposition to integrate the linear evolution equation L in Fourier space is used rather than the discrete Fourier transform, the nonlinear equation N is integrated in real space. In both cases the time integration can be performed using a symplectic method such as the Störmer-Verlet method.

8 Lagrangian and action based methods for PDEs

Variational integrators for a variety of problems, including Hamiltonian ones, can be constructed from a discrete version of Lagrangian mechanics, based on a discrete variational principle. They have the advantage that much of the structure of Lagrangian systems can be replicated on a discrete level, with variational proofs (such as Noether's theorem) extending from the continuous to the discrete setting. When applied to PDEs they can give rise to a natural multi-symplectic setting. For ODEs they lead to many symplectic rules such as the Störmer-Verlet method, the Newmark method in structural dynamics and the Moser-Veselov method for integrating the equations of motion for a rigid body considered earlier. A very complete account of these methods is given in the review by Marsden and West [99].

To give an example of the application of Lagrangian based methods, the methods described in the previous section can be extended to a wider class of partial differential equations satisfying Dirichlet, Neumann or periodic boundary conditions that are derived as variational derivatives of a suitable energy function $\mathscr{G}(u, u_x)$ in the manner

$$u_t = \left(\frac{\partial}{\partial x}\right)^{\alpha} \frac{\delta \mathscr{G}}{\delta u}, \tag{41}$$

where we define an analogous function $\mathscr{G}$ to the Hamiltonian $\mathscr{H}$ by

$$\mathscr{G}(u) = \int G(u)\, dx$$

and assume that u satisfies the following boundary condition

$$\left[\frac{\partial G}{\partial u_x}\frac{\partial u}{\partial t}\right]_0^L = 0,$$

which is true for problems with Dirichlet, natural or periodic boundary conditions.

This class of partial differential equations includes some of the Hamiltonian examples described earlier, for example the first order wave equation

$$u_t = u_x, \quad \text{where} \quad G(u) = \frac{u^2}{2}, \quad \alpha = 1,$$

and the KdV equation

$$u_t = \frac{\partial}{\partial x}\left(\frac{u^2}{2} + u_{xx}\right), \quad \text{where} \quad G = \frac{u^3}{6} - \frac{u_x^2}{2}, \quad \alpha = 1.$$

In particular, if α is *odd* then

$$\frac{\partial \mathscr{G}}{\partial t} = 0. \tag{42}$$

However, this class also includes other dissipative (non Hamiltonian) problems such as the nonlinear diffusion equation

$$u_t = (u^n)_{xx}, \quad \text{where} \quad G = -\frac{u_x^{n+1}}{n+1}, \quad \alpha = 0,$$

and the Cahn-Hilliard equation

$$u_t = (pu + ru^3 + qu_{xx})_{xx},$$

where

$$G = \left(p\frac{u^2}{2} + r\frac{u^4}{4} - q\frac{u_x^2}{2}\right), \quad p < 0,\ q < 0,\ r > 0, \quad \alpha = 2.$$

Indeed, when α is even we have

$$(-1)^{\alpha/2+1}\frac{\partial \mathscr{G}}{\partial t} \leqslant 0. \tag{43}$$

This broader class of problems is considered by Furihata [57] and we consider his derivation of a discretisation for this class of problems here. In particular Furihata considers schemes which preserve the conditions (42,43) together with certain other conserved quantities. For a very complete discussion of integrators based upon action integrals, see the review article [99]

To derive a geometrically based method, Furihata considers that the integral $\mathscr{G}$ be replaced by a discrete trapezium rule sum $\mathscr{G}_d$ of a discrete form G_d of G in which u_x is replaced by a suitable finite difference equivalent. Note that this differs from the methods considered by McLachlan. Following this procedure we obtain

$$J_d(U) = T\sum_{k=0}^{N} G_d(U)_k \Delta x$$

where the operator $T\sum_{k=0}^{N} f_k$ refers to the Trapezium rule sum

$$\left(\frac{1}{2}f_0 + \sum_{k=1}^{N-1} f_k + \frac{1}{2}f_N\right).$$

The operation of integration by parts (and its repeated applications) can then be replaced under this discretisation by the operation of summation by parts (and its repeated applications). This is a crucial observation as it allows many of the properties of the variational derivative to be directly inherited by the discretisation. In particular the summation by parts identity

$$T\sum_{k=0}^{N} f_k(\delta_k^+ g_k)\Delta x + T\sum_{k=0}^{N}(\delta_k^- f_k) g_k \Delta x = \left[\frac{f_k(s_k^+ g_k) + (s_k^- f_k) g_k}{2}\right]_{k=0}^{N}$$

where, for the sequence $f_1, f_2, \ldots f_k, \ldots$ we have operators

$$s_k^+ f_k = f_{k+1}, \quad s_k^- f_k = f_{k-1}, \quad \delta_k^+ f_k = \frac{f_{k+1} - f_k}{\Delta x}, \quad \delta_k^- f_k = \frac{f_k - f_{k-1}}{\Delta x}.$$

By doing this the discrete variation in G_d can be calculated to satisfy the identity

$$\mathscr{G}_d(U) - \mathscr{G}_d(V) = T\sum_{k=0}^{N} \frac{\delta \mathscr{G}_d}{\delta(U,V)_k}(U_k - V_k)\Delta x,$$

where the variational derivative is replaced by a discrete analogue $\delta\mathscr{G}_g/\delta(U,V)_k$. The derivation of the expression for the variational derivative is a key result given in [57] and can be expressed most easily for discrete functionals of the form

$$G_d(U)_k = \sum_{l=1}^{m} f_l(U_k) g_l^+(\delta_k^+ U_k) g_l^-(\delta_k^- U_k),$$

where f, g^+, g^- are arbitrary functions. By repeated application of summation by parts it can be shown that the variational derivative of $\mathscr{G}_d$ has (for this formulation) the following discrete form

$$\frac{\delta \mathscr{G}_d}{\delta(U,V)_k} = \sum_{l=1}^{m}\left(\frac{df_l}{d(U_k,V_k)} \frac{g_l^+(\delta_k^+ U_k) g_l^-(\delta_k^- U_k) + g_l^+(\delta_k^+ V_k) g_l^-(\delta_k^- V_k)}{2}\right.$$
$$\left. - \delta_k^+ W_l^-(U,V)_k - \delta_k^- W_l^+(U,V)_k\right). \tag{44}$$

Here the functions W above correspond to the derivative of G with respect to u_x so that

$$W_l^+(U,V)_k = \left(\frac{f_l(U_k) + f_l(V_k)}{2}\right)\left(\frac{g_l^-(\delta_k^- U_k) + g_l^-(\delta_k^- V_k)}{2}\right)\frac{dg_l^+}{d(\delta_k^+ U_k, \delta_k^+ V_k)},$$

$W_l^-(U,V)$ is defined similarly with all signs reversed and

$$\frac{df}{d(a,b)} = \frac{f(a) - f(b)}{a - b} \quad \text{if} \quad a \neq b,$$

and

$$\frac{df}{d(a,b)} = \frac{df}{da} \quad \text{if} \quad a = b.$$

The expression (44) gives a discrete representation of the variational derivative when finite difference methods are applied. The differential equation can then be discretised in space by replacing the right hand side of the original equation (41) by the discrete variational derivative (44) and a suitable time discretisation then used for the left hand side. In its simplest form this leads to the discrete evolutionary equation

$$\frac{U_k^{(n+1)} - U_k^{(n)}}{\Delta t} = \delta_k^{<\alpha>} \frac{\delta \mathscr{G}_d}{\delta(U^{(n+1)}, U^{(n)})_k}, \tag{45}$$

where

$$\delta_k^{<1>} = \frac{s_k^+ - s_k^-}{2\Delta x}, \quad \delta_k^{<2>} = \frac{s_k^+ - 2 + s_k^-}{\Delta x^2}, \quad \delta_k^{<2m+1>} = \delta_k^{<1>}\delta_k^{<2m>}.$$

It is shown in [57] that if α is odd then both $\mathscr{G}$ *and* $\mathscr{G}_d$ are conserved during the evolution along with the total discrete mass $T\sum U_k \Delta x$ if the continuous mass is also conserved.

In contrast, if α is *even* then both $\mathscr{G}$ and $\mathscr{G}_d$ decrease along solution trajectories and hence both the underlying problem and its discretisation are dissipative.

Example Following [57] we consider the KdV equation as given by

$$u_t = \frac{\partial}{\partial x}\left(\frac{u^2}{2} + u_{xx}\right), \quad G(u, u_x) = \frac{1}{6}u^3 - \frac{1}{2}u_x^2,$$

together with periodic boundary conditions

$$u(x+L, t) = u(x, t).$$

The KdV equation conserves both $\mathscr{G}$ and the total mass of the solution and it is integrable by means of the inverse scattering transformation, with soliton solutions. Many numerical methods to integrate the KdV equation have been considered, some of which share many of the properties of the splitting methods for the nonlinear wave equation described in the last section. A selection of these methods are described in [56, 65, 61, 76, 92, 120, 126, 140, 148].

To construct a numerical method for integrating the KdV equation which is directly based on the action integral, we start with a 'natural' discretisation G_d of G given by

$$G_d(U)_k = \frac{1}{6}(U_k)^3 - \frac{1}{2}\frac{(\delta_k^+ U_k)^2 + (\delta_k^- U_k)^2}{2}.$$

From this it immediately follows that

$$\frac{\delta \mathscr{G}_d}{\delta(U^{(n+1)}, U^{(n)})_k} = \frac{1}{2}\frac{\left(U_k^{(n+1)}\right)^2 + U_k^{(n+1)}U_k^{(n)} + \left(U_k^{(n)}\right)^2}{3} + \delta_k^{<2>}\frac{U_k^{(n+1)} + U_k^{(n)}}{2}.$$

Following the procedure described above then leads to the following implicit scheme

$$\begin{aligned}\frac{U_k^{(n+1)} - U_k^{(n)}}{\Delta t} = \delta_k^{<1>} \Bigg(& \frac{1}{2}\frac{\left(U_k^{(n+1)}\right)^2 + U_k^{(n+1)}U_k^{(n)} + \left(U_k^{(n)}\right)^2}{3} \\ & + \delta_k^{<2>}\frac{U_k^{(n+1)} + U_k^{(n)}}{2}\Bigg).\end{aligned} \tag{46}$$

This scheme conserves both the integrals of G and of u during the evolution, although it is not symplectic. In [57] it is claimed that (46) is unconditionally stable although no proof is given.

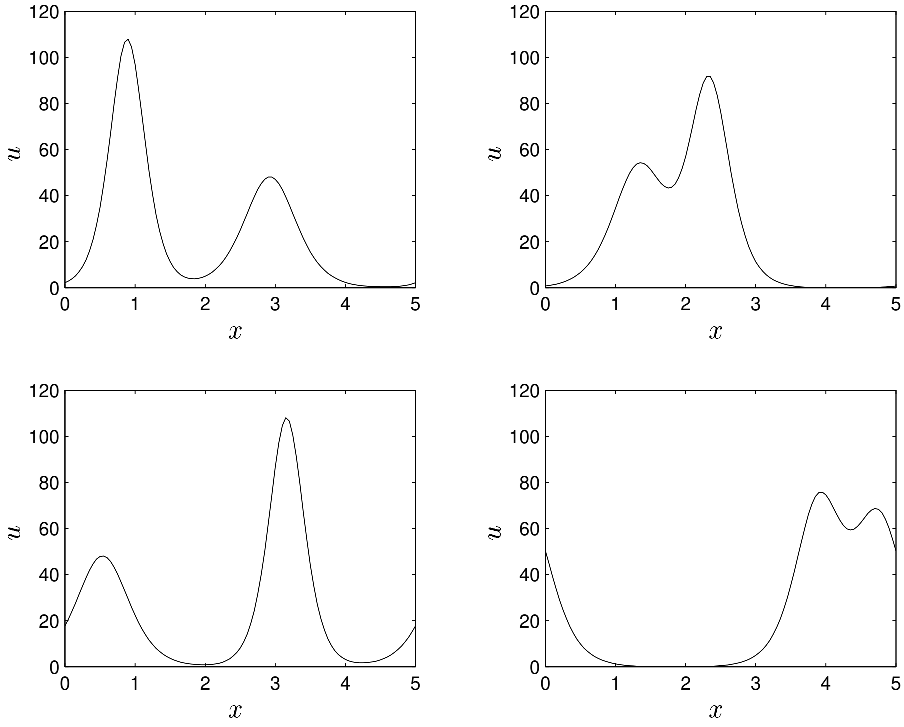

Figure 14: *Interaction of two solitons obtained using the scheme (46).*

In figure 14 we present a calculation of the evolution of the KdV system comprising two colliding solitons which is obtained using the above method in which we take interval of $[0, 5]$ a discrete step size $\Delta x = 5/100$ and a discrete time step of $\Delta t = 1/2000$. The implicit equations in (46) were solved at each time step using the Powell-hybrid solver SNSQE.

This rather brief survey has not included a detailed discussion about suitable treatments of the various types of boundary conditions encountered in the partial differential equations described by such actions. For more details on this topic see [57] and the references therein. Further application of the method described in [57] to a series of nonlinear wave equations and also to the Cahn-Hilliard equation are given in [58], [59], [100], [101]. In [99] variationally based methods for many other PDE problems are discussed, including the development of circulation preserving integrators for fluid systems.

9 Methods for partial differential equations that preserve all symmetries

In this section we review some of the work of Dorodnitsyn and his co-workers in studying methods, fully invariant under the action of all symmetries. Whereas the two previous sections have considered discretisations with a *constant* spatial mesh, we now relax this condition to allow for meshes which vary in both space and time.

As discussed earlier, symmetries are fundamental features of the differential equations of mathematical physics and if possible should be retained when the equations are discretised on either a fixed or an adaptive mesh.

In a very similar manner to that discussed earlier, we can consider the action of Lie point symmetries on a partial differential equation. Dorodnitsyn lists the following reasons for considering the action of such symmetries:

- The group action transforms one set of solutions into another.
- There exists a standard procedure [118] for obtaining (differential) invariants for a symmetry group. This can allow a reduction of the PDE to an ODE under certain circumstances (for example we can study self-similar solutions).
- The action of the symmetry can reduce the order of the equation.
- The invariance of the PDE is a necessary condition for the application of Noether's theorem on variational problems to obtain conservation laws. We return to this point later in this section.
- Lie point transformations have a clear geometrical interpretation and one can construct the orbits of a group in a finite dimensional space of independent and dependent variables.

Dorodnitsyn and his group have concentrated on constructing adaptive mesh methods that inherit all symmetries of the system. We describe these here and in the next section the use of them in finding discrete analogues of Noether's theorem. In the section after that we look at the special case of scaling symmetries.

Suppose that the partial differential equation in which we consider u to be a function of x and t which is to be discretised is given by

$$F(x, t, u_t, u, u_x, u_{xx}) = 0. \tag{47}$$

In the section on ordinary differential equations we studied the action of Lie groups on a manifold. Similarly we can consider a Lie group to act on this partial differential equation noting that the action of the group is now to couple the temporal and the spatial structures. The action of the Lie point transformations on then can be considered by looking at the one-parameter transformation groups given by

$$X = \xi^t \frac{\partial}{\partial t} + \xi^x \frac{\partial}{\partial x} + \eta \frac{\partial}{\partial u} + \dots .$$

Here the functions ξ^x, ξ^t and η are considered to be functions of t, x and u.

The case of constant functions ξ^x, ξ^t and η corresponds to an invariance of the partial differential equation to translations in the appropriate variables, for example any autonomous differential equation is invariant under the translation $t \to t + T$ generated by the action $X = \partial_t$ and, for example the wave equation is invariant under spatial translations of the form $x \to x + L$ generated by the action $X = \partial_x$. (Solutions invariant under the two actions are simply travelling waves.)

The case of linear functions

$$\xi^t = \alpha t, \quad \xi^x = \beta x, \quad \text{and} \quad \eta = \gamma u,$$

corresponds to scaling symmetries of the form

$$t \to \lambda^\alpha t, \quad x \to \lambda^\beta x, \quad u \to \lambda^\gamma u,$$

which were considered earlier in the context of ODEs and presently in the context of PDEs.

In general, the group generated by X transforms a solution point $(x, t, u, u_t, u_x, u_{xx})$ to a new one and also transforms the associated partial differential equation.

Dorodnitsyn et. al. consider discretising (47) on a mesh comprising a finite set of points in time and space $z^1, z^2 \ldots$ to give a difference equation

$$F(z) = 0. \tag{48}$$

Now, when discretising any partial differential equation using a finite difference or a finite element method it is essential to also define a mesh. This mesh should ideally also reflect the underlying symmetries of the differential equation. In particular, suppose that the mesh is defined by an equation of the form

$$\Omega(z, h) = 0. \tag{49}$$

If we seek a discretisation of the differential equation which is invariant to the Lie group action then both the difference scheme (48) and the mesh equation (49) need to be invariant under the action of the group. In particular we require the two conditions

$$XF(z) = 0 \quad \text{and} \quad X\Omega(z, h) = 0 \tag{50}$$

to be satisfied iff $F = \Omega = 0$. If this can be done (and this is a significant challenge) for *all* the possible invariant group actions then the method is termed *fully invariant*. More usually it can only be achieved for a subset of the possible group actions.

Dorodnitsyn et. al. specifically consider the use of uniform grids that are invariant under all group actions. We relax this condition in the next section, but consider their approach in more detail here. A uniform mesh is given when the left spatial step at any point in space equals the right spatial step so that

$$h^+ = h^-.$$

We note that a *uniform* mesh, in which the mesh spacing can evolve with time, should not be confused with a *constant* mesh which does not evolve with time.

In this case we can define D_{+h} and D_{-h} as right and left difference derivative operators with corresponding shift operators S_{+h} and S_{-h}. It is shown in [44], see also [5] that the exact representation of total differentiation D_x in the space of difference operators is then given by a prolonged form of the above given by

$$D^+ = \frac{\partial}{\partial x} + \hat{D}_{+h}\frac{\partial}{\partial u} + \ldots, \quad \hat{D}_{+h} = \sum_{n=1}^{\infty} \frac{(-h)^{n-1}}{n} D^n_{+h}.$$

If the symmetry group action is given by the one-parameter transformation group generated by the operator

$$X = \xi^x \frac{\partial}{\partial x} + \eta \frac{\partial}{\partial u}$$

then the action of this must be prolongated on the discrete mesh to give

$$X = \xi^x \frac{\partial}{\partial x} + \eta \frac{\partial}{\partial u} + \ldots + \left[S_{+h}(\xi^x) - \xi^x\right] \frac{\partial}{\partial h^+} + \left[\xi^x - S_{-h}(\xi^x)\right] \frac{\partial}{\partial h^-}.$$

A *uniform* mesh then retains its invariance under this prolonged action if

$$S_{+h}(\xi^x) - 2\xi^x + S_{-h}(\xi^x) = 0 \quad \text{or} \quad D_{+h}D_{-h}(\xi^x) = 0.$$

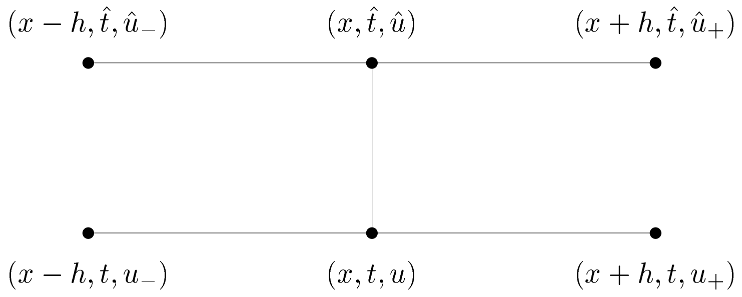

Figure 15: Stencil for an orthogonal mesh

Similarly it is uniform under the action of the operator η^t (in time) if

$$D_{+\tau}D_{-\tau}(\xi^t) = 0,$$

where $+\tau$ and $-\tau$ are temporal time steps. It is often desirable that orthogonality should also be preserved under the action of the group. It is shown in [45] that a necessary and sufficient condition for this is that

$$D_{+h}(\xi^t) + D_{+\tau}(\xi^x) = 0.$$

A further simple condition, given by

$$D_{+h}D_{+\tau}(\xi^t) = 0,$$

preserves the flatness of a layer of the grid in the time direction.

Example 1 Nonlinear diffusion with a source.

We discuss here an example investigated by Dorodnitsyn and Kozlov [48] (see also [87]) with regard to a fully invariant discretisation. In the next section we look at the same problem using an equidistribution based method.

The nonlinear diffusion equation with a source describes the diffusion and reaction of a chemical in a porous medium. For example the flow of pollutant materials through rock. It is given by the equation

$$u_t = (u^\sigma u_x) + au^n. \tag{51}$$

It admits two translation groups and one scaling group given by

$$X_1 = \frac{\partial}{\partial t}, \quad X_2 = \frac{\partial}{\partial x}, \quad X_3 = 2(n-1)t\frac{\partial}{\partial t} + (n-\sigma-1)x\frac{\partial}{\partial x} - 2u\frac{\partial}{\partial u}.$$

This set satisfies the conditions for a uniform, orthogonal mesh. The operators for the stencil and the mesh are given in figure 15.

Corresponding to time translation, space translation and scaling we have seven difference invariants of the Lie algebra given by

$$\frac{\hat{u}}{u}, \quad \frac{u_+}{u}, \quad \frac{u_-}{u}, \quad \frac{\hat{u}_+}{\hat{u}}, \quad \frac{\hat{u}_-}{\hat{u}}, \quad \frac{\tau^{\frac{n-\sigma-1}{2(n-1)}}}{h}, \quad \tau u^{n-1}.$$

An example of an invariant implicit scheme is then given by

$$\frac{\hat{u}-u}{\tau} = \frac{1}{(\sigma+1)h^2}\left(\hat{u}_+^{\sigma+1} - 2\hat{u}^{\sigma+1} + \hat{u}_-^{\sigma+1}\right) + a\hat{u}^n. \tag{52}$$

Example 2 The semilinear heat equation.

A weakly reacting chemical system can be described by the equation

$$u_t = u_{xx} + \delta u \log(u).$$

This is invariant under the one-parameter groups generated by the operators

$$X_1 = \frac{\partial}{\partial t}, \quad X_2 = \frac{\partial}{\partial x}, \quad X_3 = 2e^{\delta t}\frac{\partial}{\partial x} - \delta e^{\delta t} x u \frac{\partial}{\partial u}.$$

Unlike the previous example an orthogonal mesh cannot be used to model this equation with an invariant scheme, although we can use one with flat time layers. The four differential invariants are given by

$$J^1 = dt \quad J^2 = \left(\frac{u_x}{u}\right)^2 - \frac{u_{xx}}{u}, \quad J^3 = 2\frac{u_x}{u} + \frac{dx}{dt} \quad J^4 = \frac{1}{u}\frac{du}{dt} - \delta \log(u) + \frac{1}{4}\left(\frac{dx}{dt}\right)^2.$$

Using these we may reformulate the differential equation in a more suggestive manner. Setting $J^3 = 0$ gives a Lagrangian condition for the evolution of the mesh so that

$$\frac{dx}{dt} = -2\frac{u_x}{u}. \tag{53}$$

Similarly, setting $J^2 = J^4$ gives the following equation for the evolution of the solution:

$$\frac{du}{dt} = u_{xx} + \delta u \log(u) - 2\frac{u_x^2}{u}.$$

Thus explicit conservation of the differential invariants of this system is achieved by both a motion of the mesh and an evolution of the solution. Observe that we now have to solve two equations, one for the solution and another for the mesh. This is exactly analogous to the extended system that we investigated when we looked at time adaptivity in Section 5.3. Following Kozlov we now examine the difference invariants for the systems defined using a similar (but non-orthogonal) stencil as for the nonlinear diffusion equation. The following are difference invariants

$$I^1 = \tau, \quad I^2 = h^+, \quad I^3 = h^-, \quad I_4 = \hat{h}^+, \quad I^5 = \hat{h}^-$$

$$I^6 = (\log(u))_x - (\log(u))_{\bar{x}}, \quad I^7 = (\log(\hat{u}))_x - (\log(\hat{u}))_{\bar{x}})$$

where

$$u_x = \frac{u_+ - u}{h} \quad \text{and} \quad u_{\bar{x}} = \frac{u - u_-}{h}$$

$$I^8 = \delta \Delta x + 2(e^{\delta\tau} - 1)\left(\frac{h^-}{h^+ + h^-}(\log(u))_x + \frac{h^+}{h^+ + h^-}(\log(u))_{\bar{x}}\right),$$

$$I^9 = \delta \Delta x + 2(1 - e^{-\delta\tau})\left(\frac{\hat{h}^-}{\hat{h}^+ + \hat{h}^-}(\log(\hat{u}))_x + \frac{\hat{h}^+}{\hat{h}^+ + \hat{h}^-}(\log(\hat{u}))_{\bar{x}}\right),$$

$$I^{10} = \delta(\Delta x)^2 + 4(1 - e^{-\delta\tau})\Big(\log(\hat{u}) - e^{\delta\tau}\log(u)\Big)$$

where $\Delta x = \hat{x} - x$.

Again, by exploiting these invariants we may construct fully invariant difference schemes (effectively discretisations of the above coupled systems) which evolve both the mesh and the solution on the mesh. In [87] it is suggested that an explicit scheme can be constructed so that

$$I^8 = 0 \quad \text{and} \quad I^{10} = \frac{8}{\delta}\frac{(e^{\delta I^1} - 1)^2}{I^2 + I^3} I^6.$$

Thus the equation for the evolution of the mesh becomes

$$\delta \Delta x + 2(e^{\delta\tau} - 1)\left(\frac{h^-}{h^+ + h^-}(\log(u))_x + \frac{h^+}{h^+ + h^-}(\log(u))_{\bar{x}}\right) = 0, \tag{54}$$

which is a discretisation of (53). Similarly, the equation for the evolution of the solution then becomes

$$\delta(\Delta x)^2 + 4(1 - e^{-\delta\tau})\left(\log(\hat{u}) - e^{\delta\tau}\log(u)\right) = \frac{8}{\delta}\frac{(e^{\delta\tau} - 1)^2}{h^+ + h^-}[(\log(u))_x - (\log(u))_{\bar{x}}]. \tag{55}$$

It is shown in [87] that this discretisation admits an invariant solution which has a mesh evolving in the manner

$$x = x_0 \frac{e^{\delta t} + \alpha}{1 + \alpha}$$

and a solution which evolves in the manner

$$u(x,t) = \exp\left(e^{\delta t}\left(f(0) - \frac{e^{\delta\tau} - 1}{2}\sum_{j=1}^{n-1}\frac{e^{-\delta t_j}}{1 + \alpha e^{-\delta t_j}}\right) - \frac{\delta e^{\delta t}}{\alpha + e^{\delta t}}\frac{x^2}{4}\right).$$

Here $x = x_i^j$ and $t = t_j$ and f is a function determined from the initial conditions. For constant α this solution is invariant under the action of the combined operation $2\alpha X_2 + X_3$.

10 Noether's theorem for discrete schemes

A combination of the action based methods for partial differential equations with the symmetry preserving methods described in the last section leads to difference schemes that inherit a discrete form of Noether's theorem relating symmetries of a Lagrangian to conservation laws. An account of these methods is given in the articles [47], [46] by Dorodnitsyn and the thesis [87] of Koslov and we follow the latter treatment here. See also the discussion of Lagrangian based integrators in [99]. For convenience we have considered only the case of ordinary differential equations. The application of the same methods to partial differential equations follows very similar lines and is described in [87].

Suppose that a differential equation is derived from the variation of a Lagrangian functional $\mathcal{L}$ with

$$\mathcal{L} = \int L(x, u, du/dx)dx.$$

This functional achieves its extremal values when $u(t)$ satisfies the Euler-Lagrange equations

$$\frac{\delta \mathcal{L}}{\delta u} = \frac{\partial L}{\partial u} - D\left(\frac{\partial L}{\partial u'}\right) = 0$$

where D is the total derivative operator

$$D = \frac{\partial}{\partial x} + u'\frac{\partial}{\partial u} + \ldots$$

If X is a Lie point symmetry given by

$$X = \xi \frac{\partial}{\partial x} + \eta \frac{\partial}{\partial u} \tag{56}$$

then X is an *infinitesimal divergence symmetry* if there is a function $B(x, u)$ such that

$$X(L) + LD(\xi) = D(B). \tag{57}$$

Note that this is a statement about symmetries of the Lagrangian, rather than of the underlying differential equation. Noether's theorem applied to this system then leads to a conservation law generated by X as follows

THEOREM (Noether) *If X is an infinitessimal divergence symmetry of the functional $\mathcal{L}$ then there is a first integral J of the Euler-Lagrange equations given by*

$$J \equiv N(L) - B = const \quad where \quad N = \xi + (\eta - \xi u') \frac{\partial}{\partial u'}. \tag{58}$$

Proof See [118]

Now we seek a discrete version of this theorem. The Lagrangian functional can be discretised directly in a very similar manner to that described by Furihata. Suppose that the numerical method is constructed over a one-dimensional lattice given by

$$h_+ = \varphi(x, x_+, u, u_+),$$

where x_-, x and x_+ are adjacent mesh points with $h_- = x - x_-$, $h_+ = x_+ - x$ and u_-, u, u_+ (and also ξ_-, ξ, ξ_+) are defined on these points. An appropriate discretisation of $\mathcal{L}$ then takes the form

$$\mathcal{L}_d = \sum_{\Omega_h} L_d(x, x_+, u, u_+) h_+.$$

The definition of an infinitesimal divergence symmetry can then be extended to the discrete case in the manner

$$\xi \frac{\partial L_d}{\partial x} + \xi^+ \frac{\partial L_d}{\partial x_+} + \eta \frac{\partial L_d}{\partial u} + \eta^+ \frac{\partial L_d}{\partial u_+} + L_d D_h(\xi) = D_h(B), \tag{59}$$

together with an invariance condition on the mesh given by

$$S_h(\xi) - \xi = X(\varphi). \tag{60}$$

Here the discrete operators D_h and S_h are defined by

$$S_h(f(x)) = f(x_+) \quad \text{and} \quad D_h(f) = (S_h(f) - f)/h_+,$$

and there is a function $B = B(x, u, x_+, u_+)$.

Finding conditions for the extremals of the discrete Lagrangian leads to conditions on both the solution and on the mesh. Corresponding to the Euler-Lagrange equations are two *quasiextremals* given by

$$\frac{\delta L_d}{\delta x} = h_+ \frac{\partial L_d}{\partial x} + h_- \frac{\partial L_d^-}{\partial x} + L_d^- - L_d \quad \text{and} \quad \frac{\delta L_d}{\delta u} = h_+ \frac{\partial L_d}{\partial u} + h_- \frac{\partial L_d^-}{\partial u}.$$

If the functional $\mathcal{L}_d$ is stationary along the orbits of the group generated by X and the complete group acting on the system is at least two dimensional then both of the quasiextremals must vanish so that

$$\frac{\delta L_d}{\delta x} = 0 \quad \text{and} \quad \frac{\delta L_d}{\delta u} = 0. \tag{61}$$

This leads to a condition on both the solution and the mesh.

The discrete version of Noether's theorem is then given as follows

THEOREM *Let the discrete Lagrangian $\mathcal{L}_d$ be divergence invariant under the action of a Lie group G of dimension $n \geqslant 2$. If the quasiextremals (61) vanish then symmetry X leads to the invariant*

$$J = h_- \eta \frac{\partial L_d}{\partial u} + h_- \eta \frac{\partial L_d}{\partial x} + \eta L_d^- - B.$$

Proof See [46].

Example The following example of an application of these methods to the Pinney equation, is given in [87]. Consider the following second order ordinary differential equation

$$u'' = u^{-3}.$$

This is the Euler-Lagrange equation corresponding to the Lagrangian

$$L = u'^2 - \frac{1}{u^2}.$$

It is invariant under the action of a three dimensional Lie group G generated by the operators

$$X_1 = \frac{\partial}{\partial x}, \quad X_2 = 2x\frac{\partial}{\partial x} + u\frac{\partial}{\partial u}, \quad X_3 = x^2\frac{\partial}{\partial x} + xu\frac{\partial}{\partial u}.$$

The action of the (prolongation of) the symmetry operators X_i leads to the invariances

$$X_1 L + LD(\xi_1) = 0, \quad X_2 L + LD(\xi_2) = 0, \quad X_3 L + LD(\xi_3) = 2u'u = D(u^2).$$

Applying Noether's theorem then gives the following first integrals

$$J_1 = u'^2 + \frac{1}{u^2}, \quad J_2 = 2\frac{x}{u^2} - 2(u - u'x)u', \quad J_3 = \frac{x^2}{u^2} + (u - xu')^2.$$

A natural discretisation of L is given by

$$L_d = \left(\frac{u_+ - u}{h_+}\right)^2 - \frac{1}{uu_+}.$$

This admits the invariances

$$X_1 L_d + L_d D_h(\xi_1) = 0, \quad X_2 L_d + L_d D_h(\xi_2) = 0, \quad X_3 L_d + L_d D_h(\xi_3) = D_h(u^2).$$

The corresponding quasiextremals (invariant under X_i are given by

$$\frac{\delta L_d}{\delta u} : 2(u_x - u_{\bar{x}}) - \frac{h_+}{u^2 u_+} + \frac{h_-}{u^2 u_-} = 0$$

$$\frac{\delta L_d}{\delta x} : (u_x)^2 + \frac{1}{uu_+} - (u_{\bar{x}})^2 - \frac{1}{uu_-} = 0.$$

Here

$$u_x \equiv \frac{u_+ - u}{h_+} \quad u_{\bar{x}} \equiv \frac{u_- u_-}{h_-}.$$

The discrete form of Noether's theorem then gives the following three conserved discrete integrals

$$J_1 = u_x^2 + \frac{1}{uu_+}, \quad J_2 = \frac{x + x_+}{uu_+} - u_x((u + u_+) - (x + x_+)u_x),$$

$$J_3 = \frac{xx_+}{uu_+} + \left(\frac{u + u_+}{2} - \frac{x + x_+}{2}u_x\right)^2.$$

11 Spatial adaptivity, equidistribution and scaling invariance

11.1 Scaling invariance of partial differential equations

As we have demonstrated in Section 9, problems described by a partial differential equation often involve a complex interaction between temporal and spatial structures. As for ordinary differential equations this coupling can take many forms, however, as in our discussion on ordinary equations, a common feature of the equations of mathematical physics is that a frequently encountered group of transformations are *scaling transformations*. These generalise those we investigated for ordinary differential equations in that changes in the temporal scale and scale of the solution are also related to changes in the spatial scale. Thus partial differential equations often fall naturally into the class of problems (considered earlier in the context of ordinary differential equations) which are invariant under the action of a scaling transformation.

Although scaling symmetries are (perhaps) the most important example of differential invariants and play a key role in the analysis of partial differential equations, in comparison with the work on ordinary differential equations scaling symmetries have been less exploited in the development of numerical algorithms. There are several good reasons for this. Firstly, a partial differential equation is often acted upon independently by several symmetry groups (indeed sometimes by a continuum of such) and it is unlikely that one discretisation can preserve invariance under all of these, so some choice has to be made in advance. An example of this is given by considering the linear *heat equation.*

$$u_t = u_{xx}. \tag{62}$$

This equation, in the absence of boundary conditions, is invariant under arbitrary translations in time t and space x and to any *scaling* transformation of the form

$$t \to \lambda t, \quad x \to \lambda^{1/2} x, \quad u \to \lambda^{\alpha} u, \qquad \forall\, \alpha \quad \text{and} \quad \lambda > 0, \tag{63}$$

where α is determined by other conditions such as boundary conditions or integral constraints. (This invariance can also be expressed very naturally in terms of the action of elements in the tangent bundle.) The classical self-similar point source solution is precisely the solution of the linear heat equation invariant under the action of (63) with constant first integral so that $\alpha = -1/2$. In contrast if we consider the nonlinear heat equation

$$u_t = u_{xx} + u^2, \tag{64}$$

then this is invariant under the scaling group (63) in the case of $\alpha = -1$ only. This invariance plays a key role in the understanding of singular behaviour of the solutions of (64) when the initial data is large.

A second reason for the lack of methods which exploit scaling invariance is that in a practical situation, a partial differential equation is defined for arbitrary initial and boundary conditions. Although the equation in the absence of these can be invariant under the action of a group, a general solution will not be so. Often the group invariance is asymptotic in the sense that it describes the *intermediate asymptotic behaviour* of the solutions after a sufficiently long period of evolution that the effects of boundary and initial conditions have become unimportant, and before the system has reached an equilibrium state [10]. This behaviour is very evident for the problem (62), where solutions from an almost arbitrary initial condition evolve to become asymptotically invariant under the action of (63).

A third, and rather subtle reason, is that in many cases the precise nature of the action of a symmetry group on a partial differential equation can only be determined *after* the equation has been solved. For example, in many travelling wave problems, the solutions invariant under the group actions of translation in space and time are precisely travelling waves, the study of which reduces to that of an ordinary differential equation. However the wave speed is in general undetermined until *after* the equation has been solved — indeed determining it is a nonlinear eigenvalue problem. Thus it is difficult *a priori* to find a coordinate system travelling along with the solution in which the solution is invariant.

11.2 Spatial adaptivity

It is possible to capture much of this scaling behaviour using an adaptive method based upon geometric ideas. We now describe a general method for adapting the spatial mesh and then show how geometric ideas can naturally be incorporated into it to give a scale invariant method for partial differential equations which generalises our earlier scale invariant method for ordinary differential equations.

Consider a general partial differential equation discretised on a non-uniform mesh with spatial points $X_{i,j}$. In an analogous manner to the way in which we constructed an adaptive temporal mesh through a time reparameterization or transformation function, where the time t was described in terms of a differential equation in a fictive variable τ, we can think of the spatial mesh $X_{i,j}$ as being point values of a function $X(\xi, \tau)$ of a fictive spatial variable ξ such that X satisfies a (partial differential) equation in ξ. Here we will assume that this function has a high degree of regularity (i.e. we progress beyond thinking of a mesh as a piece-wise constant function of ξ). The study and implementation of adaptive methods then becomes the analysis of the coupled systems describing both the underlying discrete solution $U(\xi, \tau)$ and of the mesh $X(\xi, \tau)$. Invoking a new system to describe the mesh makes the whole discrete system rather larger and more complex and apparently harder to analyse. However, just as in the case of the ODE systems we looked at in Section 5.3, a close geometrical coupling of the equations for the mesh and for the solution actually simplifies their analysis. A widely used, (and from a geometrical point of view natural) procedure for generating such a mesh is that of *equidistribution* of an appropriate *monitor* function.

The approach we describe here to study adaptive discretisations of partial differential equations in one-dimension is based on the framework which is developed in [80]. It is possible to use similar ideas in higher dimensions, see [81], but this is naturally a more complex process. Equidistribution can be loosely thought of as a process for changing the *density* of the mesh points in response to the solution (in contrast to Lagrangian methods which tend to change the mesh points themselves). Our discussion will be confined to the one-dimensional case.

We define the physical mesh, that is the mesh upon which the physical problem is posed, in terms of a mesh function $X(\xi, t)$ which maps the computational (fictive) coordinate $\xi \in [0,1]$ onto a physical coordinate (which we assume without loss of generality to be in $[0,1]$) such that

$$X\left(\frac{j}{N}, t\right) = X_j(t), \qquad j = 0, \ldots, N.$$

Therefore our $N+1$ mesh points $X_j(t)$, which are permitted to vary with time, are simply the image of a uniform *computational* mesh under a time dependent mesh function.

We now introduce a monitor function $M(t, x, u, u_x, u_{xx})$ which classically represents some measure of computational difficulty in the problem, and invoke the principle of equidistribution by defining our mesh function X through the relation

$$\int_0^X M \; dx = \xi \int_0^1 M \; dx. \tag{65}$$

Differentiating with respect to ξ we see that the mesh-density X_ξ satisfies the equation

$$X_\xi = \frac{1}{M} \int_0^1 M \; dx, \tag{66}$$

so that the mesh density is inversely proportional to M. The equation above may be differentiated again to give the following partial differential equation for the mesh — referred to as MMPDE1 (moving mesh partial differential equation 1)

$$(M X_\xi)_\xi = 0.$$

This equation may then be solved for the mesh by discretising the function X appropriately [80]. In practice this can lead to an unstable system and many related partial differential equations have been derived to stabilise this process — with details given in [80]. An example of such a stabilisation is MMPDE6 given by

$$\varepsilon X_{t\xi\xi} = -(M X_\xi)_\xi$$

where ε is a small relaxation parameter. A further advantage of this approach is that it allows the use of an initially uniform mesh (although we note that starting with such a mesh can lead to a stiff system as the equilibrium manifold of an equidistributed mesh is approached). Ideally the stabilisation process should also inherit the symmetries of the original.

To solve the original partial differential equation, both the partial differential equation for the mesh function X and the partial differential equation for $u(x,t)$ are discretised. (It often pays to use a high order discretisation in both cases). One of the mesh equations may then be coupled with the original PDE, giving a new system.

The new coupled system may or may not inherit the qualitative features of the original problem. The geometric integration viewpoint is to produce a mesh in which the mesh equation inherits as many qualitative features as possible. For the purposes of this section, we follow the analysis presented for ordinary differential equations and seek a mesh so that the new system has the same scaling invariances as the original. As the mesh is governed by the monitor function M this problem reduces to that of choosing M such that the coupled system is invariant with respect to the same scaling transformation group as the original equation. By doing this we ensure that all of the scaling symmetry structure of the underlying partial differential equation will be inherited by the resulting numerical method. It is possible to do this for a wide variety of problems with relatively simple choices of M leading to some elegant scaling invariant methods.

We shall now look at a specific example in which we can compare these ideas with the symplectic methods considered earlier.

11.3 Singularities in the nonlinear Schrödinger equation (NLS)

In section 7 we looked at the integrable partial differential equation described by the one-dimensional nonlinear Schrödinger equation. In higher dimensions the radially symmetric solutions of the cubic nonlinear Schrödinger equation satisfy the partial differential equation

$$iu_t + u_{xx} + \frac{d-1}{x} u_x + u|u|^2 = 0. \tag{67}$$

Here d is the dimension of the spatial variable and x is the distance from the origin. This is a natural extension of the one-dimensional nonlinear Schrödinger equation discussed earlier. However it has two very significant differences, firstly it is not an integrable equation if $d > 1$. Furthermore, if $d \geqslant 2$ then this problem has solutions for a wide variety of initial data which blow-up so that they develop singularities at the origin in a finite time T (in a manner similar to that of gravitational collapse) so that the solution tends to infinity in an increasingly narrow (in space) peak.

As remarked earlier, the nonlinear Schrödinger equation is a model for the modulational instability of water waves and plasma waves, and is important in studies of nonlinear optics where the refractive index of a material depends upon the intensity of a laser beam. In the latter case, blow-up corresponds to a self-focusing of the wave. A general discussion of the singularity formation of the NLS equation is given in [137].

The NLS in higher dimensions remains unitary, and can also be written in precisely the same Hamiltonian form as in one dimension. However in higher dimensions it is no longer integrable and has far fewer conserved quantities. Indeed, during the evolution the following are the only two invariant quantities

$$\int_0^\infty |u|^2 x^{d-1}\, dx \quad \text{and} \quad \int_0^\infty \left(|u_x|^2 - \frac{1}{2}|u|^4 \right) x^{d-1}\, dx. \tag{68}$$

The integration strategy for the one-dimensional NLS described in Section 7 strongly exploited its Hamiltonian structure. It is much less clear in the context of higher dimensions whether this approach is the correct one as there is now a play-off between symplectic methods and scale invariant methods.

We now briefly discuss a numerical method to solve (67) when $d \geqslant 2$ which is based upon scale invariant geometrical ideas and which is very effective at computing the blow-up solutions. Details of this method are given in [22]. It is based on preserving the scaling symmetries of the problem rather than either of the two invariant quantities (68) or indeed the overall Hamiltonian structure.

To apply this procedure we consider the scaling and translational groups under which NLS is invariant. In particular (67) is invariant under the action of either of the transformations

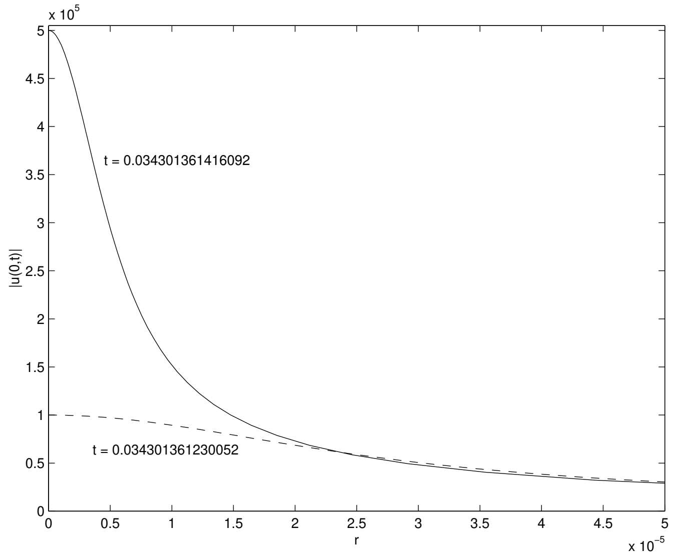

Figure 16: *The solution when* $|u(0,t)|$ *= 100000 and 500000*

the *scaling transformation*

$$t \to \lambda t, \quad x \to \lambda^{1/2} x, \quad u \to \lambda^{-1/2} u, \tag{69}$$

and *translations in phase* given by

$$u \to e^{i\varphi} u, \quad \varphi \in \mathbb{R}.$$

We seek a numerical method which inherits both the scaling and phase invariance symmetries, and achieve this through the use of adaptivity of both the temporal and spatial meshes.

The temporal and spatial adaptivity used for this example are given by solving the following equations

$$\frac{dt}{d\tau} = \frac{1}{|u(0,t)|^2},$$

coupled with MMPDE6. The choice of monitor function

$$M = |u|^2$$

results in a combined system for the mesh and the solution which is invariant under the full set of transformations involving changes both in scale and in phase.

The resulting coupled system is discretised in space using a collocation method. This leads to a system of ordinary differential equations which are scale invariant but do not (necessarily) inherit the Hamiltonian structure of the underlying partial differential equation. It is thus highly appropriate to discretise the resulting ordinary differential equation system using a scale invariant temporal adaptive method as described in Section 5.3, but less appropriate to use a symplectic solution method for the same system. (It is an unresolved question of how we may systematically include all the geometrical features of a partial differential equation into an adaptive method, indeed the equations for the mesh obtained above do not in general have a symplectic structure, even if the underlying partial differential equation does have this structure.) Accordingly, we do not use a symplectic method

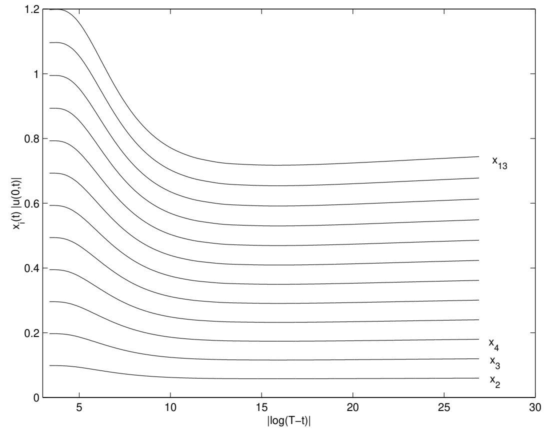

Figure 17: *The scaled mesh* $X_i(t)|u(0,t)|$

to integrate the ordinary differential equations but use instead a stable, scale invariant, spatially adaptive BDF discretisation [73]. The resulting method has proved very effective at computing singular solutions using only a modest number ($N = 81$) of mesh points in the computational domain. The computations have revealed much new geometrical structure in the problem of blow-up in the NLS including new multi-bump blow-up structures [23].

We now present the results of a computation using this method which evolves towards the singular blow-up self-similar solution which has a monotone profile.

Figure 16 shows two solutions taken when $d = 3$ with initial data $u(0,x) = 6\sqrt{2}\exp(-x^2)$ if $0 \leqslant x \leqslant 5$, and $u(0,x) = 0$ if $x > 5$. In this case the estimated value of T is $T = 0.0343013614215$. These two solutions are taken close to the blow-up time when the amplitude of $|u|$ is around 10^5 and the peak has width around 10^{-5}. Observe that the resolution of the peak is very good, indicating that the mesh points are adapting correctly.

In figure 17 we present a plot of $X_i(t)|u(0,t)|$ as a function of $|\log(T-t)|$ for a range in which u varies from 100 to 500000. According to (69) the quantity ux is an invariant of the scaling transformation and is therefore also a constant for a self-similar solution. Observe that in the computations these values rapidly evolve towards constants, demonstrating that the mesh and the discrete solution are both evolving in a self-similar manner.

Thus, as in the case of applying a scale invariant temporal adaptive approach to the ordinary differential equations describing gravitational collapse, the application of a scale invariant spatial approach to adaptivity has led to an attracting self-similar solution being precisely recreated by the numerical solution and the mesh.

A more refined approach to integrate this PDE which combines both the scale invariance and the Hamiltonian structure is described in [24].

11.4 The nonlinear diffusion equation

In Section 9 we looked at the methods described by Dorodnitsyn to integrate the nonlinear diffusion equation. We now compare and contrast these with methods based on scale invariance and equidistribution. We consider here the special case of

$$u_t = (uu_x)_x\,. \tag{70}$$

This equation admits four continuous transformation groups, the two groups of translations in time and space and the two dimensional vector space of scaling symmetry groups spanned by the operators

$$X_1 = t\frac{\partial}{\partial t} + \frac{1}{2}x\frac{\partial}{\partial x} \quad \text{and} \quad X_2 = t\frac{\partial}{\partial t} - u\frac{\partial}{\partial u}.$$

The equation (70) admits a family of self-similar solutions of the form

$$u(x,t) = t^{\gamma} v(x/t^{\beta}) \tag{71}$$

for any values of β and γ which satisfy the algebraic condition

$$2\beta - \gamma = 1.$$

Without additional conditions any such solution is possible, however, if we impose the condition that $u(x,t)$ decays as $|x| \to \infty$ then a simple calculation shows that if the mass I of the solution is given by

$$I = \int u(x,t)\ dx \tag{72}$$

then I is constant for all t. The only self-similar solution with this property has $\gamma = -1/3$ and $\beta = 1/3$. Reducing the partial differential equation down to an ordinary differential equation and solving this gives a one-parameter family of compactly supported self-similar solutions of the form

$$u(x,t) = t^{-1/3}(a - x^2/t^{2/3})_+.$$

These solutions were discovered independently by Barenblatt and Pattle, see [10].

Some of these results can be found in the paper [21]. As described, the equation

$$u_t = (uu_x)_x = (u^2/2)_{xx},$$

has self-similar solutions of constant first integral (72). Both these, and the solution from general compactly supported initial data, are compactly supported and have interfaces at points s_- and s_+ which move at a finite speed. To discretise this equation we introduce and adaptive mesh $X(\xi,t)$ such that $X(0,t) = s_-$ and $X(1,t) = s_+$. To determine X we use a monitor function and a moving mesh partial differential equation. As the evolution of the porous medium equation is fairly gentle it is possible to use the mesh equation MMPDE1 without fear of instability in the mesh. This then allows a wide possible choice of scale invariant monitor functions of the form $M(u) = u^{\gamma}$. A convenient function to use is

$$M(u) = u$$

the choice of which is strongly motivated by the conservation law

$$\int_{s_-}^{s_+} u\ dx = C.$$

Here C is a constant which we can take to equal 1 without loss of generality. Setting $M = u$ and $C = 1$ in the equidistribution principle gives

$$\int_{s_-}^{X} u\ dx = \xi, \tag{73}$$

so that differentiation with respect to ξ we have

$$uX_{\xi} = 1 \tag{74}$$

as the equation for the mesh which we will discretise. Note that this is invariant under the group action $u \to \lambda^{-1/3}u$, $X \to \lambda^{1/3}X$. Now, differentiating (73) with respect to t gives

$$0 = X_t u + \int_{s_-}^{X} u_t \, dx = X_t u + \int_{s_-}^{X} (uu_x)_x \, dx = u(X_t + u_x).$$

Thus, for the continuous problem we also have that X satisfies the Lagrangian equation

$$X_t = -u_x. \tag{75}$$

Substituting (74) and (75) into the rescaled equation gives, after some manipulation, the following equation for u in the computational coordinates:

$$u(\xi,t)_t = \frac{1}{2}u^2(u^2)_{\xi\xi}. \tag{76}$$

The equations (74), (75) and (76) have a set of self-similar solutions of the form

$$\hat{u}(\xi,t) = (t+C)^{-1/3}w(\xi), \quad \hat{X}(\xi,t) = (t-C)^{1/3}Y(\xi),$$

where C is arbitrary and the functions w and Y satisfy differential equations in ξ only. Now, consider semi-discretisations of (74) and (76) so that we introduce discrete approximations $U_i(t)$ and $X_i(t)$ to the continuous functions $u(\xi,t)$ and $X(\xi,t)$ over the computational mesh

$$\xi = i/N, \quad 1 \leqslant i \leqslant (N-1),$$

with $U_0(t) = U_N(t) = 0$. A simple centred semi-discretisation of (76) for $1 \leqslant i \leqslant (N-1)$ is given by

$$\frac{dU_i}{dt} = \frac{N^2}{2}U_i^2\left(U_{i+1}^2 - 2U_i^2 + U_{i-1}^2\right). \tag{77}$$

To define the mesh X_i we discretise (74) to give the algebraic system

$$(X_{i+1} - X_i)(U_{i+1} + U_i) = \frac{2}{N}, \quad 0 \leqslant i \leqslant (N-1). \tag{78}$$

We observe that this procedure has the geometric property of automatically conserving the discrete mass

$$\sum_{i=0}^{N-1} (X_{i+1} - X_i)\left(U_{i+1} + U_i\right). \tag{79}$$

An additional equation is needed to close the set of equations for the unknowns X_i and we do this by insisting that (as in the true solution) the discrete centre of mass is conserved (without loss of generality at 0) so that

$$\sum_{i=0}^{N-1} (X_{i+1}^2 - X_i^2)(U_{i+1} + U_i) = 0. \tag{80}$$

Observe that equation (77) for the solution and the equations (78), (80) for the mesh have decoupled in this system. This makes it much easier to analyse. In particular (77) has two key geometrical features. *Firstly*, it is invariant under the group action

$$t \to \lambda t, \quad U_i \to \lambda^{-1/3}U_i.$$

Thus it admits a (semi) discrete self-similar solution of the form

$$\hat{U}_i(t) = (t+C)^{-1/3}W_i \tag{81}$$

where $W_i > 0$ satisfies an algebraic equation approximating the differential equation for $w(\xi)$. Observe, that for all C we have

$$t^{1/3}\hat{U}_i \to W_i.$$

Secondly, the discretisation satisfies a maximum principle, so that if $U_i(t)$ and $V_i(t)$ are two solutions with $U_i(0) < V_i(0)$ for all i then $U_i(t) < V_i(t)$ for all i. (See [27]).

The consequences of these two results are profound. Suppose that $U_i(0) > 0$ is a general set of initial data. By choosing values of C appropriately (say $C = t_0$ and $C = t_1$) we can write

$$t_0^{-1/3} W_i < U_i(0) < t_1^{-1/3} W_i, \quad 1 \leqslant i \leqslant N-1.$$

Consequently, applying the maximum principle to the self-similar solution we then have that for all t

$$(t+t_0)^{-1/3} W_i < U_i(t) < (t+t_1)^{-1/3} W_i, \quad 1 \leqslant i \leqslant N-1,$$

and hence we have the convergence result

$$t^{1/3} U_i(t) \to W_i, \tag{82}$$

showing that the solution U_i and hence the mesh X_i converges *globally* to the self-similar solution. Hence the numerical scheme is predicting precisely the correct asymptotic behaviour. This is precisely because the discretisation has same underlying geometry as the partial differential equation.

We illustrate this result by performing a computation in which the differential-algebraic equations are decoupled. The resulting ODEs are solved with a BDF method and a linear system is inverted to give the mesh. Figure 18 shows a solution with arbitrary initial data being *squeezed* between two discrete self-similar solutions. The self-similar solutions shown here are those with C taking the values 0.9 and 2.3.

12 The Euler equations and some problems from meteorology

12.1 The Euler equation

Before we consider the problems with a purely meteorological flavour we shall now discuss the two-dimensional Euler equations describing inviscid incompressible fluid flow. This problem appears extensively in the mathematics literature as well as the meteorology literature where it is sometimes referred to as the baratropic vorticity equation. The Euler equation has the form

$$\dot{\omega} = \frac{\partial(\omega, \Psi)}{\partial(x,y)}, \tag{83}$$

where the right hand side of (83) is simply the Jacobian determinant $\omega_x \Psi_y - \omega_y \Psi_x$, and the streamfunction Ψ ($\Psi_x = v, \Psi_y = -u$) is related to the vorticity $\omega = v_x - u_y$ through the relation

$$\omega = \nabla^2 \Psi.$$

This is another example of a problem which may be written in Hamiltonian form (see [118, 98]), with Hamiltonian functional given by the energy

$$\mathscr{H} = \frac{1}{2}\int d\mathbf{x}\, |\mathbf{u}|^2 = \frac{1}{2}\int d\mathbf{x}\, |\nabla\Psi|^2 = -\frac{1}{2}\int d\mathbf{x}\, \Psi\omega$$

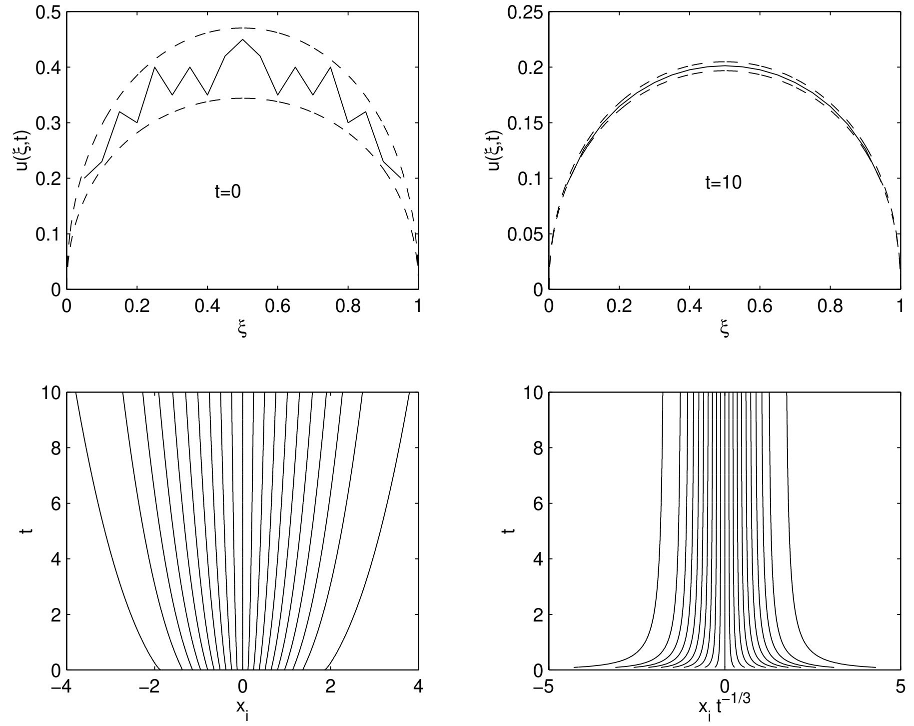

Figure 18: *Convergence of the solution in the computational domain and invariance of the computed mesh.*

and Poisson bracket given by

$$\{\mathscr{F},\mathscr{G}\} = -\int d\mathbf{x}\frac{\delta\mathscr{F}}{\delta\rho(\mathbf{x})}\left(\frac{\partial\left(\omega(\mathbf{x}),\frac{\delta\mathscr{G}}{\delta\rho(\mathbf{x})}\right)}{\partial(x,y)}\right) = \int d\mathbf{x}\,\omega(\mathbf{x})\left(\frac{\partial\left(\frac{\delta\mathscr{F}}{\delta\rho(\mathbf{x})},\frac{\delta\mathscr{G}}{\delta\rho(\mathbf{x})}\right)}{\partial(x,y)}\right),$$

and therefore, following the notation of section 7.1.1, we have

$$\mathscr{D}\bullet = -\frac{\partial(\omega,\bullet)}{\partial(x,y)}.$$

12.1.1 The Arakawa Jacobian

With the correct assumptions on boundary conditions this problem can be shown to preserve the domain integrated vorticity, the enstrophy and the energy, given respectively by

$$\int \omega\; d\mathbf{x}, \quad \int \omega^2\; d\mathbf{x}, \quad \text{and} \quad \int |\nabla\Psi|^2\; d\mathbf{x}. \tag{84}$$

Numerical methods for solving the Euler equations may be subject to nonlinear instabilities, in particular aliasing errors where there is a spurious transfer of energy from large spatial scales to unresolvable smaller spatial scales. Although finite element discretisations automatically obey discrete analogues of (84), the same is not in general true for finite difference spatial approximations. However, Arakawa [4] constructed finite difference analogues of the Jacobian operator in (83) which do preserve discrete analogues of (84). This property of a method can be shown to prevent the nonlinear instabilities described above. Following the notation of Durran [50] and expanding Ψ into a Fourier series

$$\Psi = \sum_{k,l}\Psi_{k,l}, \quad \Psi_{k,l} = a_{k,l}e^{i(kx+ly)},$$

we can now show that the enstrophy and energy in Fourier space are

$$\overline{\nabla\Psi\cdot\nabla\Psi} = -\overline{\Psi\nabla^2\Psi} = \sum_{k,l}\kappa^2\overline{\Psi_{k,l}^2}$$

and

$$\overline{\omega^2} = \overline{(\nabla^2\omega)^2} = \sum_{k,l}\kappa^4\overline{\Psi_{k,l}^2}$$

where overbar denotes domain integration and $\kappa = \sqrt{k^2+l^2}$ is the total wave number. We can therefore define a new invariant for this system — the average wave number

$$\kappa_{\text{avg}} = \sqrt{\frac{\overline{\omega^2}}{\overline{\nabla\Psi\cdot\nabla\Psi}}}.$$

The conservation of which demonstrates that there can be no net transfer of energy into small length scales. The Arakawa discretisation of the Jacobian prevents nonlinear instabilities by preserving discrete analogues of the enstrophy and energy and therefore also the discrete form of the average wave number. Arakawa's first second order approximation to the Jacobian operator on a uniform grid ($\Delta x = \Delta y = d$) is given by

$$\left.\frac{\partial(\omega,\Psi)}{\partial(x,y)}\right|_{i,j} \approx \frac{1}{3}(J_{i,j}^{++}(\omega,\Psi) + J_{i,j}^{+\times}(\omega,\Psi) + J_{i,j}^{\times+}(\omega,\Psi)),$$

where

$$J_{i,j}^{++}(\omega,\Psi) = -\frac{1}{4d^2}[(\omega_{i+1,j}-\omega_{i-1,j})(\Psi_{i,j+1}-\Psi_{i,j-1}) - (\omega_{i,j+1}-\omega_{i,j-1})(\Psi_{i+1,j}-\Psi_{i-1,j}),$$

and $J_{i,j}^{+\times}$, $J_{i,j}^{\times+}$ are given by similar expressions, see Arakawa [4] for more details. A procedure for preserving arbitrary conserved integrals in PDEs is given by McLachlan [105].

12.1.2 Sine bracket type truncation

For references to this material see [7, 102, 110, 150]. We begin with our advection equation in the following form

$$\frac{\partial\omega}{\partial t} = \frac{\partial(\omega,\Psi)}{\partial(x,y)} \equiv \omega_x\Psi_y - \omega_y\Psi_x, \tag{85}$$

We assume (2π) periodic boundary conditions and therefore we evolve on a torus T^2. We now decompose our system into Fourier modes

$$\omega = \sum_{\mathbf{m}}\omega_{\mathbf{m}}e^{i(\mathbf{m},\mathbf{x})}$$

($(\mathbf{m},\mathbf{x}) = \mathbf{m}\cdot\mathbf{x}$) and consider the resulting system of infinitely many ODEs describing their evolution in time. Decomposing Ψ in a similar manner and using the above relation between ω and Ψ we arrive at

$$\Psi_{\mathbf{m}} = \frac{\omega_{\mathbf{m}}}{|\mathbf{m}|^2}.$$

If we substitute into (85) we get after some cancellations

$$\dot{\omega}_{\mathbf{m}}(t) = \sum_{\mathbf{n}\neq\mathbf{0}}\frac{\mathbf{m}\times\mathbf{n}}{|\mathbf{n}|^2}\,\omega_{\mathbf{m}+\mathbf{n}}\,\omega_{-\mathbf{n}}$$

where $\mathbf{m} \times \mathbf{n} = m_1 n_2 - m_2 n_1$, and for real ω we have that $\omega_{-\mathbf{n}} = \omega_{\mathbf{n}}^{\star}$.

This turns out to be Lie-Poisson with the following

$$H(\omega) = \frac{1}{2} \sum_{\mathbf{n} \neq \mathbf{0}} \frac{\omega_{\mathbf{n}} \omega_{-\mathbf{n}}}{|\mathbf{n}|^2}, \quad \nabla H(\omega)_{\mathbf{k}} = \frac{\omega_{-\mathbf{k}}}{|\mathbf{k}|^2},$$

and Poisson structure (structure constants) defined by

$$J_{\mathbf{mn}}(\omega) = (\mathbf{m} \times \mathbf{n}) \omega_{\mathbf{m}+\mathbf{n}} \equiv \sum_{\mathbf{k}} C_{\mathbf{mn}}^{\mathbf{k}} \omega_{\mathbf{k}}, \quad C_{\mathbf{mn}}^{\mathbf{k}} = (\mathbf{m} \times \mathbf{n}) \delta_{\mathbf{m}+\mathbf{n}-\mathbf{k},\mathbf{0}}.$$

So that finally we may write our system in the form

$$\dot{\omega}_{\mathbf{m}} = \sum_{\mathbf{k},\mathbf{l},\mathbf{n}} a^{\mathbf{nl}} \, C_{\mathbf{mn}}^{\mathbf{k}} \, \omega_{\mathbf{k}} \, \omega_{\mathbf{l}},$$

and the metric (inverse inertia tensor) is given by

$$a^{\mathbf{nl}} = \frac{1}{|\mathbf{n}|^2} \delta_{\mathbf{n}+\mathbf{l},\mathbf{0}}.$$

The finite dimensional truncation of our bracket is now achieved by defining the new structure constants (N finite)

$$C_{\mathbf{mn}}^{\mathbf{k}} = \frac{N}{2\pi} \sin\left(\frac{2\pi}{N} (\mathbf{m} \times \mathbf{n})\right) \delta_{\mathbf{m}+\mathbf{n}-\mathbf{k},\mathbf{0}}$$

and so we have the finite dimensional (Poisson) bracket

$$J_{\mathbf{mn}} = \frac{N}{2\pi} \sin\left(\frac{2\pi}{N} (\mathbf{m} \times \mathbf{n})\right) \omega_{\mathbf{m}+\mathbf{n}} \Big|_{\text{mod N}}.$$

Note that these structure constants are those for the algebra $\mathfrak{su}(N)$, and the consistency of this truncation relies on the fact that, in some sense, $SU(N) \to \mathrm{Diff}_{\mathrm{Vol}}(T^2)$ as $N \to \infty$.

We then reduce indices modulo N to the periodic lattice $-M \leqslant m_1, m_2 \leqslant M$ where $N = 2M + 1$. The Hamiltonian is truncated to a finite sum and we can now write down the Sine-Euler equations

$$\begin{aligned} \dot{\omega}_{\mathbf{m}} &= J_{\mathbf{mn}}(\omega) \nabla H_{\mathbf{n}}(\omega) \\ &= \sum_{\substack{n_1, n_2 = -M \\ \mathbf{n} \neq \mathbf{0}}}^{M} \frac{N}{2\pi |\mathbf{n}|^2} \sin\left(\frac{2\pi}{N} (\mathbf{m} \times \mathbf{n})\right) \omega_{\mathbf{m}+\mathbf{n}} \, \omega_{-\mathbf{n}}. \end{aligned} \tag{86}$$

McLachlan [102] constructs a Poisson integrator for (86) which is explicit, fast, and preserves analogues of $N-1$ Casimir's to within round-off error. Mclachlan et. al. [110] were able to study baroclinic instability in a two-layer quasi-geostrophic type model using these ideas.

12.2 The semi-geostrophic equations, frontogenesis and prediction ensembles

To put this work into some context we will now consider how a variety of geometrical integration ideas have been used in combination to tackle certain problems which arise in the numerical solution of meteorological problems. These complex problems abound with geometrical features (such as the conservation of potential vorticity) and are very challenging numerically as they involve solving large systems of equations over long periods of time, often with the formation of singular structures. We now consider two meteorological problems for which a geometric integration based numerical approach to their solution appears to give some improvement over existing methods of solution.

The three-dimensional Boussinesq equations of semi-geostrophic theory describe the ideal, inviscid flow of a fluid on a plane with constant coriolis force f. If u and v are the wind velocities then they may be written in the form (for many further details see [78, 40, 41])

$$\left.\begin{aligned} \frac{Du_g}{Dt} - fv + \frac{\partial \varphi}{\partial x} &= \frac{Du_g}{Dt} - f(v - v_g) = 0, \\ \frac{Dv_g}{Dt} + fu + \frac{\partial \varphi}{\partial y} &= \frac{Dv_g}{Dt} + f(u - u_g) = 0, \end{aligned}\right\} \tag{87}$$

$$\frac{D\theta}{Dt} = 0, \tag{88}$$

$$\nabla_x \cdot \mathbf{u} = 0,$$

$$\nabla_x \varphi = \left(f v_g, -f u_g, g\frac{\theta}{\theta_0} \right).$$

Here (u_g, v_g) is the geostrophic wind, θ the potential temperature, and φ the geopotential. The energy integral E defined by

$$E = \int_D \left(\frac{1}{2}(u_g^2 + v_g^2) - \frac{g\theta z}{\theta_0} \right) dx\, dy\, dz$$

is an invariant of this set of equations. This equation set is of interest for many reasons, one being that it allows the study of idealised atmospheric weather fronts. That is, just as for the nonlinear Schrödinger equation it admits solutions which form singularities in finite time (although the nature of these singularities is quite different).

It is usual to define a coordinate transformation from $(x, y, z)^T$ coordinates to isentropic geostrophic momentum coordinates

$$\mathbf{X} \equiv (X, Y, Z)^T = \left(x + \frac{v_g}{f}, y - \frac{u_g}{f}, \frac{g\theta}{f^2\theta_0} \right)^T. \tag{89}$$

In a similar manner to the previous section we can think of $(X, Y, Z)^T$ as being (fictive) computational coordinates introduced in earlier sections, (89) then describes the evolution of a spatial mesh. In terms of these new coordinates (87) and (88) transform to

$$\frac{D\mathbf{X}}{Dt} = \mathbf{u}_g \equiv (u_g, v_g, 0)^T, \tag{90}$$

and hence the motion in these new coordinates is exactly geostrophic, as well as nondivergent $\nabla_X \cdot \mathbf{u}_g = 0$. A numerical method based on (90) will perform in an adaptive way — a Lagrangian form of mesh adaptivity where the mesh is moved at exactly the speed of the underlying velocity field.

The ratio of volume elements in dual space to that of physical space is given by

$$q = \frac{\partial(X, Y, Z)}{\partial(x, y, z)}.$$

This relates the scaling of the spatial mesh to the computational mesh in an analogous manner to the use of monitor functions described earlier. The expression q defines a consistent form of the Ertel potential vorticity (PV) in SG theory, satisfying

$$\frac{Dq}{Dt} = 0.$$

It is possible to write our coordinate transformation as $\mathbf{X} = \nabla_x P$ where

$$P(\mathbf{x}) = \frac{\varphi}{f^2} + \frac{1}{2}(x^2 + y^2).$$

Hence q, the PV, is equivalently the determinant of the Hessian of P with respect to the coordinates $\mathbf{x}$,

$$q = \det(\mathrm{Hess}_x(P)).$$

Also, $\mathbf{x} = \nabla_{\mathbf{X}} R$, where $P(\mathbf{x})$ and $R(\mathbf{X})$ are a pair of Legendre transforms related by

$$P + R = \mathbf{x} \cdot \mathbf{X}.$$

We can now introduce a stream function for the geostrophic velocities,

$$\Psi = f^2 \left(\frac{1}{2}(X^2 + Y^2) - R(\mathbf{X}) \right), \quad (u_g, v_g) = \frac{1}{f} \left(-\frac{\partial \Psi}{\partial Y}, \frac{\partial \Psi}{\partial X} \right). \tag{91}$$

Defining ρ (the pseudo-density) to be

$$\rho \equiv q^{-1} = \det(\mathrm{Hess}_X(R)), \tag{92}$$

it can be shown that

$$\frac{D_X \rho}{Dt} \equiv \frac{\partial \rho}{\partial t} - \frac{1}{f} \frac{\partial(\rho, \Psi)}{\partial(X, Y)} = 0 \tag{93}$$

It is now possible to compute the evolution of this system using the following procedure,

1. given an initial distribution of a pseudo-density solve the nonlinear elliptic equation of Monge-Ampère type (92) for R,
2. using the streamfunction (91) compute a new velocity field (u_g, v_g),
3. advect the pseudo-density distribution using (93) and return to start.

We thus have two distinct numerical problems to solve. The first being the computation of a solution to the Monge-Ampère equation (92). This is obviously linked to determining the coordinate transformation (89) in exactly the manner of the adaptive mesh methods described earlier, since for a given R we have

$$\mathbf{x} = \nabla_{\mathbf{X}} R,$$

and hence fits in well with our discussions of coordinate transformations and adaptivity earlier.

The second numerical challenge is that of solving the advection equation (93). We will now show that this also has a nice geometric structure very similar to the Euler equations considered in the previous subsection. We shall then return to the connection with two-dimensional adaptivity through a unifying geometrical framework.

12.2.1 Hamiltonian formulations

We now combine the theory described earlier for Hamiltonian partial differential equations with the meteorological equations and consider Hamiltonian formulations for this problem. Roulstone and Norbury [123] discuss two Hamiltonian formulations of the semi-geostrophic equations. The first, a canonical (infinite-dimensional extension of (2)) representation of the equations of motion (90), with Hamiltonian functional

$$\mathscr{H}[\mathbf{X}] = f \int d\mathbf{a} \left(\frac{1}{2}(X^2(\mathbf{a}) + Y^2(\mathbf{a})) - R(\mathbf{X}(\mathbf{a})) \right),$$

where $\mathbf{a}$ is a Lagrangian particle labelling coordinate. The standard canonical Poisson bracket is given by

$$\{\mathscr{F}, \mathscr{G}\}_c = \int d\mathbf{a} \left(\frac{\delta \mathscr{F}}{\delta X(\mathbf{a})} \frac{\delta \mathscr{G}}{\delta Y(\mathbf{a})} - \frac{\delta \mathscr{F}}{\delta Y \mathbf{a})} \frac{\delta \mathscr{G}}{\delta X(\mathbf{a})} \right).$$

As for the rigid body bracket (28), refer to [98, 118] and [123] for further details of this bracket operation. It is possible to prove conservation of PV (equivalently pseudo-density) along trajectories by demonstrating that

$$\{q, \mathscr{H}\}_c = 0.$$

Again following [123] we may write the advection equation (93) in Hamiltonian form. Using the previous Hamiltonian, this time evaluated in phase space solely as a functional of ρ. That is,

$$\mathscr{H}[\rho] = f \int d\mathbf{X}\, \rho(\mathbf{X}) \left(\frac{1}{2}(X^2 + Y^2) - R(\mathbf{X}) \right), \quad \frac{\delta \mathscr{H}}{\delta \rho} = f^2 \left(\frac{1}{2}(X^2 + Y^2) - R \right) \equiv \Psi.$$

We are now in a position to write the equations of motion (93) as

$$\frac{\partial \rho(\mathbf{X})}{\partial t} = \{\rho(\mathbf{X}), \mathscr{H}\}, \tag{94}$$

where the noncanonical Poisson bracket (see [123, 98, 118]) is given by

$$\{\mathscr{F}, \mathscr{G}\} = \int_\Gamma d\mathbf{X} \frac{\delta \mathscr{F}}{\delta \rho(\mathbf{X})} \left(\frac{\partial \left(\rho(\mathbf{X}), \frac{\delta \mathscr{G}}{\delta \rho(\mathbf{X})} \right)}{\partial (X, Y)} \right).$$

Note that in these coordinates, and with this bracket, the pseudo-density becomes a Casimir invariant for the system, $\{\rho, \mathscr{F}\} = 0$ for all functionals $\mathscr{F}(\rho)$, (c.f. the quantity S in the rigid body problem).

The geometric integration problem of numerically integrating these equations whilst preserving the pseudo-density or potential vorticity along the flow turns out to be intimately related to preserving the Hamiltonian (or Poisson bracket) structure of the problem. See [123] for more details, and also [102, 110] for some applications to similar problems where explicit methods capturing the Hamiltonian structure and the Casimir invariants are derived.

12.2.2 Links with moving mesh theory

We now take a closer look at the coordinate transformation from physical to geostrophic or dual coordinates, we also choose to sometimes use the term computational coordinates for X since these are the variables in which computing will be carried out. Recall from earlier we had

$$\mathbf{X} \equiv (X, Y, Z) = \left(x + \frac{v_g}{f}, y - \frac{u_g}{f}, \frac{g\theta}{f^2\theta_0} \right)^T,$$

and

$$q = \frac{\partial(X, Y, Z)}{\partial(x, y, z)} = \det(\mathrm{Hess}_x(P)), \tag{95}$$

we shall now show some links with the theory of moving mesh partial differential equations.

It is possible to write the continuous form of the first one-dimensional moving mesh partial differential equation (MMPDE) in the form (c.f. (66))

$$\frac{\partial x}{\partial \xi} = \frac{1}{M}$$

where M is our monitor function. Notice the similarity with (95) if we take $M = q$, and identify the computational coordinates X and ξ. In particular in one-dimension we simply have that $M = P_{xx}$.

In three dimensions the Russell et. al. approach [81] to construct coordinate transformations ($\xi = \xi(\mathbf{x}, t)$) is to minimize the following integral

$$I[\xi] = \frac{1}{2} \int \sum_{i=1}^{3} \left(\nabla \xi^i\right)^T G_i^{-1} \nabla \xi^i \, d\mathbf{x},$$

where the G_i are monitor functions, three by three symmetric positive definite matrices (concentrates mesh points in regions where G_i is large). The Euler-Lagrange equations for which are

$$-\frac{\delta I}{\delta \xi^i} = \nabla \cdot \left(G_i^{-1} \nabla \xi^i\right) = 0, \quad i = 1, 2, 3.$$

But now notice what happens when we take our monitor functions to be equal $G_i \equiv G$ and

$$G = \mathrm{Hess}_x(P).$$

For a start the determinant of our monitor function is simply the potential vorticity, and one possible solution to the Euler-Lagrange equations is $\xi = \nabla_x P$,since then (using the symmetry of the Hessian if necessary),

$$G^{-1} \nabla \xi^i = \mathbf{e}_i, \quad i = 1, 2, 3; \qquad \mathbf{e}_1 = (1, 0, 0)^T, \text{ etc.}$$

We have thus shown a link between the usual analytical transformation found in the literature and the moving mesh adaptivity ideas discussed in previous sections. A key point to take on board from these is that the equations governing the mesh transformation should be solved to high order, i.e. a smooth mesh should be used. This contrasts with the piecewise constant mesh transformation discussed in [40], as well as the geometric method (a numerical method based on the piecewise constant construction, see [36]).

We hope to employ some of the geometric integration ideas discussedin this paper to the semi-geostrophic equations, with the aim of obtaining the superior results we observed for the nonlinear Schrödinger, and other equations.

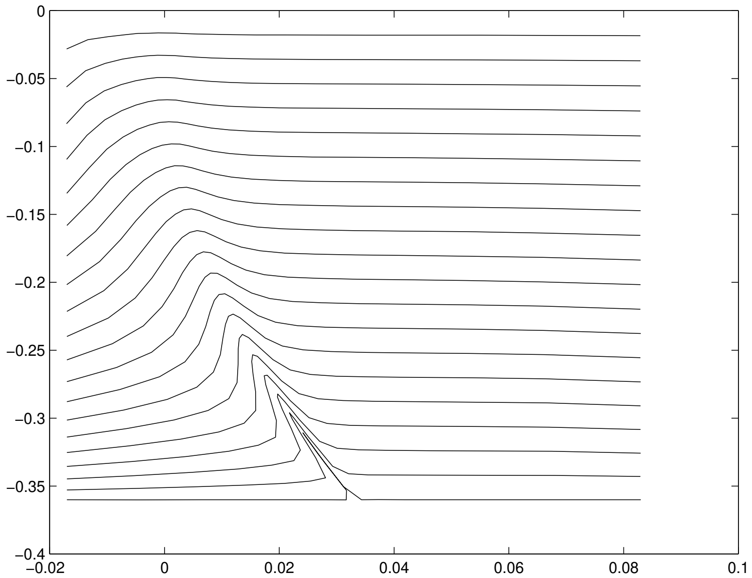

Figure 19: *The structure of the transformation obtained via the parabolic umbilic example.*

We now show some results from a very early calculation based on the above results. Figure 19 demonstrates the singular structure in the coordinate transformation (89) for an example discussed by Chynoweth et. al. [37] where the parabolic umbilic is used as a simple example of an atmospheric front. Figure 20 shows a corresponding mesh which was computed using the potential vorticity as a monitor functionn.

12.2.3 Calculating Lyapunov exponents

Weather forecasting makes *prediction ensembles* to see how reliable a forecast is. This involves discretising the underlying partial differential equations in space to get a system of ordinary differential equations, then looking for the p largest modes of error growth of this system. A systematic way of finding such modes is to calculate Lyapunov exponents of the system.

The calculation of Lyapunov exponents is a natural candidate for a geometric integration based approach as it involves integrating matrix ordinary differential equations which require the preservation of structural properties of the matrices. An interesting algorithm to do this was proposed in [43] and involved integrating systems of equations defining orthogonal matrices. An alternative procedure [75] is to solve the system

$$\dot{Y} = A(t)Y, \quad Y \in M^{n\times p}$$

and to find a singular value decomposition (see [141]) of Y using

$$Y = U(t)S(t)V(t),$$

where U is an $n \times p$ matrix with orthogonal columns, V is a $p \times p$ matrix with orthogonal columnsand S is a diagonal $p \times p$ matrix of singular values. The growth rates of the dominant modes can then be calculated via the Lyapunov exponents

$$\lambda_i = \lim_{t\to\infty} \left[\frac{1}{t} \log S_{ii}(t) \right].$$

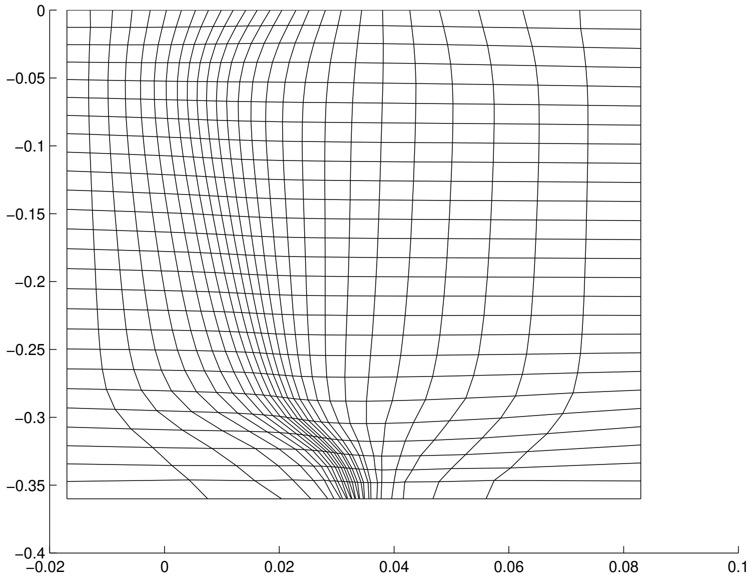

Figure 20: *The mesh computed for the parabolic umbilic example with potential vorticity as our monitor function.*

Essential to this calculation is determining the matrices U and V. An efficient way to proceed is to determine ordinary differential equations for U and V which typically take the form

$$\dot{U} = AU + U(H - U^T AU) \tag{96}$$

where H is a derived $p \times p$ matrix and U the $n \times p$ matrix with orthogonal columns. Equation (96) is a naturally arising evolutionary system in which keeping the columns of U orthogonal is important for the accuracy of the estimates of the Lyapunov exponents. Conventional integrators will not do this easily, however this structure is amenable to methods based on the Lie group invariance of such systems [84]. The geometric integration approach is to decompose U as a product of Householder reflections [141] and solve the ordinary differential equations that define the reflections. The advantage of using such a procedure for (96) is that it has very efficient estimates (exponential convergence) of subspaces to spaces spanned by the fastest growing modes, although great care needs to be taken when singular values coalesce.

13 Conclusion

We have demonstrated in this review that the consideration of qualitative properties in ordinary and partial differential equations is important when designing numerical schemes and we have given some examples of general methods and techniques which may be employed to capture geometric features in discretisations of continuous problems. Traditionally numerical analysts have not necessarily followed this philosophy, they have tended to prefer the black box approach as described in the left hand side of the diagram in Section 1. This approach has led to excellent results in many situations and the numerical analyst has been able to avoid looking too far into the underlying structure of their problems. In this brief article on a subject which is growing and evolving at a fast rate we have hopefully shown using some theory as well as examples the possible advantages which the geometric integration approach to numerical analysis may yield. We have looked at methods applied to both ordinary and partial differential equation problems with Hamiltonian structure, singularity formation, and evolution on manifolds, as well as discussing the possibility of applying these ideas to some problems arising in meteorology and numerical weather prediction — although work on this area is ongoing. In many examples geometric integration has shown that a consideration of the underlying structure of a problem may well be worthwhile since this opens up the possibility of discretising the problem in such a way that the structure is not totally destroyed in the discrete system, this has led to robust methods which are both more accurate and stable for classes of problems. To follow the geometric integration philosophy numerical analysts will therefore need to be conversant with both current results and any new developments in the qualitative theory of differential equations.

Geometric integration is still a relatively new subject area and much work has yet to be done, and with every new development in the underlying theory of differential equations this task will grow. In this review we have shown that it is possible to incorporate qualitative features of many diverse types and for many different problems into numerical algorithms. However a study of the feasibility and practicality of such methods for a wide range of industrial sized real world problems is required. With our brief discussion of some possible meteorological applications we have shown that there is some hope in this direction, but also that there is the possibility of a real two way exchange of ideas between numerical analysis and application areas, where techniques used for specific problems may be generalised to a wider class of problems. Geometric integration also allows us the chance of thinking about old and popular methods in a new light, maybe to improve or generalise, or maybe to help explain behaviour and performance not done so before, or even to help us discover behaviour previously not noticed.

Acknowledgements Much of this work was completed under the financial support of the EPSRC Computational Partial Differential Equations grant GR/M30975. We are especially grateful to Reinout Quispel, JF Williams and Sergio Blanes for reading and commenting on earlier versions of this article.

References

[1] L. Abia and J.M. Sanz-Serna, *Partitioned Runge-Kutta methods for separable Hamiltonian problems*, Math. Comput. **60**, (1993), 617–634.

[2] M. Ablowitz and B.M. Herbst, *On homoclinic structure and numerically induced chaos for the nonlinear Schrödinger equation*, SIAM J. Appl. Math. **50**, (1990), 339–351.

[3] M.P. Allen and D.J. Tildesley, *Computer simulations of liquids*, Clarendon Press, Oxford, (1987).

[4] A. Arakawa, *Computational design for long-term numerical integration of the equations of fluid motion: two-dimensional incompressible flow*, J. Comput. Phys. **1**, (1966), 119–143.

[5] W.F. Ames, R.L. Anderson, V.A. Dorodnitsyn, E.V. Ferapontov, R.K. Gazizov, N.H. Ibragimov and S.R. Svirshevskii, *CRC Hand-book of Lie Group Analysis of Differential Equations Volume 1, Exact solutions and conservation laws*, CRC press, (1994).

[6] V.I. Arnold, *Mathematical Methods of Classical Mechanics,* Springer-Verlag, New York, (1978).

[7] V.I. Arnold and B.A. Khesin, *Topological methods in hydrodynamics*, Springer-Verlag, New York, (1998).

[8] A. Aubry and P. Chartier, *Pseudo-symplectic Runge-Kutta methods*, BIT **38**, (1998), 439–461.

[9] M.A. Austin, P.S. Krishnaprasad and L.-S. Wang, *Almost Poisson Integration of Rigid Body Systems*, J. Comp. Phys. **107**, (1993), 105–117.

[10] G.I. Barenblatt, *Scaling, self-similarity and intermediate asymptotics.* CUP, (1996).

[11] E. Barth and B. Leimkuhler, *Symplectic Methods for Conservative Multibody Systems* Communications of the Fields Institute, **10**, (1996)

[12] G. Benettin and A. Giorgilli, *On the Hamiltonian interpolation of near-to-the-identity symplectic mappings with applications to symplectic integration algorithms*, J. Stat. Phys. **74**, (1994), 1117–1143.

[13] W.J. Beyn, *On invariant closed curves for one-step methods*, Num. Math. **51**, (1987), 103–122.

[14] S. Blanes, F. Casas and J. Ros, *High order optimized geometric integrators for linear differential equations*, accepted for publication, BIT.

[15] S. Blanes and P.C. Moan, *Practical symplectic partitioned Runge-Kutta and Runge-Kutta-Nyström methods*, accepted for publication, J. Comp. Appl. Math.

[16] P.B. Bochev and C. Scovel, *On quadratic invariants and symplectic structure*, BIT **34**, (1994), 337–345.

[17] S.D. Bond and B.J. Leimkuhler, *Time-transformations for reversible variable stepsize integration*, Numer. Algor. **19**, (1998), 55–71.

[18] T.J. Bridges, *Multi-symplectic structures and wave propogation*, Math. Proc. Camb. Phil. Soc. **121**, (1997), 147–190.

[19] T.J. Bridges and S. Reich, *Multi-symplectic integrators: numerical schemes for Hamiltonian PDEs that conserve symplecticity*, Phys. Lett. A **284**, (2001), 184–193.

[20] D.S. Broomhead and A. Iserles (eds.) *The dynamics of numerics and the numerics of dynamics*, Oxford: Clarendon Press, (1992).

[21] C.J. Budd, G.J. Collins, W-Z Huang and R.D. Russell, *Self-similar discrete solutions of the porous medium equation*, Phil. Trans. Roy. Soc. Lond. A **357**, (1999), 1047–1078.

[22] C.J. Budd, S. Chen and R.D. Russell, *New self-similar solutions of the nonlinear Schrödin ger equation with moving mesh computations*, J. Comp. Phys. **152**, (1999), 756–789.

[23] C.J. Budd, *Asymptotics of new blow-up self-similar solutions of the nonlinear Schrödinger equation*,to appear in SIAM J. Appl. Math.

[24] C.J. Budd and V.A. Dorodnitsyn, *Scale invariant, symplectic adaptive numerical methods for the nonlinear Schrödinger equation in dimensions two and three*, (2001), submitted.

[25] C.J. Budd and A. Iserles (editors), *Geometric integration: numericalsolution of differential equations on manifolds.* Phil. Trans. Roy. Soc. Lond. A. **357**, (1999), 943–1133.

[26] C.J. Budd, B. Leimkuhler and M.D. Piggott, *Scaling invariance and adaptivity.* University of Bath Mathematics preprint 99/18, (1999).

[27] C.J. Budd and M.D. Piggott, *The geometric integration of scale invariant ordinary and partial differential equations.* J. Comp. Appl. Math. **128**, (2001), 399–422.

[28] S.R. Buss, *Accurate and efficient simulations of rigid-body rotations.* J. Comp. Phys. **164**, (2000), 377–406.

[29] M.P. Calvo and J.M. Sanz-Serna, *The development of variable-step symplecic integrators, with application to the two-body problem*, SIAM J. Sci. Comput. **14**, (1993), 936–952.

[30] M.P. Calvo, M.A. López-Marcos and J.M. Sanz-Serna, *Variable step implementation of geometric integrators*, Appl. Numer. Math. **28**, (1998), 1–16.

[31] J. Candy and W. Rozmus, *A symplectic integration algorithm for separable Hamiltonian functions.* J. Comput. Phys. **92**, (1991), 230–256.

[32] E. Celledoni and A. Iserles, *Approximating the exponential from a Lie algebra to a Lie group.* Math. of Comp. **69**, (2000), 1457–1480.

[33] P.J. Channel and C. Scovel, *Symplectic integration of Hamiltonian systems.* Nonlinearity **3**, (1990), 231–259.

[34] S.J. Chapman, J.R. King and K.L. Adams, *Exponential asymptotics and Stokes lines in nonlinear ordinary differential equations*, Proc. Roy. Soc. Lond. A, **454**, (1998), 2733–2755.

[35] Y.G. Chen, *Asymptotic behaviours of blowing-up solutions for finite difference analogue of* $u_t = u_{xx} + u^{1+\alpha}$. J. Fac. Sci. Univ. Tokyo; SecIA, Math. **33**, (1986), 541–574.

[36] S. Chynoweth, *The semi-geostrophic equations and the Legendre transform*, Ph.D thesis, University of Reading, UK, (1987).

[37] S. Chynoweth, D. Porter and M.J. Sewell, *The parabolic umbilic and atmospheric fronts*, Proc. R. Soc. Lond. A **419**, (1988), 337–362.

[38] S. Cirilli, E. Hairer and B. Leimkuhler, *Asymptotic error analysis of the adaptive Verlet method*, BIT **39**, (1999), 25–33.

[39] M.J.P. Cullen, J. Norbury, and R.J. Purser, *Generalised Lagrangian solutions for atmospheric and oceanic flows.* SIAM J. Appl. Math. **51**, (1991), 20–31.

[40] M.J.P. Cullen and R.J. Purser, *An extended Lagrangian theory of semi-geostrophic frontogenesis.* J. Atmos. Sci., **41**, (1984), 1477–1497.

[41] M.J.P. Cullen and R.J. Purser, *Properties of the Lagrangian semi-geostrophic equations.* J. Atmos. Sci. **46**, (1987), 2684–2697.

[42] M. Cullen, D. Salmond and P. Smolarkiewicz, *Key numerical issues for the development of the ECMWF model*, Proccedings of ECMWF workshop on *Developments in numerical methods for very high resolution global models*, (2000).

[43] L. Dieci, R.D. Russell and E.S. Van Vleck, *On thecomputation of Lyapunov exponents for continuous dynamical systems.* SIAM J. Numer. Anal. **34**, No. 1, (1997), 402–423.

[44] V.A. Dorodnitsyn, *Transformation groups in mesh spaces*, J. Sov. Math. **55**, 1490–1517.

[45] V.A. Dorodnitsyn, *Finite-difference models exactly inheriting symmetry of original differential equations*, in *Modern group analysis: Advanced analytical and computational methods in mathematical physics*, N.H. Ibragimov et. al. (eds.), Kluwer, 191–201, (1993).

[46] V.A. Dorodnitsyn, *Finite difference analog of the Noether theorem*, Dokl. Akad. Nauk, **328**, (1993), 678.

[47] V.A. Dorodnitsyn, *Noether-type theorems for difference equations.* IHES/M/98/27, Bures-sur-Yvette(France), (1998).

[48] V.A. Dorodnitsyn and R. Kozlov, *The whole set of symmetry preserving discrete versions of a heat transfer equation with a source*, preprint 4/1997, NTNU, Trondheim, Norway, (1997).

[49] P.G. Drazin and R.S. Johnson, *Solitons: an introduction*, CUP, (1989).

[50] D. Durran, *Numerical methods for wave equations in geophysical fluid dynamics*, Springer-Verlag, New York, (1999).

[51] D.J.D. Earn and S. Tremaine, *Exact numerical studies of Hamiltonian maps: Iterating without roundoff error*, Physica D **56**, (1992), 1–22.

[52] K. Engø and S. Faltinsen, *Numerical integration of Lie-Poisson systems while preserving coadjoint orbits and energy*, SIAM J. Numer. Anal. **39**, (2001), 128–145.

[53] K. Engø, A. Marthinsen and H.Z. Munthe-Kaas, *DiffMan: an object oriented MATLAB toolbox for solving differential equations on manifolds*, Technical Report No. 164, Dept. of Informatics, University of Bergen, (1999).

[54] Feng Kang, *On difference schemes and symplectic geometry*, Proc. 1984 Beijing symp. diff. geometry and diff. equations, Beijing, Science Press, (1985), 42–58.

[55] L.E. Fraenkel, *An introduction to maximum principles and symmetry in elliptic problems*, CUP, (2000).

[56] J. de Frutos and J.M. Sanz-Serna, *Accuracy and conservation properties in numerical integration: the case of the Korteweg-de Vries equation*, Numer. Math. **75**, (1997), 421–445.

[57] D. Furihata, *Finite difference schemes for* $\partial u/\partial t = (\partial/\partial x)^\alpha \delta G/\delta u$ *that inherit energy conservation or dissipation property*, J. Comp. Phys. **156**, (1999), 181–205.

[58] D. Furihata, *A stable and conservative finite difference scheme for the Cahn-Hilliard Equation*, Numer. Math. **87**, (2001), 675–699.

[59] D. Furihata, *Finite Difference Schemes for Nonlinear Wave Equation that Inherit Energy Conservation Property*, to appear in J. Comput. Appl. Math.

[60] Z. Ge and J.E. Marsden, *Lie-Poisson Hamilton-Jacobi theory and Lie-Posson integrators*, Phys. Lett. A. **133**, (1988), 134–139.

[61] K. Goda, *On the instability of some finite difference schemes for the Korteweg-de-Vries equation*, J. Phys. Soc. Japan **39**, (1975), 229–236.

[62] H. Goldstein, *Classical Mechanics*, Second edition, Addison-Wesley Publishing, 1980.

[63] M. Golubitsky, Schaeffer and I. Stewart, *Singularites and Groups in Bifurcation theory*, Springer.

[64] O. Gonzalez, *Time integration and discrete Hamiltonian systems*, J. Nonlinear Sci. **6**, (1996), 449–467.

[65] I.S. Grieg and J.L. Morris, *A hopscotch method for the Korteweg-de-Vries equation*, J. Comp. Phys. **20**, (1976), 64–80.

[66] D.F. Griffiths and J.M. Sanz-Serna, *On the scope of the method of modified equations*, SIAM J. Sci. Stat. Comput. **7**, (1986), 994–1008.

[67] P. Grindrod, *Patterns and waves.* Oxford University Press, New York, (1991).

[68] E. Hairer, *Variable time step integration with symplectic methods*, Appl. Numer. Math. **25**, (1997), 219–227.

[69] E. Hairer, *Numerical geometric integration.* Unpublished lecture notes, (1999), available on http://www.unige.ch/math/folks/hairer/.

[70] E. Hairer, *Geometric integration of ordinary differential equations on manifolds.* to appear, BIT, (2000).

[71] E. Hairer and Ch. Lubich, *The life-span of backward error analysis for numerical integrators*, Numer. Math. **76**, (1997), 441–462.

[72] E. Hairer and Ch. Lubich, *Asymptotic expansions and backward analysis for numerical integrators*, In *Dynamics of Algorithms*, (eds. R. de la Llave, L.R. Petzold and J. Lorenz), Springer IMA Volumes in Mathematics and its Applications, vol. 118, (2000), 91–106.

[73] E. Hairer, S.P. Nørsett and G. Wanner, *Solving ordinary differential equations I*, Second edition, Springer series in computational mathematics **8**, Springer-Verlag, Berlin, (1993).

[74] E. Hairer and D. Stoffer, *Reversible long-term integration with variable stepsizes*, SIAM J. Sci. Comput. **18**, (1997), 257–269.

[75] R. Hauser, *Private communication*, (2000).

[76] R. Herman and C. Knickerbocker, *Numerically induced phase shift in the KdV soliton*, J. Comp. Phys. **104**, (1993), 50–55.

[77] T. Holder, B. Leimkuhler and S. Reich, *Explicit variable step-size and time-reversible integration* BIT, to appear.

[78] B.J. Hoskins, *The geostrophic momentum approximation and the semi-geostrophic equations.* J. Atmos. Sci. **32**, (1975), 233–242.

[79] W. Huang and B. Leimkuhler, *The adaptive Verlet method*, SIAM J. Sci. Comput. **18**, (1997), 239–256.

[80] W. Huang, Y. Ren and R.D. Russell, *Moving mesh partial differential equations (MM-PDES) based on the equidistributional principle.* SIAM J. Numer. Anal. **31**, (1994), 709–730.

[81] W. Huang and R.D. Russell, *Moving mesh strategy based on a gradient flow equation for two-dimensional problems*, SIAM J. Sci. Comput. **20**, (1999), 998–1015.

[82] A. Iserles, *On Cayley-transform methods for the discretization of Lie-group equations.* Tech. Report 1999/NA4, DAMTP, University of Cambridge.

[83] A. Iserles and S. Norsett, *On the solution of linear differential equations in Lie groups*, Phil. Trans. Roy. Soc. Lond. A., **357**, (1999), 983–1019.

[84] A. Iserles, H.Z. Munthe-Kaas, S.P. Nørsett and A. Zanna, *Lie-group methods*, Acta Numerica (2000), 215–365.

[85] T. Itoh adn K. Abe, *Hamiltonian-Conserving Discrete Canonical Equations Based on Variational Difference Quotients*, J. Comp. Phys. **77**, (1988), 85–102.

[86] C. Kane, J.E. Marsden and M. Ortiz, *Symplectic-energy-momentum preserving variational integrators*, J. Math. Phys. **40**, (1999), 3353–3371.

[87] R. Kozlov, *Symmetry applications to difference and differential-difference equations*, PhD Thesis 2000:117 Institutt for matematiske fag, NTNU Trondheim, (2000).

[88] J.S.W. Lamb and J.A.G. Roberts, *Time-reversal symmetry in dynamical systems: a survey.* Physica D **112**, (1998), 1–39.

[89] F.M. Lasagni, *Canonical Runge-Kutta methods*, Z. Agnew. Math. Phys. **39**. 952–953.

[90] B. Leimkuhler, *Reverible adaptive regularization: perturbed Kepler motion and classical atomic trajectories*, Phil. Trans. Roy. Soc. Lond. A. **357**, (1999), 1101–1133.

[91] R.J. Le Veque and H.C. Yee, *A study of numerical methods for hyperbolic conservation laws with stiff source terms*, J. Comput. Phys. **86**, (1990), 187–210.

[92] P.W. Li *On the numerical study of the KdV equation by the semi-implicit and leap-frog methods*, Computer Physics Communications **88**, (1995), 121–127.

[93] S. Li and Vu-Quoc *Finite difference calculus invariant structure of a class of algorithms for the nonlinear Klein-Gordon equation*, SIAM J. Numer. Anal. **32**, (1995), 1839–1875.

[94] A.J. Lichtenberg and M.A. Lieberman, *Regular and stochastic motion*, Springer-Verlag, New York, (1983).

[95] M.A. López-Marcos, J.M. Sanz-Serna and J.C. Diaz, *Are Gauss-Legendre methods useful in molecular dynamics*, J. Comp. Appl. Math. **67**, (1996), 173–179.

[96] R.S. MacKay, *Some aspects of the dynamics and numerics of Hamiltonian systems.* in *The dynamics of numerics and the numerics of dynamics.* D. Broomhead and A. Iserles eds., Clarendon Press, Oxford, (1992), 137–193.

[97] W. Magnus, *On the exponential solution of differential equations for a linear operator*, Commun. Pure Appl. Math., **VII**, (1954), 649–673.

[98] J.E. Marsden and T.S. Ratiu, *Introduction to mechanics and symmetry*, Second edition, Springer-Verlag, (1999).

[99] J.E. Marsden and M. West, *Discrete mechanics and variational integrators*, Acta Numerica (2001), 357–514.

[100] T. Matsuo and D. Furihata, *Dissipative and Conservative Finite Difference Schemes for Complex-Valued Nonlinear Partial Differential Equations*, to appear in J. Comput. Phys.

[101] T. Matsuo, M.Sugihara, D. Furihata and M. Mori, *Spatially Accurate Dissipative or Conservative Finite Difference Schemes Derived by the Discrete Variational Method*, submitted to Japan J. Indust. Appl. Math.

[102] R.I. McLachlan, *Explicit Lie-Poisson integration and the Euler equations.* Phys. Rev. Lett. **71**, (1993), 3043–3046.

[103] R.I. McLachlan, *Symplectic integration of Hamiltonian wave equations.* Numer. Math. **66**, (1994), 465–492.

[104] R.I. McLachlan, *On the numerical integration of ordinary differential equations by symmetric composition methods*, SIAM J Sci Comp. **16**, (1995), 151–168.

[105] R.I. McLachlan, *Spatial discretization of partial differential equations with integrals*, submitted to SIAM J. Numer. Anal.

[106] R.I. McLachlan and P. Atela, *The accuracy of symplectic integrators.* Nonlinearity **5**, (1992), 541–562.

[107] R.I. McLachlan and G.R.W. Quispel, *Six lectures on the geometric integration of ODEs*, in *Foundations of computational mathematics*, eds. R. DeVore, A. Iserles and E. Süli, London Mathematical Society Lecture note series 284, (2001), 155–210.

[108] R.I. McLachlan, G.R.W. Quispel and N. Robodoux, *Geometric integration using discrete gradients*, Phil. Trans. Roy. Soc. Lond. A. **357**, (1999), 1021–1045.

[109] R.I. McLachlan, G.R.W. Quispel and G.S. Turner, *Numerical integrators that preserve symmetries and reversing symmetries*, SIAM J. Numer. Anal. **35**, (1998), 586–599.

[110] R. McLachlan, I. Szunyogh and V. Zeitlin, *Hamiltonian finite-dimensional models of baroclinic instability.* Phys. Lett. A **229**, (1997), 299–305.

[111] C. Moler and C. Van Loan, *Nineteen dubious ways to compute the exponential of a matrix.* SIAM Review **20**, (1978), 801–836.

[112] H. Munthe-Kaas, *Runge-Kutta methods on Lie groups*, BIT **38**, (1998), 92–111.

[113] H. Munthe-Kaas and B. Owren, *Computations in a free Lie algebra*, Phil. Trans. Roy. Soc. Lond. A. **357**, (1999), 957–981.

[114] H. Munthe-Kaas and A. Zanna, *Numerical integration of differential equations on homogeneous manifolds*, in *Foundations of computational mathematics*, (eds. F. Cucker and M. Shub), Springer, Berlin, 305–315, (1997).

[115] N. Murray and M. Holman, *The origin of chaos in the outer solar system*, Science **283**, (1999), 1877–1881.

[116] A. Murua and J.M. Sanz-Serna, *Order conditions for numerical integrators obtained by composing simpler integrators*, Phil. Trans. Roy. Soc. Lond. A. **357**, (1999), 1079–1100.

[117] D. Okunbor and R.D. Skeel, *An explicit Runge-Kutta-Nyström method is canonical if and only if its adjoint is explicit*, SIAM J. Numer. Anal. **29**, No. 2, (1992), 521–527.

[118] P.J. Olver, *Applications of Lie Groups to differential equations*, Springer, New York, (1986).

[119] P.J Olver, *Moving frames — in geometry, algebra, computer vision and numerical analysis*, in 'Foundations of computational mathematics', ed. R. DeVore, A. Iserles and E. Süli, London Mathematical Society Lecture note series 284, (2001), 267–297.

[120] K. Pen-Yu and J.M. Sanz-Serna, *Convergence of methods for the numerical solution of the Korteweg-de-Vriess equation*, IMA J. Num. Anal. **1**, (1981), 215–221.

[121] S. Reich, *Backward Error Analysis for Numerical Integrators*, SIAM J. Numer. Anal. **36**, (1999), 1549–1570.

[122] S. Reich, *Multi-symplectic Runge-Kutta collocation methods for Hamiltonian wave equations*, J. Comp. Phys. **157**, (2000), 473–499.

[123] I. Roulstone and J. Norbury, *A Hamiltonian structure with contact geometry for the semi-geostrophic equations.* J. Fluid. Mech. **272**, (1994), 211–233.

[124] R.D. Ruth, *A canonical integration technique.* IEEE Trans. Nucl. Sci. **30**, 2669–2671.

[125] A. Samarskii, V. Galaktionov, S. Kurdyumov and A. Mikhailov, *Blow-up in quasilinear parabolic equations.* Walter de Gruyter, (1995).

[126] J.M. Sanz-Serna, *An explicit finite-difference scheme with exact conservation properties*, J. Comp. Phys. **47**, (1982), 199-210.

[127] J.M. Sanz-Serna, *Runge-Kutta schemes for Hamiltonian systems*, BIT **28**, (1988), 877–883.

[128] J.M. Sanz-Serna, *Geometric Integration* in *The state of the art in numerical analysis.*, (eds. I.S. Duff and G.A. Watson), Oxford: Clarendon, 121–143, (1997).

[129] J.M. Sanz-Serna and M.P. Calvo, *Numerical Hamiltonian problems.* Chapman and Hall, London, (1994).

[130] J.M. Sanz-Serna and A. Portillo, *Classical numerical integrators for wave-packet dynamics*, J. Chem. Phys. **104**, (1996), 2349–2355.

[131] Ch. Schlier and A. Seiter, *Symplectic Integration and Classical Trajectories: A Case Study*, J. Chem. Phys. A **102**, (102), 9399–9404, (1998).

[132] R.D. Skeel and C.W. Gear, *Does variable step size ruin a symplectic integrator?*, Physica D **60**, (1992), 311–313.

[133] D.M. Stoffer, *Some geometric and numerical methods for perturbed integrable systems*, Ph. D. Thesis, ETH Zürich, (1988).

[134] D.M. Stoffer, *Variable steps for reversible integration methods*, Computing **55**, (1995), 1–22

[135] D. Stoffer and K. Nipp, *Invariant curves for variable step size integrators*, BIT **31**, (1991), 169-180.

[136] A.M. Stuart and A.R. Humphries, *Dynamical Systems and Numerical Analysis*, Cambridge, (1996).

[137] C. Sulem and P-L Sulem, *The nonlinear Schrödinger equation.* Applied Mathematical Sciences **139**, Springer, (1999).

[138] Y.B. Suris, *The canonicity of mappings generated by Runge-Kutta type methods when integrating the system* $\ddot{x} = -\partial U/\partial x$, U.S.S.R. Comput. Maths. Phys. **29**, (1989), 138–144.

[139] G.J. Sussman and J. Wisdom, *Chaotic evolution of the solar system*, Science **257**, (1992), 56–62.

[140] T.R. Taha and M.J. Ablowitz, *Analytical and numerical aspects of certain nonlinear evolution equations. III. Numerical, Korteweg-de-Vries equation*, J. Comp. Phys. **55**, (1984), 231–253.

[141] L.N. Trefethen and D. Bau III, *Numerical linear algebra.* SIAM, (1997).

[142] V.S. Varadarajan, *Lie groups, Lie algebras, and their representations*, Prentice-Hall, (1974).

[143] L. Verlet, *Computer "experiments" on classical fluids. I.Thermodynamic properties of Lennard-Jones molecules.* Phys. Rev. **159**, (1967), 98–103.

[144] R. de Vogelaere, *Methods of integration which preserve the contact transformation property of Hamiltonian equations*, Tech. report No. 4, Dept. Math., Univ. Notre Dame, (1956).

[145] J. Wisdom and M. Holman, *Symplectic maps for the* N*-body problem.* Astron. J. **102**, (1991), 1528–1538.

[146] H. Yoshida, *Construction of higher order symplectic integrators*, Phys. Lett. A **150**, (1990), 262–268.

[147] H. Yoshida, *Recent progress in the theory and application of symplectic integrators*, Celestial Mechanics and Dynamical Astronomy **56**, (1993), 27–43.

[148] N.J. Zabusky and M.D. Kruskal, *Interaction of 'solitons' in a collisionless plasma and the recurrence of initial states*, Phys. Rev. Lett. **15**, (1965), 240–243.

[149] A. Zanna, *Collocation and relaxed collocation for the Fer and the Magnus expansions*, SIAM J. Numer. Anal. **36**, (1999), 1145–1182.

[150] V. Zeitlin, *Finite-mode analogues of 2D ideal hydrodynamics: Coadjoint orbits and local canonical structure*, Physica D **49**, (1991), 353–362.